Revisiting Generalization Measures Beyond IID: How Image Corruption and Perturbation Affect Robustness of Generalization Measures

Anonymous authors
Paper under double-blind review

Abstract

Predicting generalization from quantities available before target-test evaluation remains a central challenge in deep learning. The systematic benchmark of Jiang et al. (2020) evaluated many generalization measures, but it focused on independent and identically distributed (IID) settings. We revisit this problem for image classifiers evaluated under controlled corruptions and perturbations. Our study uses CIFAR-10-C/P, where the label space and task remain fixed while the input images are degraded or perturbed. This setting also allows us to revisit the robustness concerns raised by Dziugaite et al. (2020), who showed that the apparent reliability of generalization measures can depend strongly on experimental conditions. Our experiments show that the usefulness of generalization measures is strongly regime-dependent. When the selector must commit to a measure family before target-test evaluation, Calibration & Confidence provides the most favorable family-level downside profile in our CIFAR-10-C/P protocol, achieving the lowest normalized-regret point estimate and the highest top-20% hit rate among non-oracle families. Optimization-based measures, Information Criteria, and Sharpness-based measures provide additional regime-dependent signals in correlation or local-reliability analyses. Together, these findings suggest that model selection should not rely only on measures favored by IID evaluation. Instead, generalization measures should be treated as regime-dependent ranking signals and validated on a target-like proxy for the expected corruption or perturbation setting.

1 Introduction

Deep learning models can fit large training sets and still perform well on held-out data, but predicting this behavior remains difficult (Zhang et al., 2017; Nagarajan & Kolter, 2019; Kawaguchi et al., 2022). For image classification, this question becomes sharper when clean IID evaluation is replaced by controlled image corruptions or perturbations. A useful generalization measure should indicate, before evaluating on the shifted test images, which trained models are likely to retain smaller train-to-test or clean-to-shifted performance gaps (Jiang et al., 2020; Dziugaite et al., 2020).

Many generalization measures have been proposed using model complexity, optimization dynamics, information theory, margins, and loss-landscape geometry. The number of candidates makes empirical evaluation important. Jiang et al. (2020) benchmarked 40 measures on CIFAR-10 and SVHN, and Dziugaite et al. (2020) showed that measure reliability can change under different experimental conditions. These studies provide the starting point for our work, but they mainly assess clean IID behavior. Two image-classification questions remain open:

i. Image corruption and perturbation robustness: Existing IID benchmarks do not show whether a measure ranks models correctly when the same classifier is evaluated on corrupted or perturbed images such as CIFAR-10-C/P (Hendrycks & Dietterich, 2019).

ii. Confidence calibration: A classifier's confidence can carry information about its errors (Guo et al., 2017; Krishnan & Tickoo, 2020). Recent studies connect calibration and generalization behavior (Wald

et al., 2021; Tada & Naganuma, 2023; Yoshida & Naganuma, 2024), but Calibration & Confidence measures are rarely evaluated as generalization measures in large-scale benchmarks.

We therefore revisit the empirical evaluation of generalization measures beyond IID, but only in the controlled image-shift setting defined by CIFAR-10-C/P. This scope is intentional. CIFAR-10-C and CIFAR-10-P keep the label space and task fixed while modifying the input images, so they allow us to ask whether IID-validated measures remain reliable for corruption and perturbation robustness without changing object categories or task semantics.

We follow the experimental philosophy of Jiang et al. (2020), which evaluates more than 40 generalization measures from multiple perspectives, and adapt it to CIFAR-10-C/P evaluation. In addition to conventional Baseline & Output-based, Norm & Margin-based, Sharpness-based, and Optimization-based measures, we include Calibration & Confidence and Information Criteria as candidate generalization-measure families. Through our evaluations, Sharpness-based measures are promising under IID settings, which is consistent with earlier observations that sharpness-related quantities can track model generalization. The main new finding is scoped to image corruptions and perturbations: some categories that are overlooked because they correlate weakly with the IID generalization gap, or because they have not usually been treated as generalization measures, can become more informative for CIFAR-10-C/P gaps than for the IID gap. Calibration & Confidence measures provide the most favorable family-level downside profile when the selector must commit to a family before target-test evaluation, while Optimization-based measures, Information Criteria, and Sharpness-based measures provide additional regime-dependent signals under CIFAR-10-C/P. In addition, motivated by the concerns raised by Dziugaite et al. (2020), we analyze sign-error distributions to examine robustness across hyperparameter variations. The results show that several families can provide useful CIFAR-10-C/P ranking signals in some hyperparameter environments, but this does not make any family a uniformly reliable selector. The detailed definitions of the additional measure families are provided in Appendix A, and supplementary CIFAR-10 measure-level summaries and sign-error analyses are reported in Appendices C.1 and C.4. Thus, our results argue against treating any single generalization measure or measure family as a fixed proxy across clean IID and CIFAR-10-C/P regimes. They instead support a regime-aware view in which measures for corruption or perturbation robustness should be selected from multiple candidate families and validated in the relevant hyperparameter environment.

Our key contributions are as follows:

- Systematic expansion of the experimental framework. We extend the benchmark of Jiang et al. (2020) from IID evaluation to CIFAR-10-C/P corruptions and perturbations, while adding Calibration & Confidence measures and Information Criteria to the conventional measure families.
- Empirical evidence of regime-dependent predictability. We show that IID predictivity does not reliably imply predictivity on CIFAR-10-C/P. Calibration & Confidence measures, Optimization-based measures, Information Criteria, and Sharpness-based measures can be useful candidates under these controlled image shifts, with different levels of correlation and local reliability.
- From correlation to model selection. We complement rank-correlation and sign-error analyses with a decision-level model-selection protocol. This protocol shows that Calibration & Confidence has the most favorable family-level downside profile when selection must be made at the family level, while other promising signals can fail locally across hyperparameter axes or at the decision stage.

2 Related Work

2.1 Generalization Measures

To estimate the generalization performance of a trained model without relying on target test data, prior work has proposed many theoretical and empirical measures. Capacity-based measures, such as VC-dimension (Vapnik, 1991; Bartlett et al., 2019), depend mainly on the hypothesis space and do not account for the learned solution (Neyshabur et al., 2014). Norm- and margin-based measures instead use properties of the learned

classifier, including parameter scale and distance to the decision boundary (Krogh & Hertz, 1991; Neyshabur et al., 2015; Bartlett et al., 2017; Jiang et al., 2018). PAC-Bayes measures bound generalization risk through a posterior distribution over parameters relative to a prior (Dziugaite & Roy, 2017). Dynamics- and Sharpness-based measures use optimization behavior or the local curvature of the loss around the trained solution (Keskar et al., 2017; Foret et al., 2020).

Jiang et al. (2020) conducted a large-scale evaluation of such measures and found that PAC-Bayes and some Sharpness-based measures correlated well with IID generalization, while many traditional norm-based measures were less reliable. Dziugaite et al. (2020) further showed that these conclusions can depend on the experimental setup. The behavior of these measures is still less clear when the same image task is evaluated under corruptions and perturbations. Our study addresses this narrower question and adds Calibration & Confidence measures and Information Criteria to the candidate set.

2.2 Image Corruption, Perturbation, and Confidence Calibration

Clean IID evaluation does not fully describe the behavior of image classifiers under input degradation. Benchmarks such as ImageNet-C and CIFAR-10-C/P show that models with strong clean accuracy can lose accuracy under common corruptions or small perturbation sequences (Hendrycks et al., 2020; Hendrycks & Dietterich, 2019; Geirhos et al., 2018). These benchmarks are useful for our purpose because they modify the image input while keeping the task fixed.

Confidence calibration measures whether predicted probabilities match empirical correctness (Guo et al., 2017). Modern neural networks can be overconfident, and this overconfidence can become more visible under corrupted or perturbed inputs. Prior work has connected calibration with generalization behavior (Ovadia et al., 2019; Wald et al., 2021), but Calibration & Confidence measures (Naeini et al., 2015; Nixon et al., 2019) have rarely been evaluated as standalone predictors in large-scale generalization-measure benchmarks. We therefore include Calibration & Confidence metrics as candidate measures for CIFAR-10-C/P performance gaps.

3 Experimental Protocol

Our main experimental protocol centers on the CIFAR-10 suite. Building on the ranking-based benchmark of Jiang et al. (2020) and the robustness concerns raised by Dziugaite et al. (2020), we ask whether generalization measures induce model rankings that remain valid when evaluation moves from the clean CIFAR-10 test set to CIFAR-10-C/P. This design keeps the training distribution, label space, and model family fixed while changing the test images, allowing us to isolate whether a measure that is useful for IID model selection remains useful for corruption and perturbation robustness. We organize the evaluation into three stages: correlation analysis identifies promising measure families, local sign-error analysis checks whether their rankings are reliable along hyperparameter axes, and decision-level model selection tests whether they choose better models for CIFAR-10-C/P before target labels are used for evaluation. We also broaden the set of measures by incorporating Calibration & Confidence measures and Information Criteria in addition to the traditional families of complexity, norm, sharpness, and Optimization-based measures. Details of the hyperparameter grids and model-specific settings are provided in Appendix B.

3.1 Primary CIFAR-10 Suite, Datasets, and Models

CIFAR-10 suite. We adopt CIFAR-10 (Krizhevsky et al., 2009) as the primary IID benchmark and use CIFAR-10-C/P (Hendrycks & Dietterich, 2019) as the matched corruption and perturbation evaluation suite. The suite therefore consists of three matched evaluation targets: the standard CIFAR-10 test set for IID generalization, CIFAR-10-C for common corruptions, and CIFAR-10-P for perturbations. CIFAR-10-C and CIFAR-10-P preserve the same classification task while changing the test-time input images, making them suitable for testing whether measure-induced model rankings transfer from clean evaluation to controlled image shifts. For this primary suite, we use a three-layer CNN (SimpleCNN), ResNetV2-32 (He et al., 2016), and Network in Network (NiN) (Lin et al., 2013).

Supplementary appendix analyses. We also report supplementary analyses in the appendix. Appendix C.1 provides the clean-to-shifted-test degradation scatter plot and measure-level summaries, and Appendix C.4 provides the full sign-error distributions across architectures and targets.

All hyperparameter grids, model-specific settings, and random seeds for the CIFAR-10 suite are provided in Appendix B.

3.2 Training Protocol

For the primary CIFAR-10 suite, each run is trained for 100 epochs. The sweep includes training hyperparameters such as optimizer, learning rate, batch size, dropout, weight decay, and random seed; for NiN, depth and width are also swept. These controlled sweeps are central to our protocol because they create many candidate models whose rankings can be compared under clean, corrupted, and perturbed test targets. Additional training details are provided in Appendix B.

3.3 Generalization Measures

We classify generalization measures into six categories, partially adopting the taxonomy of Jiang et al. (2020).

Baseline & Output-based Measures. This category comprises structural capacity proxies and simple statistics of the predictive distribution that do not require gradient or optimization information. These serve as baselines reflecting architectural scale or output-shape properties. Representative metrics include VC-dimension approximations, total parameter counts, and output statistics such as cross-entropy or negative entropy.

Norm & Margin-based Measures. These measures capture the geometric properties of the learned function by combining decision boundary separation with parameter complexity. This family includes metrics quantifying the classifier margin, such as the inverse logit margin, as well as various measures of scale, such as parameter ℓ_2 norms, spectral norms, and distances from initialization.

Sharpness-based Measures. Sharpness metrics quantify the sensitivity of the empirical loss to perturbations around the learned parameters, operationalizing the concept of local minima flatness. This category encompasses worst-case loss increases under structured perturbations, curvature approximations like the Hessian top eigenvalue, and PAC-Bayes bounds that interpret stability under stochastic perturbations (Foret et al., 2020).

Optimization-based Measures. These measures summarize the properties of gradients to capture training dynamics, stability, and local sensitivity. Unlike static baselines, these metrics explicitly leverage differential information. Examples include the variance of parameter gradients, which reflects the stochasticity of the training process, and the norms of gradients with respect to parameters or inputs.

The first four categories were included in the evaluations of Jiang et al. (2020) and Dziugaite et al. (2020). We add the following two categories because they may capture behavior under corrupted or perturbed inputs:

Information Criteria. Information criteria balance goodness-of-fit with complexity corrections. This family includes classical criteria like AIC, as well as measures adapted for deep learning that account for posterior variability or local geometry, such as WAIC and TIC. These metrics penalize the model's negative log-likelihood by terms reflecting effective complexity.

Calibration & Confidence. Finally, we include measures that evaluate the alignment between predicted probabilities and empirical accuracy. This category focuses on the reliability of the model's uncertainty estimates, employing metrics such as Expected Calibration Error, Maximum Calibration Error, and adaptive binning variants.

In our implementation, these Calibration & Confidence measures are computed on the source-domain CIFAR-10 training split available before shifted-test evaluation. The training script first partitions the CIFAR-10

training set into an 80% training split and a 20% clean validation split, and then passes the training loader as the measure loader to the common evaluator. The calibration implementations compute bin-wise accuracy from the labels in the supplied loader, so their labels are source-domain labels. Calibration & Confidence measures are therefore not label-free quantities; they are source-supervised pre-target measures. Our claim is not that calibration can be computed without labels, but that source-domain labels can provide a useful pre-target ranking signal without using shifted-test labels. Clean validation labels are also source-domain information and are used only by source/clean baseline selectors. Clean CIFAR-10 test quantities are not used by the main selectors. CIFAR-10-C/P labels, shifted-test accuracies, shifted-test losses, shifted-test gaps, target ranks, and empirical correlation signs are not used before selection.

More detailed descriptions of the metrics are provided in Appendix A.

3.4 Correlation-based Evaluation

We first evaluate each generalization measure as a ranking signal. The purpose of this stage is screening: we ask whether a measure ranks candidate models in the same order as a clean, corrupted, or perturbed target gap. This perspective follows Jiang et al. (2020): a useful generalization measure should help identify, among trained candidate models, which one is likely to suffer a larger or smaller train–test degradation before accessing the target test labels.

Target quantities. For the CIFAR-10 suite, we evaluate both clean and shifted target quantities. We denote the standard CIFAR-10 train–test gap by `GenGap_CIFAR10`. For CIFAR-10-C/P, we use two complementary targets. First, `OODGenGap_C` and `OODGenGap_P` are train-to-shifted-test gaps, defined as the difference between CIFAR-10 training accuracy and CIFAR-10-C/P test accuracy. Second, `OODTestGap_C` and `OODTestGap_P` are clean-to-shifted-test degradation targets, defined as the difference between clean CIFAR-10 test accuracy and CIFAR-10-C/P test accuracy. The first target matches the train–test generalization-gap perspective of prior work, while the second isolates shifted-test degradation by removing the training-accuracy term.

Granulated Kendall score Ψ. Following Jiang et al. (2020), and matching our correlation-analysis implementation, we avoid computing a single global correlation over all runs, since such a score can be dominated by large architectural or hyperparameter changes. Instead, we form local subspaces in which exactly one hyperparameter varies while all others are fixed. For a valid subspace s with n_s runs, measure values μ_i, and target gaps g_i, we compute Kendall's tau-a as

$$\tau_s(\mu, g) = \frac{2}{n_s(n_s - 1)} \sum_{i<j} \operatorname{sign}(\mu_i - \mu_j) \operatorname{sign}(g_i - g_j), \tag{1}$$

where ties contribute zero through the sign function. We then average over valid subspaces:

$$\Psi(\mu, g) = \frac{1}{|\mathcal{S}|} \sum_{s \in \mathcal{S}} \tau_s(\mu, g). \tag{2}$$

A positive Ψ indicates that larger measure values tend to rank models as having larger target gaps, while values near zero indicate little reliable ranking signal. Comparing Ψ across clean and CIFAR-10-C/P targets tests whether the measure-induced ordering is preserved under image corruptions and perturbations.

3.5 Local Reliability Evaluation

The correlation stage identifies promising measure families on average, but an average Kendall score can hide local ranking failures. We therefore evaluate local reliability using sign-error distributions, following the robustness motivation of Dziugaite et al. (2020). The goal is to detect whether a measure fails along particular hyperparameter axes, such as learning rate or weight decay, even when its aggregate correlation is favorable.

Sign-error distributions. Matching our sign-error implementation, we define a hyperparameter configuration, excluding random seed, as a combo. An environment is a pair of combos (h_1, h_2) that differ in exactly

one hyperparameter. For each environment, we compare repeated runs from the two combos and compute the pairwise sign-error between the measure μ and target gap g:

$$\ell_{ij} = \frac{1 - \operatorname{sign}(\mu_i - \mu_j)\operatorname{sign}(g_i - g_j)}{2}. \tag{3}$$

Thus, $\ell_{ij} = 0$ when the measure and target agree on the ordering of the two runs, $\ell_{ij} = 1$ when they disagree, and ties contribute 1/2. When noise filtering is enabled, pairs are weighted using the Hoeffding-based weight

$$w_{ij} = \max\left\{0,\ \left(1 - 2\exp\left[-2n\left(\frac{|g_i - g_j|}{2}\right)^2\right]\right)^2 - 0.5\right\}, \tag{4}$$

where n is the relevant test-set size. Environments with small effective sample size

$$n_{\text{eff}} = \frac{(\sum w_{ij})^2}{\sum w_{ij}^2} \tag{5}$$

are filtered out. The environment-level sign-error is then estimated as

$$\widehat{\text{SE}} = \frac{\sum w_{ij}\ell_{ij}}{\sum w_{ij}}. \tag{6}$$

We report the distribution of $\widehat{\text{SE}}$ across environments and hyperparameter axes. This exposes failure modes that can be hidden by a single mean score, such as measures that look predictive on average but fail badly for particular hyperparameter changes.

3.6 Decision-level Model Selection Evaluation

The third CIFAR-10 evaluation asks a more direct question: can a measure be used to select one model that performs well on CIFAR-10-C/P before target labels are used for evaluation? The decision-level analysis checks whether measure-induced rankings lead to useful model choices for corrupted or perturbed images. Each selector observes only source-domain quantities and pre-target generalization-measure values, chooses one run from a candidate set, and is then evaluated using the held-out shifted-test metric.

Candidate sets and selectors. We form candidate sets at the architecture–sweep–target level. Each set contains finished CIFAR-10-C/P runs that share the same architecture, sweep identity, and shifted target; the selector must choose one run from that set. We compare three selector classes: generalization-measure selectors, source/clean baselines based on training or clean CIFAR-10 validation quantities, and reference selectors Random and Oracle OOD. Clean validation labels are treated as available source-domain information. Clean-test quantities are excluded from the main source/clean baselines and reported only as optimistic references in the appendix. For lower-is-better selectors, the selected run is

$$\hat{r}_q(C) = \arg\min_{r \in C} s_q(r), \tag{7}$$

with the lower-is-better direction fixed a priori for all generalization-measure selectors. Higher-is-better source accuracy baselines are written in the same minimization form by defining $s_q(r)$ as the negative accuracy. Oracle OOD is not an available selector; it is used only as the zero-regret reference.

Selection metrics. No selector uses CIFAR-10-C/P target labels, accuracies, losses, gaps, correlation signs, or target ranks when choosing a run. These target quantities are used only after selection to compute evaluation metrics. Thus, Calibration & Confidence selectors use only source-split labels through their pre-target measure values, not shifted-test labels. For a candidate set C, let $y(r)$ be the held-out shifted-test metric of run r, let $d \in \{\text{higher}, \text{lower}\}$ be its direction, let $r^\star$ be the oracle OOD run, let r^- be the worst run on the shifted target, and let $\hat{r}_q$ be the run selected by selector q. The regret is

$$R_q(C) = \begin{cases} y(r^\star) - y(\hat{r}_q), & d = \text{higher}, \\ y(\hat{r}_q) - y(r^\star), & d = \text{lower}. \end{cases} \tag{8}$$

We normalize this regret by the oracle-to-worst range:

$$\bar{R}_q(C) = \begin{cases} \dfrac{R_q(C)}{y(r^\star) - y(r^-)}, & d = \text{higher}, \\ \dfrac{R_q(C)}{y(r^-) - y(r^\star)}, & d = \text{lower}, \end{cases} \tag{9}$$

with zero normalized regret assigned when the oracle-to-worst range is degenerate. We report mean normalized regret, top-10% and top-20% hit rates, and the number of candidate sets. Appendix C.5 gives the full definitions, leakage check, candidate-set filtering, Random handling, family-level aggregation procedure, and bootstrap confidence-interval procedure.

Leakage boundary. The boundary in our protocol is target-test information, not all labeled source information. Source-domain labels, including the clean validation split, are allowed for source/clean baselines and calibration-style measures. In contrast, clean CIFAR-10 test quantities and all CIFAR-10-C/P target labels, accuracies, losses, gaps, ranks, and empirical signs are unavailable to the selectors.

4 Results

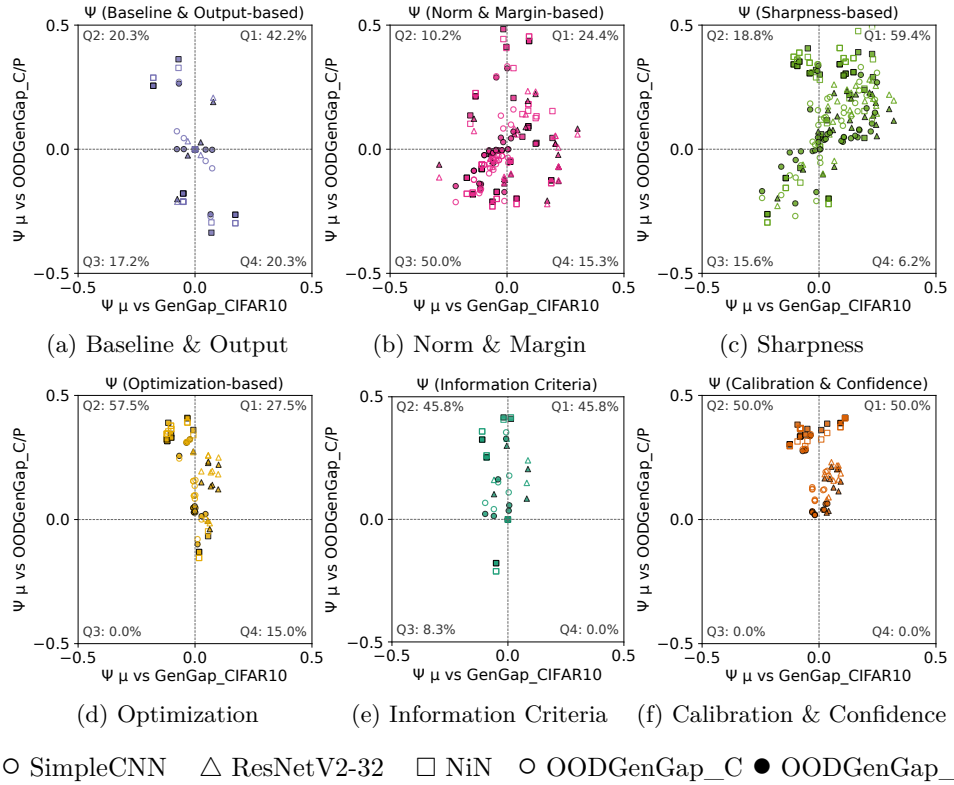

(a) Baseline & Output (b) Norm & Margin (c) Sharpness

(d) Optimization (e) Information Criteria (f) Calibration & Confidence

○ SimpleCNN △ ResNetV2-32 □ NiN ○ OODGenGap_C ● OODGenGap_P

Figure 1: CIFAR-10 suite under corruptions and perturbations: relationship between IID generalization-gap correlation and shifted generalization-gap correlation. Each point is a measure by architecture by shifted target combination. The x-axis is Ψ for `GenGap_CIFAR10`, and the y-axis is Ψ for `OODGenGap_C` or `OODGenGap_P`. Q1 contains measures with positive IID and shifted-test correlations. Q2 contains measures that are weak or negative for IID but positive for CIFAR-10-C/P. Q1 and Q2 are the shifted-test-favorable regions. The main pattern is that Sharpness-based measures remain comparatively stable, while Optimization-based measures, Information Criteria, and Calibration & Confidence measures concentrate more strongly in Q1/Q2 than expected from their IID-only behavior.

4.1 Corruptions and Perturbations Reveal Shift-oriented Measure Families

We begin with CIFAR-10 models evaluated on CIFAR-10-C and CIFAR-10-P. This setting keeps the training distribution, label space, and model families fixed while changing the test-time input images, making it a controlled regime for asking whether an IID generalization measure remains useful for corrupted or perturbed images. Figure 1 compares each measure family's summarized Granulated Kendall score for the IID generalization gap against its score for the train-to-shifted-test gaps, `OODGenGap_C` and `OODGenGap_P`. Each plotted point corresponds to one measure, architecture, and shifted target. The quadrant annotations in each panel summarize the global sign pattern: Q1 contains measures that are positively predictive in both clean and shifted regimes, whereas Q2 contains measures that are weak or negative under IID evaluation but become positive under CIFAR-10-C/P. We read Q1 and Q2 as shifted-test-favorable regions, with Q2 marking signals that IID-only analysis would tend to miss. We do not interpret the quadrant summaries as architecture-invariant effect sizes. They are descriptive screening summaries; the architecture-specific tables and decision-level results are needed to assess whether these signals persist beyond the aggregate visualization.

Sharpness remains the main continuity with IID evaluation. Sharpness-based measures provide the clearest continuity with the IID-centered picture. Many sharpness measures fall in the positive shifted-test region and often remain positive in IID as well, indicating that this family continues to capture a useful sensitivity signal under controlled corruptions and perturbations. This is an important consistency check rather than the main new point: sharpness-related quantities were already among the more informative families in prior IID-centered evaluations (Jiang et al., 2020).

Corruptions and perturbations expose overlooked families. The more distinctive finding is visible in Figures 1d–1f. Optimization-based measures, Information Criteria, and Calibration & Confidence measures move toward the shifted-test-favorable quadrants, especially Q1 and Q2, even though several of them are not strong IID predictors. This means that IID-only evaluation can miss measure families whose signal becomes visible when the target is corruption or perturbation robustness. For Calibration & Confidence, the main positive shifted-test signal is concentrated in NiN: Table 5 reports OOD-C $\Psi = 0.355$ for NiN, whereas SimpleCNN and ResNetV2-32 are near zero with OOD-C $\Psi = 0.044$ and 0.092, respectively. This architecture dependence prevents us from interpreting Calibration & Confidence as a uniformly strong correlation signal across all architectures. Its main advantage appears more clearly at the decision level, where the family has a lower-downside profile after averaging over candidate sets. In contrast, Baseline & Output-based and Norm & Margin-based measures are less reliable as category-level signals: their signs are more mixed, and many measures remain weak or negative for the shifted targets. Information Criteria should be interpreted here as comparatively informative correlation signals and useful candidates for further validation, not as uniformly strong selectors.

The same qualitative conclusion is not an artifact of including training accuracy in the target gap. Appendix C.1 reports the clean-to-shifted degradation analysis, where `OODTestGap_C` and `OODTestGap_P` remove the training-accuracy term and compare clean CIFAR-10 test performance directly against CIFAR-10-C/P test performance. The signal is generally weaker under this stricter target, but Optimization-based measures, Information Criteria, and Calibration & Confidence measures remain more favorable than many Baseline & Output-based or Norm & Margin-based alternatives. Appendix C.3 provides the corresponding measure-level tables across architectures and targets.

4.2 Local Reliability Depends on the Hyperparameter Axis

From average association to local reliability. The scatter plots above answer which measure families are promising on average, but model selection is usually a local ranking problem. A practitioner often compares models that differ along one hyperparameter axis, and a measure with a favorable average Ψ can still be unreliable if it reverses these local orderings. We therefore audit the CIFAR-10-C/P signals with sign-error distributions. For NiN on CIFAR-10-C, Figure 2 reports environment-level sign-error rates separated by the hyperparameter axis that defines the local comparison. Lower values indicate that the measure preserves the target-gap ordering more reliably, whereas values near 0.5 indicate chance-level local ranking.

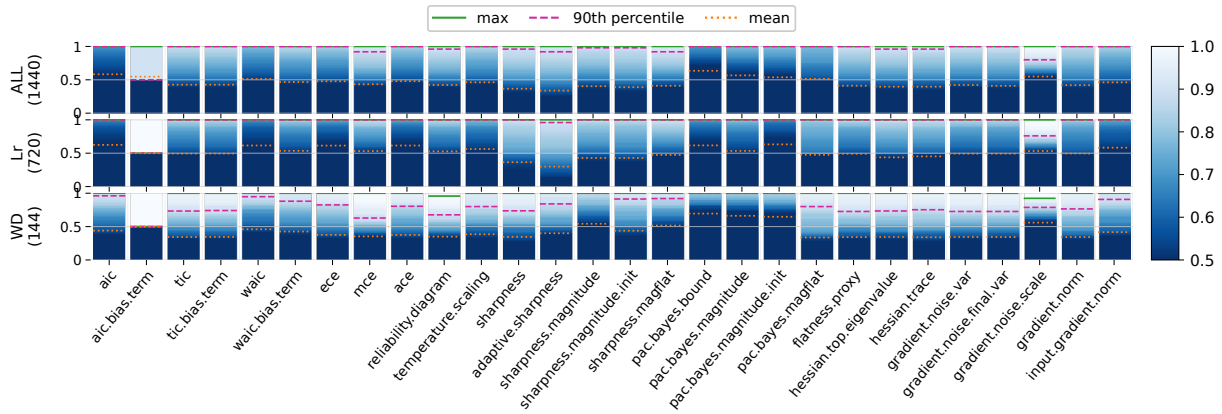

Figure 2: Local reliability on CIFAR-10-C: sign-error distributions for NiN. Each column shows the distribution of environment-level sign-error values for one generalization measure, separated by the hyperparameter axis that defines the local environment. The plot reveals that average shifted-test correlation is not enough: several promising measures remain difficult to use along the learning-rate axis but become much more reliable along weight-decay environments. The orange, magenta, and green lines indicate the mean, 90th percentile, and maximum, respectively.

Hyperparameter-axis dependence. The main lesson is that reliability is strongly axis-dependent. Learning-rate environments remain difficult: many measures have mean sign-errors close to or above chance level, and their upper tails indicate badly misranked local comparisons. Weight-decay environments show a different pattern, with lower sign-errors for a broader set of measures, including Calibration & Confidence measures, Information Criteria, and several sharpness- or optimization-related quantities. Thus, a high average CIFAR-10-C/P correlation is not sufficient for model selection; the measure must also be reliable over the hyperparameter direction actually being searched.

Reproducibility across CIFAR-10-C/P. The CIFAR-10-P results in Appendix C.4 show the same qualitative structure for NiN, and the appendix also reports the corresponding distributions for SimpleCNN, ResNetV2-32, and the clean-to-shifted degradation targets. This supports a narrow interpretation of the CIFAR-10-C/P results: Optimization-based measures, Information Criteria, and Calibration & Confidence measures are useful candidates, but they should be used only after checking local sign-error behavior in the relevant hyperparameter environment.

4.3 Decision-level Model Selection Tests Family-level Utility

Selection task. The correlation and sign-error analyses identify candidate measure families, but they do not directly answer whether these measures can choose a model before CIFAR-10-C/P target labels are used for evaluation. We therefore evaluate the decision-level model-selection protocol defined in Section 3.6. For each architecture–sweep–target candidate set, a selector chooses one run without observing the target shifted-test metric; the selected run is then compared with the oracle OOD run using normalized regret and top-k hit rates.

Family-level results. Table 1 shows that the correlation-level findings translate into selection gains, though imperfectly. Calibration & Confidence has the lowest mean normalized-regret point estimate among all non-oracle selector families (0.178) and the highest top-20% hit rate (0.543). Optimization-based selectors have a slightly higher top-10% hit rate (0.393 versus 0.379), but their normalized-regret point estimate is worse. Source/clean baselines also have higher normalized regret and lower hit rates than Calibration & Confidence. Thus, the evidence supports Calibration & Confidence as the family-level choice with the most favorable downside profile in this CIFAR-10-C/P protocol, not as evidence of uniform dominance. Paired candidate-set bootstrap comparisons support this pattern: Calibration & Confidence reduces normalized

regret relative to Source/clean baselines, Optimization-based selectors, and Random. Appendix C.5 reports the paired differences and intervals.

The family-level aggregation in Table 1 is designed to evaluate robustness when a user must commit to a family, not to identify the lowest-regret individual measure after seeing the results. For each candidate set, we average selector metrics within a family and then average those candidate-set values over the 28 candidate sets. Bootstrap intervals resample candidate sets, not individual selector rows. This aggregation can hide heterogeneity within a family, so individual selector results remain important. This family-level result should not be read as saying that every calibration measure dominates every optimization or sharpness measure. In fact, some individual Optimization-based and Sharpness-based selectors achieve lower regret, but their families exhibit larger within-family spread; the Calibration & Confidence advantage is therefore a stability and downside result at the family level. Appendix C.5 reports the corresponding individual-selector results in Table 24 and architecture-specific family breakdowns in Tables 25–27. It also reports within-family spread and an equal-architecture macro average in Tables 28 and 29. Architecture-specific breakdowns show that this pattern is not equally strong for every architecture. In particular, for ResNetV2-32, the intervals for Calibration & Confidence, Optimization-based selectors, and Information Criteria overlap substantially. We therefore interpret the pooled result as evidence for a favorable family-level downside profile, not as architecture-uniform dominance. Information Criteria are useful candidates for correlation and local-reliability analysis, but their decision-level regret is close to Random.

Failure cases and interpretation. The weaker families are also informative. Norm & Margin-based selectors perform worse than Random in normalized regret and have much lower top-k hit rates, indicating that traditional Norm & Margin-based complexity proxies are unreliable for this CIFAR-10-C/P selection task. Baseline & Output-based measures and Information Criteria are close to Random at the family level, even though individual measures can still be useful in particular regimes. These results separate three roles of the analysis: Kendall correlation screens for promising measures, sign-error analysis checks local ranking reliability, and decision-level selection tests whether these signals lead to better choices on corrupted or perturbed images. The evidence supports Calibration & Confidence as the most conservative family-level default on CIFAR-10-C/P, while keeping the conclusion limited to controlled image shifts.

Table 1: Decision-level model selection on CIFAR-10-C/P. The table reports family-level averages over pre-target selectors. For each family, each individual selector is evaluated on each candidate set, selector metrics are averaged within the family for that candidate set, and the resulting candidate-set values are then averaged over 28 candidate sets. Source/clean baselines exclude clean-test quantities; clean-test references are reported in Appendix C.5. Lower normalized regret is better; higher top-k hit rates are better.

Selector family	Mean normalized regret ↓	95% CI	Top-10% hit ↑	Top-20% hit ↑	# candidate sets
Oracle	0.000	[0.000, 0.000]	1.000	1.000	28
Calibration & Confidence	0.178	[0.123, 0.238]	0.379	0.543	28
Source/clean baselines	0.253	[0.187, 0.325]	0.286	0.405	28
Optimization-based	0.267	[0.210, 0.326]	0.393	0.500	28
Sharpness-based	0.339	[0.272, 0.410]	0.307	0.420	28
Information Criteria	0.365	[0.265, 0.472]	0.345	0.429	28
Baseline & Output-based	0.380	[0.305, 0.454]	0.277	0.357	28
Norm & Margin-based	0.640	[0.561, 0.719]	0.063	0.102	28
Random	0.385	[0.338, 0.431]	0.111	0.200	28

5 Discussion

5.1 How Corruptions and Perturbations Change Measure Validity

The central empirical lesson is that the validity of a generalization measure depends on the evaluation regime. In the CIFAR-10 suite, the shifts are controlled: corruptions and perturbations alter the input while preserving the label space and the underlying task. In this setting, Optimization-based measures and Information Criteria, which are weak or mixed under IID evaluation, become comparatively informative

correlation signals for `OODGenGap_C/P`, often alongside Sharpness-based measures. This suggests that gradient dynamics, optimization noise, and complexity-penalty terms can capture forms of model fragility exposed by image degradation. They are not merely failed IID proxies, but they also should not be treated as uniformly strong model-selection signals.

This contrast reframes the role of IID evaluation. The issue is not simply that IID correlations are noisy, but that they can select the wrong families for a corruption or perturbation target. A concise statement of the result is

$$\rho(m, G_{\mathrm{IID}}) \not\Rightarrow \rho(m, G_{\mathrm{OOD}}),$$

where m denotes a generalization measure, G_{IID} is the IID generalization gap, and G_{OOD} is the relevant shifted-test gap. The implication is not that our benchmark fixes a single preferred measure family, but that each measure family has a regime-specific operating range. For controlled corruptions and perturbations, IID evidence alone is not enough to decide which measure should guide model selection.

5.2 Calibration & Confidence as Selection Signals

Calibration & Confidence measures are useful in the CIFAR-10-C/P suite, but they are not a complete solution to shifted-test model selection. Their main empirical advantage is decision-level robustness when the selector must commit to a family: among non-oracle families, they have the lowest normalized-regret point estimate and the highest top-20% hit rate on CIFAR-10-C/P candidate sets. This does not imply that every calibration measure is reliable. We interpret this result as evidence that Calibration & Confidence has smaller downside as a family-level default, not as evidence that calibration errors are superior to the lowest-regret optimization, sharpness, or loss-based individual selectors.

The CIFAR-10-C/P results also suggest that no single calibration summary should be treated as sufficient. Expected Calibration Error (ECE) is an average bin-wise discrepancy,

$$\mathrm{ECE} = \sum_{b=1}^{B} \frac{|B_b|}{n} \left|\mathrm{acc}(B_b) - \mathrm{conf}(B_b)\right|,$$

whereas Maximum Calibration Error (MCE) captures the largest bin-wise discrepancy,

$$\mathrm{MCE} = \max_{b \in \{1,\ldots,B\}} \left|\mathrm{acc}(B_b) - \mathrm{conf}(B_b)\right|.$$

Controlled corruptions and perturbations can create high-confidence errors that are not captured well by average accuracy alone. In such cases, worst-case or bin-sensitive summaries such as MCE and reliability-diagram-based measures can retain signal that average-case summaries such as ECE may miss.

We treat this explanation as a plausible interpretation rather than an identified mechanism. The present experiments do not isolate calibration-specific information from correlated source-domain quantities such as loss, accuracy, or confidence dispersion.

5.3 Guidelines for Regime-Aware Model Selection

The consequence is that no single generalization measure should be trusted on CIFAR-10-C/P only because it works well under IID evaluation. For corruption and perturbation robustness, the CIFAR-10-C/P results support a candidate set that includes Calibration & Confidence, Optimization-based measures, Information Criteria, and Sharpness-based measures. Information Criteria are supported mainly by correlation and local-reliability analyses, not by family-level decision regret. Calibration & Confidence is the lower-downside family-level default in the selection experiment, but it should still be checked in the local hyperparameter environment being searched.

For CIFAR-10-C/P-style image degradation, Optimization-based measures and Information Criteria should be evaluated alongside Sharpness-based and Calibration & Confidence measures, because these families can become more informative under controlled corruptions and perturbations than they appear under IID evaluation. However, Information Criteria should be treated as correlation and local-reliability candidates

rather than family-level decision defaults. Thus, model-selection use should check not only whether a measure has a high average Ψ, but whether it preserves rankings in the local hyperparameter environment being searched.

A concrete workflow is therefore:

CIFAR-10-C/P-style target:	evaluate the candidate families above;
Local hyperparameter search:	check sign-error behavior along the searched axis;
Before selection:	validate rankings on a proxy corruption or perturbation close to the target.

The validation step is essential. Whenever possible, practitioners should construct a proxy corruption or perturbation that resembles the expected target, compute the candidate measures before target-test selection, and retain only measures whose induced rankings remain reliable under that proxy. This protocol is more defensible than selecting a single measure because it performed well in an IID benchmark.

6 Limitations and Future Work

Scope of Experimental Benchmarking: Data, Models, and Shifts. Our empirical scope is bounded. The evaluation uses CNN-style models on CIFAR-10-C/P controlled corruptions and perturbations. CIFAR-10-C/P is a controlled image-degradation suite, not a natural distribution-shift benchmark. We therefore interpret the results as evidence about these image-shift regimes, not as guarantees for other architectures, modalities, tasks, or shift types. We do not claim that the same family-level ordering will hold for natural distribution shifts, semantic shifts, larger-scale datasets, transformers, or augmentation-heavy training recipes. Our claim is restricted to controlled CIFAR-10-C/P-style image degradation, where the label space and task semantics are fixed. The usefulness of Calibration & Confidence measures may also depend on the source split and validation protocol.

Selection Protocol and Practical Use. The family-level results do not identify a universal individual measure. Individual selectors within the same family can behave differently; therefore, the family-level result should be interpreted as a robustness summary rather than a prescription to use every member of the family. Practical use also depends on having a proxy corruption or perturbation close to the expected target. When no target-like proxy is available, the decision-level value of these measures is more limited.

Theoretical Grounding. The analysis is primarily empirical. Rank correlations, sign-error distributions, and decision-level regret quantify predictive utility, but they do not establish causal mechanisms. Our results do not isolate whether the advantage of Calibration & Confidence comes from calibration-specific information, confidence-distribution effects, or correlation with source-domain loss and accuracy. Future work should test broader model families and additional corruption or perturbation types, and should isolate why Calibration & Confidence, Information Criteria, optimization dynamics, and sharpness become useful in this setting.

7 Conclusion

This work revisits generalization-measure benchmarking beyond IID evaluation for image corruptions and perturbations. Across controlled CIFAR-10-C/P shifts, IID predictivity does not reliably transfer to shifted-test predictivity. Calibration & Confidence, Information Criteria, and Optimization-based measures can provide useful correlation or local-reliability signals, although only Calibration & Confidence shows the most favorable family-level downside profile in our decision-level selection protocol. The decision-level model-selection experiment shows that correlation-based predictivity is not sufficient by itself. In our pre-target selection protocol, Calibration & Confidence has the lowest normalized-regret point estimate and the highest top-20% hit rate among non-oracle families on CIFAR-10-C/P candidate sets. The results support a regime-aware model-selection workflow: start from measure families that are plausible for the expected image shift, compare them against source/clean baselines, and validate their rankings on a target-like proxy before using them for selection.

References

H. Akaike. A new look at the statistical model identification. *IEEE Transactions on Automatic Control*, 19 (6):716–723, 1974. doi: 10.1109/TAC.1974.1100705.

Shunichi Amari. Natural gradient works efficiently in learning. *Neural computation*, 10(2):251–276, 1998.

Peter L Bartlett, Dylan J Foster, and Matus J Telgarsky. Spectrally-normalized margin bounds for neural networks. *Advances in neural information processing systems*, 30, 2017.

Peter L Bartlett, Nick Harvey, Christopher Liaw, and Abbas Mehrabian. Nearly-tight vc-dimension and pseudodimension bounds for piecewise linear neural networks. *Journal of Machine Learning Research*, 20 (63):1–17, 2019.

Junbum Cha, Sanghyuk Chun, Kyungjae Lee, Han-Cheol Cho, Seunghyun Park, Yunsung Lee, and Sungrae Park. Swad: Domain generalization by seeking flat minima. *Advances in Neural Information Processing Systems*, 34, 2021.

Gintare Karolina Dziugaite and Daniel M. Roy. Computing nonvacuous generalization bounds for deep (stochastic) neural networks with many more parameters than training data. In *Proceedings of the 33rd Annual Conference on Uncertainty in Artificial Intelligence (UAI)*, 2017.

Gintare Karolina Dziugaite, Alexandre Drouin, Brady Neal, Nitarshan Rajkumar, Ethan Caballero, Linbo Wang, Ioannis Mitliagkas, and Daniel M Roy. In search of robust measures of generalization. *Advances in Neural Information Processing Systems*, 33:11723–11733, 2020.

Pierre Foret, Ariel Kleiner, Hossein Mobahi, and Behnam Neyshabur. Sharpness-aware minimization for efficiently improving generalization. *arXiv preprint arXiv:2010.01412*, 2020.

Robert Geirhos, Patricia Rubisch, Claudio Michaelis, Matthias Bethge, Felix A Wichmann, and Wieland Brendel. Imagenet-trained cnns are biased towards texture; increasing shape bias improves accuracy and robustness. In *International conference on learning representations*, 2018.

Chuan Guo, Geoff Pleiss, Yu Sun, and Kilian Q Weinberger. On calibration of modern neural networks. In *International conference on machine learning*, pp. 1321–1330. PMLR, 2017.

Haowei He, Gao Huang, and Yang Yuan. Asymmetric valleys: Beyond sharp and flat local minima. *Advances in Neural Information Processing Systems*, 32:2553–2564, 2019.

Kaiming He, Xiangyu Zhang, Shaoqing Ren, and Jian Sun. Identity mappings in deep residual networks. In *European conference on computer vision*, pp. 630–645. Springer, 2016.

Dan Hendrycks and Thomas Dietterich. Benchmarking neural network robustness to common corruptions and perturbations. In *International Conference on Learning Representations*, 2019.

Dan Hendrycks, Steven Basart, Norman Mu, Saurav Kadavath, Frank Wang, Evan Dorundo, Rahul Desai, Tyler Zhu, Samyak Parajuli, Mike Guo, et al. The many faces of robustness: A critical analysis of out-of-distribution generalization. *arXiv preprint arXiv:2006.16241*, 2020.

Pavel Izmailov, Dmitrii Podoprikhin, Timur Garipov, Dmitry Vetrov, and Andrew Gordon Wilson. Averaging weights leads to wider optima and better generalization. *arXiv preprint arXiv:1803.05407*, 2018.

Yiding Jiang, Dilip Krishnan, Hossein Mobahi, and Samy Bengio. Predicting the generalization gap in deep networks with margin distributions. In *International Conference on Learning Representations*, 2018.

Yiding Jiang, Behnam Neyshabur, Hossein Mobahi, Dilip Krishnan, and Samy Bengio. Fantastic generalization measures and where to find them. In *International Conference on Learning Representations*, 2020.

Kenji Kawaguchi, Leslie Pack Kaelbling, and Yoshua Bengio. Generalization in deep learning. In *Mathematical Aspects of Deep Learning*. Cambridge University Press, 2022. doi: 10.1017/9781009025096.003.

Nitish Shirish Keskar, Jorge Nocedal Dheevatsa Mudigere, Mikhail Smelyanskiy, and Ping Tak Peter Tang. On large-batch training for deep learning: Generalization gap and sharp minima. In *International Conference on Learning Representations*, 2017.

Ranganath Krishnan and Omesh Tickoo. Improving model calibration with accuracy versus uncertainty optimization. *Advances in Neural Information Processing Systems*, 33:18237–18248, 2020.

Alex Krizhevsky, Vinod Nair, and Geoffrey Hinton. Cifar-10 and cifar-100 (canadian institute for advanced research). `http://www.cs.toronto.edu/~kriz/cifar.html`, 2009. MIT License.

Anders Krogh and John Hertz. A simple weight decay can improve generalization. *Advances in neural information processing systems*, 4, 1991.

Min Lin, Qiang Chen, and Shuicheng Yan. Network in network. *arXiv preprint arXiv:1312.4400*, 2013.

Mahdi Pakdaman Naeini, Gregory Cooper, and Milos Hauskrecht. Obtaining well calibrated probabilities using bayesian binning, 2015.

Hiroki Naganuma, Taiji Suzuki, Rio Yokota, Masahiro Nomura, Kohta Ishikawa, and Ikuro Sato. Takeuchi's information criteria as generalization measures for DNNs close to NTK regime, 2022. URL `https://openreview.net/forum?id=FH_mZOKFX-b`.

Vaishnavh Nagarajan and J Zico Kolter. Uniform convergence may be unable to explain generalization in deep learning. *Advances in Neural Information Processing Systems*, 32, 2019.

Behnam Neyshabur, Ryota Tomioka, and Nathan Srebro. In search of the real inductive bias: On the role of implicit regularization in deep learning. *CoRR*, abs/1412.6614, 2014. URL `https://api.semanticscholar.org/CorpusID:6021932`.

Behnam Neyshabur, Ryota Tomioka, and Nathan Srebro. Norm-based capacity control in neural networks. In *Conference on learning theory*, pp. 1376–1401. PMLR, 2015.

Jeremy Nixon, Michael W Dusenberry, Linchuan Zhang, Ghassen Jerfel, and Dustin Tran. Measuring calibration in deep learning. In *CVPR workshops*, volume 2, 2019.

Yaniv Ovadia, Emily Fertig, Jie Ren, Zachary Nado, David Sculley, Sebastian Nowozin, Joshua Dillon, Balaji Lakshminarayanan, and Jasper Snoek. Can you trust your model's uncertainty? evaluating predictive uncertainty under dataset shift. *Advances in neural information processing systems*, 32, 2019.

Christopher J. Shallue, Jaehoon Lee, Joseph Antognini, Jascha Sohl-Dickstein, Roy Frostig, and George E. Dahl. Measuring the effects of data parallelism on neural network training. *Journal of Machine Learning Research*, 20(112):1–49, 2019.

Keigo Tada and Hiroki Naganuma. How image corruption and perturbation affect out-of-distribution generalization and calibration. In *2023 International Joint Conference on Neural Networks (IJCNN)*, pp. 1–6, 2023. doi: 10.1109/IJCNN54540.2023.10191806.

Kei Takeuchi. Distribution of information statistics and validity criteria of models. *Mathematical Science*, 153:12–18, 1976.

Vladimir Vapnik. Principles of risk minimization for learning theory. *Advances in neural information processing systems*, 4, 1991.

Yoav Wald, Amir Feder, Daniel Greenfeld, and Uri Shalit. On calibration and out-of-domain generalization. *Advances in neural information processing systems*, 34:2215–2227, 2021.

Sumio Watanabe and Manfred Opper. Asymptotic equivalence of bayes cross validation and widely applicable information criterion in singular learning theory. *Journal of machine learning research*, 11(12), 2010.

Kotaro Yoshida and Hiroki Naganuma. Towards understanding variants of invariant risk minimization through the lens of calibration, 2024.

Chiyuan Zhang, Samy Bengio, Moritz Hardt, Benjamin Recht, and Oriol Vinyals. Understanding deep learning requires rethinking generalization. In *International Conference on Learning Representations*, 2017. URL https://arxiv.org/abs/1611.03530.

Guodong Zhang, Lala Li, Zachary Nado, James Martens, Sushant Sachdeva, George E Dahl, Christopher J Shallue, and Roger Grosse. Which algorithmic choices matter at which batch sizes? insights from a noisy quadratic model. *arXiv preprint arXiv:1907.04164*, 2019.

A More Details on Generalization Measures

Table 2: Summary of generalization measures evaluated in this study, including those applicable beyond the IID regime. The measures are categorized into six groups based on their source of signal and intended use as generalization predictors.

Measure Name	Description
Baseline & Output-based Measures	
`vcdim`	Approximate VC-dimension bound based on network depth and width.
`params`	Total number of trainable model parameters.
`magnitude`	The ℓ_2 norm of the parameter vector.
`cross.entropy`	Average cross-entropy loss on the training set (or evaluation split).
`negative.entropy`	Negative entropy of the predictive distribution (measure of confidence/peakiness).
Norm & Margin-based Measures	
`inverse.margin.p10`	Inverse of the 10th percentile of the logit margin distribution.
`l2.over.margin.p10`	Ratio of parameter ℓ_2 norm to the 10th percentile margin.
`l1.over.margin.p10`	Ratio of parameter ℓ_1 norm to the 10th percentile margin.
`margin.normalized.param.norm`	Parameter norms scaled by the robust margin.
`spectral.norm.per.layer`	Sum of spectral norms computed per layer.
`spec.sum`	Sum of the spectral norms of the weight matrices.
`spec.prod`	Product of the spectral norms of the weight matrices.
`frobenius.distance`	Frobenius distance between the final weights and initialization.
`path.norm`	Path-norm; a scale-invariant capacity measure.
`fisher.rao.norm`	Fisher-Rao norm; geometry-aware norm based on the Fisher Information Matrix.
Sharpness-based Measures	
`sharpness`	Worst-case loss increase within a neighborhood (standard definition).
`adaptive.sharpness`	Sharpness measured with an adaptive neighborhood size.
`sharpness.magnitude`	Sharpness scaled by the magnitude of the parameters.
`sharpness.magnitude.init`	Sharpness scaled by the magnitude relative to initialization.
`sharpness.magflat`	Flatness measure using multiplicative perturbations proportional to weight magnitude.
`pac.bayes.bound`	PAC-Bayes generalization bound (interpreted as stability/flatness).
`pac.bayes.magnitude`	PAC-Bayes bound incorporating parameter magnitude.
`pac.bayes.magnitude.init`	PAC-Bayes bound incorporating distance from initialization.
`pac.bayes.magflat`	PAC-Bayes variant related to magnitude-proportional flatness.
`flatness.proxy`	Flatness proxy based on Elastic Weight Consolidation (EWC).
`hessian.top.eigenvalue`	The largest eigenvalue of the Hessian matrix (worst-case curvature).
`hessian.trace`	The trace of the Hessian matrix (average curvature).
Optimization-based Measures	
`gradient.noise.var`	Variance of the stochastic gradients during training.

Continued on next page

Table 2 – continued from previous page

Measure Name	Description
`gradient.noise.final.var`	Variance of the gradients measured at the final solution.
`gradient.noise.scale`	Ratio of gradient noise variance to the mean squared gradient norm.
`gradient.norm`	Aggregate norm of the gradients across minibatches.
`input.gradient.norm`	Norm of the gradient of the loss with respect to the input (sensitivity).
Information Criteria	
`aic.bias.term`	The complexity penalty term of AIC (based on parameter count).
`tic.bias.term`	The complexity penalty term of TIC (trace term).
`waic.bias.term`	The complexity penalty term of WAIC (log-likelihood variance).
Calibration & Confidence Measures	
`ece`	Expected Calibration Error; weighted average difference between confidence and accuracy in bins.
`mce`	Maximum Calibration Error; the maximum gap between confidence and accuracy across bins.
`ace`	Adaptive Calibration Error; uses adaptive binning based on quantiles.
`reliability.diagram`	Calibration error derived from bin-wise reliability diagrams.
`temperature.scaling`	Calibration error calculated after post-hoc optimal temperature scaling.

Table 2 presents the generalization measures adopted in this study. The following subsections describe the evaluated measures or their implementation families, including the Calibration & Confidence and Information Criteria families added to the original Jiang et al. (2020) taxonomy.

A.1 Baseline & Output-based Measures

`vcdim`. We report an architecture-based VC-dimension proxy. Classical VC theory motivates capacity control via VC-style complexity measures (Vapnik, 1991). In our experiments, we use the standard parameter-count proxy commonly used as a simple capacity baseline in generalization-measure evaluations (Jiang et al., 2020):

$$\text{vcdim} = W \log W, \tag{10}$$

where W is the number of trainable parameters. This proxy is also consistent with known scaling behavior of VC/pseudodimension upper bounds for piecewise-linear networks (Bartlett et al., 2019). For 4D image inputs, we instead use the μ_{VC} upper bound (Eq. 15) from Fantastic Generalization Measures and Where to Find Them by Jiang et al. (2020). We computed this measure to create a capacity-only baseline to test whether architecture scale alone predicts IID/OOD generalization gaps (Jiang et al., 2020; Dziugaite et al., 2020).

`params`, `magnitude`, `cross.entropy`, and `negative.entropy`. These measures are simple architecture- or output-based baselines. `params` is the number of trainable parameters, `magnitude` is the parameter ℓ_2 norm, `cross.entropy` is the empirical cross-entropy on the data split used for measuring the model, and `negative.entropy` is the negative predictive entropy. They are included to distinguish signals that come from model size or output confidence from signals that require margins, curvature, or optimization dynamics.

A.2 Norm & Margin-based Measures

`inverse.margin.p10`. For each sample (x_n, y_n), define a margin m_n. For all classification runs in this study, m_n is computed from logits. Margin distributions, especially lower-tail statistics, have been shown to

correlate with generalization gaps and are used in practice as predictors (Jiang et al., 2018; 2020). Let $q_{0.10}$ be the empirical 10th percentile of $\{m_n\}_{n=1}^{N}$. We compute a sign-preserving, clamped inverse:

$$\text{inverse.margin.p10} = \frac{1}{\text{clip}(q_{0.10}, -\epsilon, \epsilon)} \quad \text{where} \quad \text{clip}(z, -\epsilon, \epsilon) = \text{sign}(z)\max(|z|, \epsilon). \tag{11}$$

We computed this measure to create a low-tail separation/robustness signal (small-magnitude lower-tail margins ⇒ larger score) used as a predictor of generalization gaps (Jiang et al., 2018; Bartlett et al., 2017).

`l2.over.margin.p10`. This measure is an alias of `margin.normalized.param.norm` under default settings. Norm- and margin-based quantities are standard complexity surrogates for deep nets (Neyshabur et al., 2015; Bartlett et al., 2017; Jiang et al., 2020). Let θ be the vector of all trainable parameters (including biases by default) and let $\|\theta\|_2$ be its ℓ_2 norm. Let S denote the chosen lower-tail margin statistic (default: $p10$), computed from logits. The reported value is

$$\text{l2.over.margin.p10} = \frac{\|\theta\|_2}{\max(|S|, \epsilon)}. \tag{12}$$

We computed this measure to create a combined scale+tail-margin proxy to test whether larger parameter scale relative to worst-case margins correlates with poorer generalization (Neyshabur et al., 2015; Jiang et al., 2018; Bartlett et al., 2017).

`l1.over.margin.p10`. Same implementation family as above, but using ℓ_1 norm. ℓ_1-type norms appear in norm-based capacity control and can behave differently under sparsity/scale effects (Neyshabur et al., 2015; 2014).

$$\text{l1.over.margin.p10} = \frac{\|\theta\|_1}{\max(|S|, \epsilon)}, \tag{13}$$

with the same S definition (default statistic $p10$). We computed this measure to probe whether absolute-scale/sparsity-sensitive norms behave differently as generalization predictors under IID and shift (Jiang et al., 2020; Dziugaite et al., 2020).

`margin.normalized.param.norm`. This is the canonical implementation used by `l2.over.margin.p10` by default. With $\|\theta\|_2$ including biases and S the selected margin statistic (default $p10$), we compute

$$\text{margin.normalized.param.norm} = \frac{\|\theta\|_2}{\max(|S|, \epsilon)}. \tag{14}$$

We computed this measure to create a single scalar that merges parameter scale and lower-tail margin magnitude, evaluated as a candidate predictor of IID/OOD generalization gaps across architectures (Neyshabur et al., 2015; Bartlett et al., 2017; Jiang et al., 2018).

`spectral.norm.per.layer`. For each layer weight tensor W_ℓ, we estimate the spectral norm via power iteration on a matrix flattening of the weights. Spectral norms are central to spectrally-normalized margin bounds and Lipschitz-style capacity control for deep networks (Bartlett et al., 2017; Neyshabur et al., 2015). For convolutions, kernels are flattened (not the full convolution operator). Let $\hat{\sigma}_\ell$ denote the resulting estimate. We aggregate to a scalar mean:

$$\text{spectral.norm.per.layer} = \frac{1}{L}\sum_{\ell=1}^{L} \hat{\sigma}_\ell. \tag{15}$$

We computed this measure to create an operator-scale proxy (approximate Lipschitz/conditioning signal) to test correlation with IID/OOD generalization gaps (Bartlett et al., 2017; Jiang et al., 2020).

`spec.sum`, `spec.prod`, and `frobenius.distance`. The `spec.sum` and `spec.prod` measures use the same per-layer spectral-norm estimates as `spectral.norm.per.layer`, but aggregate them by summation or product, respectively. `frobenius.distance` measures the Frobenius norm of the displacement from initialization, $\|\theta - \theta_0\|_F$, when an initialization snapshot is available. These quantities are included because spectral products/sums and distance-from-initialization terms appear in norm-based generalization bounds and in empirical generalization-measure benchmarks (Bartlett et al., 2017; Jiang et al., 2020; Dziugaite et al., 2020).

path.norm. This measure is implementation-dependent by model family. Path- and norm-based controls are standard complexity surrogates and appear in multiple generalization-measure catalogs (Neyshabur et al., 2014; 2015; Jiang et al., 2020). For the convolutional models in this study, we use a structured layer-wise aggregation:

$$\text{path.norm} = \sum_{\ell=1}^{L} \log \left\| W_\ell \right\|_F. \tag{16}$$

We computed this measure to create a structured weight-aggregation complexity proxy, since exact path norms are intractable at scale, intended to correlate with generalization behavior (Neyshabur et al., 2014; Jiang et al., 2020; Dziugaite et al., 2020).

fisher.rao.norm. Let $p_\theta(y \mid x)$ be the predictive distribution and define $g_n = \nabla_\theta \log p_\theta(y_n \mid x_n)$. Fisher-information geometry motivates measuring parameter sensitivity through Fisher-metric–weighted quantities (Amari, 1998; Kawaguchi et al., 2022). The Fisher–Rao quantity is computed as

$$\text{fisher.rao.norm} = \sqrt{\mathbb{E}\left[(\theta^\top g)^2\right]} \approx \sqrt{\frac{1}{N}\sum_{n=1}^{N} (\theta^\top g_n)^2} = \sqrt{\theta^\top \widehat{F}\,\theta}, \tag{17}$$

where $\widehat{F} = \frac{1}{N}\sum_{n=1}^{N} g_n g_n^\top$. We computed this measure to create an information-geometric complexity measure that weights parameters by their sensitivity in log-likelihood space (Amari, 1998; Jiang et al., 2020).

A.3 Sharpness-based Measures

sharpness. Sharpness is computed in a SAM-style one-step perturbation per minibatch, then averaged over the data loader. Sharpness and sharp minima have been linked to generalization behavior (e.g., large-batch effects) (Keskar et al., 2017), and SAM operationalizes a sharpness-aware objective (Foret et al., 2020). For a batch loss $\hat{L}_b(\theta)$, define the normalized gradient direction

$$u_b = \frac{\nabla_\theta \hat{L}_b(\theta)}{\left\| \nabla_\theta \hat{L}_b(\theta) \right\|_2}. \tag{18}$$

The one-step perturbed parameters are

$$\theta_b^+ = \theta + \rho\, u_b, \tag{19}$$

and we report the average batch-wise loss increase

$$\text{sharpness} = \mathbb{E}_b\left[\hat{L}_b(\theta_b^+) - \hat{L}_b(\theta)\right]. \tag{20}$$

We computed this measure to create a scalable flatness/sensitivity proxy (one-step) that remains informative across architectures and evaluation regimes (Foret et al., 2020; Cha et al., 2021; Izmailov et al., 2018).

adaptive.sharpness. Adaptive sharpness scans over a log-spaced set of radii $\{\rho_k\}_{k=1}^{K}$, computes the SAM-style one-step sharpness at each radius, and by default returns the maximal normalized value:

$$\text{adaptive.sharpness} = \max_{k \in \{1,\ldots,K\}} \frac{\text{sharpness}(\rho_k)}{\rho_k}. \tag{21}$$

We computed this measure to create a radius-robust sharpness summary that reduces sensitivity to a single perturbation scale (Foret et al., 2020; Jiang et al., 2020; Cha et al., 2021).

sharpness.magnitude. Let the baseline empirical loss be $\hat{L}(\theta) = \frac{1}{N}\sum_{n=1}^{N} \mathrm{CE}_n(\theta)$. Magnitude-aware perturbations are commonly used in empirical generalization-measure evaluations to improve comparability across scales (Jiang et al., 2020; Dziugaite et al., 2020). For each perturbation sample k, and for each parameter tensor p, we apply additive Gaussian noise scaled by the tensor standard deviation:

$$p \leftarrow p + \epsilon, \qquad \epsilon \sim \mathcal{N}\big(0,\, (r \cdot \mathrm{std}(p))^2\big). \tag{22}$$

Let $\Delta_k = \hat{L}(\theta + \Delta\theta_k) - \hat{L}(\theta)$ be the loss increase. We aggregate across samples (default: max; optionally mean):

$$\text{sharpness_raw} = \max_k \Delta_k. \tag{23}$$

Define the magnitude factor

$$M_{\text{orig}} = \frac{\|\theta\|_2}{\sqrt{d}}, \tag{24}$$

where d is the total number of parameters. The final measure is

$$\text{sharpness.magnitude} = \text{sharpness_raw} \cdot M_{\text{orig}}. \tag{25}$$

We computed this measure to create a scale-aware sharpness signal that probes sensitivity of the learned solution to stochastic perturbations (Keskar et al., 2017; Jiang et al., 2020; He et al., 2019).

`sharpness.magnitude.init.` This measure matches **`sharpness.magnitude`** but uses an initialization-relative magnitude factor when an init snapshot θ_0 is available:

$$M_{\text{init}} = \frac{\|\theta - \theta_0\|_2}{\sqrt{d}}, \tag{26}$$

falling back to M_{orig} if θ_0 is unavailable. The final measure is

$$\text{sharpness.magnitude.init} = \text{sharpness_raw} \cdot M_{\text{init}}. \tag{27}$$

We computed this measure to capture sharpness weighted by distance traveled during training, reducing sensitivity to raw parameter scaling (Jiang et al., 2020; Dziugaite et al., 2020; Izmailov et al., 2018).

`sharpness.magflat.` With the same baseline loss $\hat{L}(\theta)$, we sample magnitude-aware perturbations

$$\Delta\theta_k = r \cdot z_k \odot (|\theta| + \epsilon_{\text{scale}}), \qquad z_k \sim \mathcal{N}(0, I), \tag{28}$$

and compute loss increases $\Delta_k = \hat{L}(\theta + \Delta\theta_k) - \hat{L}(\theta)$. We aggregate across samples (default: max; optionally mean):

$$\text{sharpness.magflat} = \max_k \Delta_k. \tag{29}$$

We computed this measure to create a magnitude-aware flatness proxy intended to improve comparability across architectures and training scales (Jiang et al., 2020; Dziugaite et al., 2020; Keskar et al., 2017).

`pac.bayes.magflat.` PAC-Bayes analysis provides nonvacuous generalization bounds for deep stochastic predictors under suitable choices of priors/posteriors (Dziugaite & Roy, 2017; Dziugaite et al., 2020). We define a diagonal Gaussian posterior centered at the learned parameters with magnitude-scaled variance:

$$Q = \mathcal{N}\big(\theta,\ \text{diag}(\sigma_{q,i}^2)\big), \qquad \sigma_{q,i}^2 = (\sigma_{\text{post}}|\theta_i|)^2, \tag{30}$$

and an isotropic Gaussian prior

$$P = \mathcal{N}(0, \sigma_{\text{prior}}^2 I). \tag{31}$$

We approximate the Gibbs empirical 0–1 risk via multiplicative noise:

$$\theta' = \theta \odot (1 + \sigma_{\text{post}}\varepsilon), \qquad \varepsilon \sim \mathcal{N}(0, I), \qquad \hat{R}_G = \mathbb{E}_{\theta'}[\text{empirical 0–1 error}]. \tag{32}$$

The KL divergence is

$$\text{KL}(Q\|P) = \frac{1}{2}\sum_i \left(\frac{\theta_i^2}{\sigma_p^2} + \frac{\sigma_{q,i}^2}{\sigma_p^2} - 1 - \log\frac{\sigma_{q,i}^2}{\sigma_p^2} \right), \qquad \sigma_p^2 = \sigma_{\text{prior}}^2. \tag{33}$$

Using a McAllester-style bound, we report

$$\text{pac.bayes.magflat} = \hat{R}_G + \sqrt{\frac{\mathrm{KL}(Q\|P) + \log\left(\frac{2\sqrt{n}}{\delta}\right)}{2n}}, \tag{34}$$

where n is the sample count used for the bound and δ is the confidence parameter. We computed this measure in our experiment to see the uncertainty and scale-aware bound, which is intended to remain informative across model families and evaluation regimes (Dziugaite & Roy, 2017; Jiang et al., 2020; Dziugaite et al., 2020).

`pac.bayes.bound`, `pac.bayes.magnitude`, and `pac.bayes.magnitude.init`. These measures use the same PAC-Bayes template as `pac.bayes.magflat`, but differ in how the posterior perturbation scale is parameterized. `pac.bayes.bound` uses the base stochastic-perturbation bound, `pac.bayes.magnitude` incorporates the learned parameter magnitude, and `pac.bayes.magnitude.init` incorporates distance from initialization. They are grouped with Sharpness-based measures because they evaluate sensitivity of the learned solution under stochastic perturbations and convert that sensitivity into a bound-like scalar.

`flatness.proxy`. We estimate the diagonal of the empirical Fisher for each parameter coordinate i using per-batch gradients:

$$F_i \approx \frac{1}{B}\sum_{b=1}^{B}\left(\frac{\partial L_b}{\partial w_i}\right)^2. \tag{35}$$

With prior precision λ (a fixed hyperparameter), define

$$\pi_i = F_i + \lambda. \tag{36}$$

We aggregate across coordinates using a configured statistic (mean/median/harmonic mean):

$$\text{flatness.proxy} = \mathrm{agg}_i(\pi_i). \tag{37}$$

We computed this measure to create a lightweight precision proxy that approximates local sensitivity without explicit Hessian computation, consistent with flatness/curvature-focused generalization analyses (Keskar et al., 2017; Cha et al., 2021; Jiang et al., 2020).

`hessian.top.eigenvalue`. Using a single-batch loss $L(\theta)$, we estimate the largest Hessian eigenvalue via power iteration with Hessian–vector products:

$$v_{t+1} = \frac{Hv_t}{\|Hv_t\|_2}, \tag{38}$$

and report the Rayleigh quotient

$$\lambda_{\max} \approx v^\top H v. \tag{39}$$

We computed this measure to create a direct curvature indicator capturing the dominant local curvature direction, aligning with curvature-based accounts of sharp/flat minima (Keskar et al., 2017; He et al., 2019; Jiang et al., 2020).

`hessian.trace`. We estimate the Hessian trace using the Hutchinson estimator with Rademacher vectors v_s:

$$\mathrm{tr}(H) \approx \frac{1}{S}\sum_{s=1}^{S} v_s^\top H v_s. \tag{40}$$

We computed this measure to create a scalar summary of total curvature that complements $\lambda_{\max}$ and is commonly used in curvature/flatness studies of generalization (Keskar et al., 2017; He et al., 2019; Jiang et al., 2020).

A.4 Optimization-based Measures

`gradient.noise.var` and `gradient.noise.final.var`. These measures estimate the variance of stochastic gradients across minibatches. `gradient.noise.var` summarizes gradient variability during training or over the configured measurement loader, while `gradient.noise.final.var` measures the same type of variability at the final trained solution. They are included as optimization-dynamics proxies because high gradient variability can reflect instability or sensitivity of the learned solution.

`gradient.noise.scale`. Let g_b be the per-batch gradient vector and let d denote the number of gradient coordinates. Gradient noise and batch-size effects are central to several empirical accounts of optimization dynamics and generalization (Shallue et al., 2019; Zhang et al., 2019). For each coordinate i,

$$\bar{g}_i = \frac{1}{B}\sum_{b=1}^{B} g_{b,i}, \qquad \mathrm{Var}_i = \frac{1}{B}\sum_{b=1}^{B}(g_{b,i} - \bar{g}_i)^2. \tag{41}$$

We compute the noise scale

$$\text{gradient.noise.scale} = \frac{1}{d}\sum_{i=1}^{d} \frac{\mathrm{Var}_i}{\bar{g}_i^2 + \epsilon}. \tag{42}$$

We computed this measure for our experiments to create a training-dynamics stability statistic that summarizes gradient stochasticity as a candidate predictor of generalization behavior (Zhang et al., 2019; Shallue et al., 2019; Keskar et al., 2017).

`gradient.norm`. For each batch, compute the gradient of the mean loss and its global norm

$$\|g\|_2 = \left(\sum_p \|g_p\|_2^2\right)^{1/2} \qquad (\text{or } \|g\|_1,\ \|g\|_\infty \text{ if configured}), \tag{43}$$

then aggregate across batches using a configured statistic (mean/max/std/median):

$$\text{gradient.norm} = \mathrm{agg}_b\big(\|g^{(b)}\|\big). \tag{44}$$

We computed this measure to create a compact summary of the gradient scale over evaluation batches, which was used to relate optimization sensitivity to IID/OOD generalization gaps (Jiang et al., 2020; Zhang et al., 2019; Dziugaite et al., 2020).

`input.gradient.norm`. This measure computes the norm of the loss gradient with respect to the input, $\|\nabla_x L(x, y; \theta)\|$, and aggregates it across batches. It is included as a sensitivity measure: larger input gradients indicate that small input perturbations can change the loss more strongly, which is directly relevant when comparing IID behavior with corruption- or perturbation-based shifted targets.

A.5 Information Criteria

`aic.bias.term`. The Akaike Information Criterion (AIC) (Akaike, 1974) is derived from maximum likelihood estimation under standard regularity conditions. It is defined as:

$$\mathrm{AIC} = 2\,\mathrm{NLL}(\hat{\theta}) + 2k, \tag{45}$$

where $\mathrm{NLL}(\hat{\theta}) = -\log L(\hat{\theta})$ is the negative log-likelihood evaluated at the MLE and k is the number of parameters. In our implementation, NLL is computed as the sum over all samples. The AIC bias term quantifies model complexity to mitigate overfitting and is given by $2k$. We take k to be the total number of trainable parameters. Optionally, when the sample size N is small relative to k, we use the finite-sample correction (AICc), in which case the bias term becomes

$$2k + \frac{2k(k+1)}{N-k-1}, \tag{46}$$

valid when $N > k + 1$.

`tic.bias.term`. The Takeuchi Information Criterion (TIC) (Takeuchi, 1976; Naganuma et al., 2022) generalizes AIC by relaxing the realizability assumption. It remains valid under model misspecification (i.e., when the true distribution is not contained in the model family), provided standard regularity conditions hold. It is defined as

$$\mathrm{TIC} = \mathrm{NLL}_{\mathrm{mean}}(\theta) + \mathrm{Tr}\big(I(\theta)^{-1}J(\theta)\big)\,, \tag{47}$$

where $I(\theta)$ is the Fisher information based on the Hessian of the mean NLL, and $J(\theta)$ is the empirical Fisher based on per-sample scores. When the model is correctly specified, $J \approx I$ and the trace term reduces to the parameter count.

The TIC bias term is $\mathrm{Tr}(I(\theta)^{-1}J(\theta))$. Since forming and inverting the full Fisher information matrix is infeasible at scale, we approximate the trace via a diagonal sandwich approximation:

$$\mathrm{bias}_{\mathrm{TIC}} = \sum_j \frac{\mathrm{diag}(J)_j}{\mathrm{diag}(I)_j + \epsilon}, \tag{48}$$

where $\mathrm{diag}(I)$ and $\mathrm{diag}(J)$ denote the diagonals of (respectively) the Hessian of the mean NLL (estimated via Hutchinson's method) and the empirical Fisher (estimated from per-sample gradients).

For completeness, the same diagonal approximation also admits a deterministic upper bound using the inequality $\sum_j \frac{b_j}{a_j} \le \frac{\sum_j b_j}{\min_j a_j}$ for positive vectors a, b:

$$\mathrm{bias}_{\mathrm{TIC}}^{\mathrm{bound}} = \frac{\sum_j \mathrm{diag}(J)_j}{\max(\min_j \mathrm{diag}(I)_j,\, \epsilon)}. \tag{49}$$

This bound is not reported as a separate measure in Table 2; the reported Information Criteria entry is `tic.bias.term`.

`waic.bias.term`. The Widely Applicable Information Criterion (WAIC) (Watanabe & Opper, 2010) is Bayesian and grounded in singular learning theory. Unlike AIC and TIC, WAIC remains valid for singular models (e.g., neural networks and mixture models) where regularity conditions fail, and it does not require realizability. WAIC is computed from the posterior predictive distribution as

$$\mathrm{WAIC} = -2\,\mathrm{LPPD} + 2k_{\mathrm{WAIC}}, \tag{50}$$

where LPPD is the log pointwise predictive density and k_{WAIC} is the effective number of parameters, typically estimated via the variance of the log-likelihood under the posterior. In our runs, posterior samples are generated by MC Dropout when the dropout probability is greater than 0; when it is 0, we use weight noise.

The WAIC bias term is twice the effective number of parameters and is computed as

$$\mathrm{bias}_{\mathrm{WAIC}} = 2\sum_{n=1}^{N} \mathrm{Var}_{\theta\sim p(\theta|D)}\big[\ln p(x_n \mid \theta)\big], \tag{51}$$

where N is the number of samples and the variance is taken over posterior samples of θ.

A.6 Calibration & Confidence Measures

`ece`. Expected Calibration Error (ECE) (Naeini et al., 2015) partitions model predictions into equally spaced confidence bins. It calculates the absolute difference between the average confidence and the accuracy within each bin, taking a weighted average based on the number of samples in each bin. Let y denote the ground-truth label and $\tilde{p}$ denote the predicted probability for a given sample, with $\tilde{y}$ representing the final predicted class. Let N be the total number of samples in the dataset used to calculate ECE, and let B_m be the set of samples falling into the m-th confidence bin. Then, ECE is calculated as follows:

$$\mathrm{ECE} = \sum_{m=1}^{M} \frac{|B_m|}{N} |Acc(B_m) - Conf(B_m)| \tag{52}$$

$Acc(B_m)$ and $Conf(B_m)$ are defined as follows

$$Acc(B_m) = \frac{1}{|B_m|} \sum_{b \in B_m} \mathbf{1}\left(\tilde{y}_b = y_b\right), \; Conf(B_m) = \frac{1}{|B_m|} \sum_{b \in B_m} \tilde{p}_b$$

`reliability diagram.` In contrast to ECE, which computes a sample-weighted average across bins, the reliability-diagram score used here calculates an unweighted average of bin-wise calibration gaps.

$$\text{Reliability Diagram} = \frac{1}{M} \sum_{m=1}^{M} |Acc(B_m) - Conf(B_m)| \tag{53}$$

`mce.` Maximum Calibration Error (MCE) represents the maximum discrepancy between accuracy and confidence across all bins. Formally:

$$\text{MCE} = \max_m |Acc(B_m) - Conf(B_m)| \tag{54}$$

`ace.` It has been pointed out that predictions from recent large-scale models tend to be concentrated in high-confidence ranges (Nixon et al., 2019). Consequently, the equally spaced binning used in ECE results in low-confidence bins containing almost no samples due to this skew. To address this, Adaptive Calibration Error (ACE) (Nixon et al., 2019) dynamically handles confidence bias by partitioning bins to contain an equal number of samples, rather than using equal intervals. Let K be the number of classes. For each class k, the prediction confidences are sorted and partitioned into M subsets of equal size. Let $B_{m,k}$ denote the m-th bin for class k.

$$\text{ACE} = \frac{1}{KM} \sum_{k=1}^{K} \sum_{m=1}^{M} |Acc(B_{m,k}) - Conf(B_{m,k})| \tag{55}$$

`temperature.scaling.` We calculate the ECE after calibrating the model's predicted distribution using Temperature Scaling (Guo et al., 2017). Specifically, Temperature Scaling involves dividing the model's output logits z by a scalar constant T. In this study, we determined the optimal T by minimizing the cross-entropy loss on the training data using the L-BFGS optimizer, and subsequently computed the ECE.

B Experimental Setup Details

All experiments were conducted on a single NVIDIA H100 GPU.

B.1 CIFAR-10

Details of the training hyperparameter sweep ranges are provided in Tables 3 and 4. Each primary CIFAR-10-suite run is trained for 100 epochs, consistent with the protocol described in Section 3. We specified different ranges for the learning rate, as the optimal values vary depending on the optimizer. CIFAR-10-C corruption severity is an evaluation setting rather than a training hyperparameter; for SimpleCNN, we evaluated severity levels 1–5. Additionally, we provided a separate table for NiN, as it is the only architecture that includes width and depth as hyperparameters.

Table 3: Hyperparameter search space for SimpleCNN and ResNetV2-32 on CIFAR-10.

Hyperparameter	SGD	RMSProp & Adam
Learning rate	$\{3.2 \times 10^{-1}, 1 \times 10^{-1}, 3.2 \times 10^{-2}, 1 \times 10^{-2}, 3.2 \times 10^{-3}\}$	$\{3.2 \times 10^{-3}, 1 \times 10^{-3}, 3.2 \times 10^{-4}, 1 \times 10^{-4}, 3.2 \times 10^{-5}\}$
Batch size	$\{32, 64, 128, 256\}$	
Dropout	$\{0, 0.5\}$	
Weight decay	$\{0, 1, 5 \times 10^{-4}\}$	
Random seed	$\{0, 1, 2, 3, 4\}$	

Table 4: Hyperparameter search space for NiN on CIFAR-10.

Hyperparameter	SGD	RMSProp & Adam
Learning rate	$\{1 \times 10^{-1}, 3.2 \times 10^{-2}, 1 \times 10^{-2}\}$	$\{1 \times 10^{-3}, 3.2 \times 10^{-4}, 1 \times 10^{-4}\}$
Batch size	$\{32, 64, 128\}$	
Dropout	$\{0, 0.5\}$	
Depth	$\{2, 8\}$	
Width	$\{2, 8\}$	
Weight decay	$\{0, 5 \times 10^{-4}\}$	
Random seed	$\{0, 1, 2, 3, 4\}$	

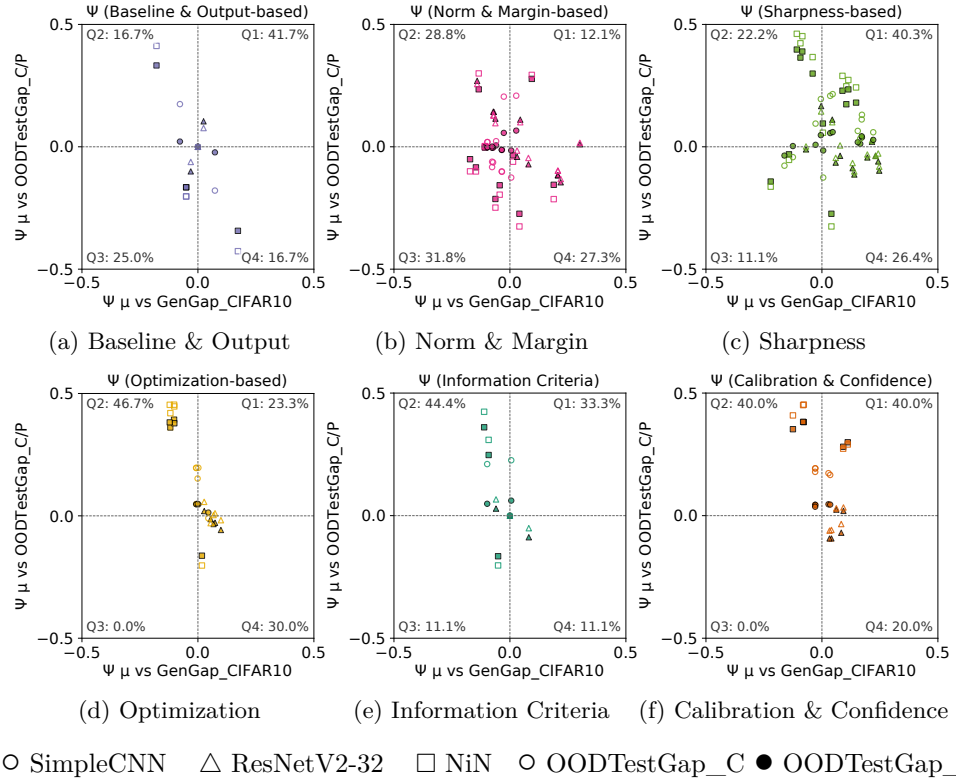

(a) Baseline & Output (b) Norm & Margin (c) Sharpness

(d) Optimization (e) Information Criteria (f) Calibration & Confidence

○ SimpleCNN △ ResNetV2-32 □ NiN ○ OODTestGap_C ● OODTestGap_P

Figure 3: CIFAR-10 suite clean-to-shifted degradation robustness check. Each panel compares IID generalization-gap sensitivity against the degradation from clean CIFAR-10 test accuracy to CIFAR-10-C/P test accuracy. The quadrant annotations show that the main CIFAR-10-C/P pattern from Figure 1 is attenuated but still visible for several Optimization-based measures, Information Criteria, and Calibration & Confidence measures.

C Additional Results

C.1 CIFAR-10 Suite: Test-Set Shifted Gap Analysis

Figure 3 reports the clean-to-shifted degradation scatter analysis used as a robustness check for the main train-to-shifted-test analysis in Figure 1. This target removes the training-accuracy term by comparing clean CIFAR-10 test performance directly against CIFAR-10-C/P test performance. The tables below provide the corresponding measure-level summaries for both train-to-shifted-test gaps and clean-to-shifted degradation targets.

C.2 CIFAR-10 Suite: Granulated-Score Uncertainty

Table 5 reports a descriptive uncertainty audit behind the family-level Ψ scatter plots in Figure 1. For each architecture and measure family, Ψ is the unweighted family mean of the measure-level "ALL" granulated scores. We report percentile bootstrap 95% intervals using measure-level resampling and subspace-level resampling within each selected measure, together with the valid-subspace count used in each family aggregate. These intervals should be interpreted as descriptive stability summaries rather than formal inferential confidence intervals, because different subspaces can share underlying trained runs and hyperparameter configurations and therefore are not guaranteed to be independent samples. The measure families and exclusions match the scatter-plot construction: raw `aic`, `tic`, and `waic` are omitted, while their bias-term variants are retained.

Table 5: Family-level granulated score Ψ with descriptive bootstrap 95% intervals and valid-subspace counts on the CIFAR-10 suite. The intervals summarize stability under measure- and subspace-level resampling, but should not be interpreted as formal inferential confidence intervals because subspaces may share trained runs and hyperparameter configurations. Valid subspaces are reported as total count across measures, followed by median per measure and range in parentheses.

Model	Family	# Measures	Valid subspaces	IID Ψ [95% boot.]	OOD-C Ψ [95% boot.]	OOD-P Ψ [95% boot.]
SimpleCNN	Information Criteria	3	1746 (582; 582–582)	-0.031 [-0.094, 0.013]	0.026 [0.000, 0.056]	0.082 [0.000, 0.173]
SimpleCNN	Calibration & Confidence	5	2910 (582; 582–582)	-0.005 [-0.034, 0.026]	0.044 [0.030, 0.059]	0.153 [0.120, 0.186]
SimpleCNN	Baseline & Output-based	4	2328 (582; 582–582)	-0.001 [-0.056, 0.052]	-0.000 [-0.006, 0.005]	-0.001 [-0.054, 0.052]
SimpleCNN	Norm & Margin-based	11	6402 (582; 582–582)	-0.049 [-0.074, -0.024]	0.002 [-0.013, 0.020]	-0.022 [-0.065, 0.033]
SimpleCNN	Sharpness-based	12	6984 (582; 582–582)	0.054 [-0.012, 0.119]	0.034 [0.006, 0.058]	0.110 [0.024, 0.187]
SimpleCNN	Optimization-based	5	2910 (582; 582–582)	0.006 [-0.016, 0.030]	0.043 [0.032, 0.052]	0.121 [0.058, 0.163]
ResNetV2-32	Information Criteria	3	1746 (582; 582–582)	0.007 [-0.060, 0.078]	0.062 [0.000, 0.112]	0.103 [0.000, 0.172]
ResNetV2-32	Calibration & Confidence	5	2910 (582; 582–582)	0.062 [0.033, 0.091]	0.092 [0.043, 0.139]	0.135 [0.092, 0.174]
ResNetV2-32	Baseline & Output-based	4	2328 (582; 582–582)	-0.002 [-0.031, 0.026]	0.001 [-0.024, 0.026]	0.002 [-0.023, 0.030]
ResNetV2-32	Norm & Margin-based	11	5863 (582; 43–582)	0.068 [-0.013, 0.155]	0.034 [-0.004, 0.073]	0.035 [-0.008, 0.075]
ResNetV2-32	Sharpness-based	12	6982 (582; 581–582)	0.126 [0.068, 0.180]	0.101 [0.056, 0.143]	0.142 [0.086, 0.194]
ResNetV2-32	Optimization-based	5	2910 (582; 582–582)	0.064 [0.035, 0.094]	0.108 [0.050, 0.151]	0.151 [0.070, 0.204]
NiN	Information Criteria	3	3888 (1296; 1296–1296)	-0.085 [-0.123, -0.049]	0.133 [-0.171, 0.325]	0.136 [-0.208, 0.352]
NiN	Calibration & Confidence	5	6480 (1296; 1296–1296)	-0.016 [-0.099, 0.072]	0.355 [0.317, 0.392]	0.362 [0.323, 0.395]
NiN	Baseline & Output-based	4	5184 (1296; 1296–1296)	-0.027 [-0.143, 0.110]	-0.091 [-0.240, 0.143]	-0.108 [-0.273, 0.156]
NiN	Norm & Margin-based	11	13678 (1296; 718–1296)	-0.040 [-0.103, 0.025]	-0.051 [-0.149, 0.076]	-0.058 [-0.163, 0.074]
NiN	Sharpness-based	12	15552 (1296; 1296–1296)	-0.016 [-0.081, 0.048]	0.172 [0.041, 0.290]	0.192 [0.035, 0.332]
NiN	Optimization-based	5	6480 (1296; 1296–1296)	-0.086 [-0.128, -0.032]	0.237 [0.049, 0.343]	0.256 [0.047, 0.375]

C.3 CIFAR-10 Suite: Measure-Level Ψ Summaries

Table 6: Average summary of IID correlations and OODGenGap_C OOD sensitivities across input directories.

Measure	lr^{IID}	lr^{OOD}	wd^{IID}	wd^{OOD}	τ^{IID}	τ^{OOD}	Ψ^{IID}	Ψ^{OOD}
spec.prod	-0.1743	-0.1827	0.2927	-0.1783	-0.1413	-0.2420	-0.0598	-0.0772
frobenius.distance	-0.3710	-0.1168	0.1300	-0.0169	-0.3393	-0.2375	-0.1300	0.0013
spec.sum	-0.2089	-0.1573	0.2964	-0.1832	-0.1339	-0.2087	-0.0565	-0.0793
vcdim	0.0005	0.0005	0.0006	0.0006	-0.0337	-0.1573	-0.0168	-0.0593
pac.bayes.bound	-0.2112	-0.1689	0.1902	-0.2437	-0.0789	-0.1410	-0.1503	-0.1379
pac.bayes.magnitude	-0.1135	-0.0988	0.2947	-0.1817	-0.0402	-0.1212	0.0303	-0.0405
magnitude	-0.1135	-0.0988	0.2947	-0.1817	-0.0402	-0.1212	0.0303	-0.0405
negative.entropy	-0.1802	-0.1207	0.3254	-0.1216	0.0503	-0.1092	0.0900	-0.0795
spectral.norm.per.layer	-0.2090	-0.1575	0.2930	-0.1824	-0.1111	-0.1085	-0.0301	-0.0250
pac.bayes.magnitude.init	-0.3319	-0.0998	0.2730	-0.1568	-0.2925	-0.0952	-0.0415	0.0355
aic.bias.term	0.0000	0.0000	0.0000	0.0000	-0.0044	-0.0755	-0.0170	-0.0595
params	0.0000	0.0000	0.0000	0.0000	-0.0044	-0.0755	-0.0170	-0.0595
l1.over.margin.p10	0.0776	-0.0323	0.3251	-0.1762	-0.0012	-0.0434	0.0043	-0.0706
gradient.noise.scale	0.1085	0.0550	0.1000	-0.0587	0.0838	-0.0328	0.0389	-0.0379
l2.over.margin.p10	0.0359	0.0059	0.2949	-0.1633	-0.0708	-0.0083	0.0007	-0.0270
margin.normalized.param.norm	0.0359	0.0059	0.2949	-0.1633	-0.0708	-0.0083	0.0007	-0.0270
pac.bayes.magflat	0.0182	0.1013	-0.2787	0.1987	0.0243	0.0126	-0.0367	-0.0154
path.norm	0.1671	-0.1081	0.4915	0.1584	0.1126	0.0178	0.1379	-0.0166
cross.entropy	0.1743	0.1173	-0.3214	0.1131	-0.0564	0.1042	-0.0957	0.0769
waic.bias.term	0.2257	0.1462	-0.1596	0.1306	-0.0987	0.1146	-0.0833	0.1259
temperature.scaling	0.2038	0.1681	-0.2368	0.1545	-0.0383	0.1266	-0.0236	0.1487
fisher.rao.norm	0.2175	0.1639	-0.1920	0.1257	0.0135	0.1388	-0.0270	0.1162
ace	0.2562	0.1573	-0.2454	0.1878	-0.0102	0.1434	-0.0254	0.1315
ece	0.2544	0.1595	-0.2429	0.1917	-0.0107	0.1436	-0.0222	0.1352
mce	0.3258	0.2379	-0.0996	0.1805	0.0636	0.1750	0.0709	0.2015
gradient.norm	0.2823	0.1810	-0.2501	0.1911	0.0407	0.1782	-0.0003	0.1661
gradient.noise.var	0.2904	0.1780	-0.2268	0.1809	0.0412	0.1800	-0.0176	0.1676
reliability.diagram	0.3413	0.2287	-0.0953	0.1864	0.0684	0.1842	0.0697	0.2009
flatness.proxy	0.2878	0.1800	-0.2362	0.1810	0.0570	0.1938	-0.0115	0.1738
gradient.noise.final.var	0.2894	0.1779	-0.2279	0.1767	0.0590	0.1956	-0.0142	0.1750
tic.bias.term	0.3198	0.2049	-0.2270	0.1924	0.0805	0.1988	-0.0080	0.1558
input.gradient.norm	0.2565	0.2030	-0.2509	0.1735	0.0437	0.2106	-0.0319	0.1754
hessian.top.eigenvalue	0.3152	0.2282	-0.2313	0.2008	0.1503	0.2448	0.0250	0.1710
hessian.trace	0.3168	0.2334	-0.2448	0.1978	0.1491	0.2460	0.0338	0.1687
inverse.margin.p10	0.3616	0.3138	-0.2205	0.2166	0.1745	0.2600	0.0508	0.1895
sharpness.magnitude	0.3544	0.2580	0.2065	-0.0033	0.2967	0.2744	0.1673	0.1603
sharpness.magnitude.init	0.3376	0.2834	0.1583	0.1036	0.2550	0.2834	0.1530	0.2084
sharpness	0.3301	0.2531	-0.1329	0.2253	0.2527	0.2898	0.1250	0.1899
sharpness.magflat	0.3970	0.2748	0.1354	0.0283	0.3571	0.3310	0.1716	0.1734
adaptive.sharpness	0.3381	0.2824	0.0118	0.1357	0.3488	0.3505	0.1940	0.1429

Table 7: Average summary of IID correlations and OODGenGap_P OOD sensitivities across input directories.

Measure	lr^{IID}	lr^{OOD}	wd^{IID}	wd^{OOD}	τ^{IID}	τ^{OOD}	Ψ^{IID}	Ψ^{OOD}
frobenius.distance	-0.3710	-0.3217	0.1300	-0.0602	-0.3393	-0.3842	-0.1300	-0.0555
spec.prod	-0.1743	-0.3157	0.2927	-0.1869	-0.1413	-0.3338	-0.0598	-0.1156
spec.sum	-0.2089	-0.2918	0.2964	-0.1859	-0.1339	-0.2940	-0.0565	-0.1032
pac.bayes.magnitude.init	-0.3319	-0.3116	0.2730	-0.1690	-0.2925	-0.2422	-0.0415	-0.0227
spectral.norm.per.layer	-0.2090	-0.2920	0.2930	-0.1883	-0.1111	-0.1905	-0.0301	-0.0428
negative.entropy	-0.1802	-0.2559	0.3254	-0.1297	0.0503	-0.1890	0.0900	-0.1327
magnitude	-0.1135	-0.2131	0.2947	-0.1873	-0.0402	-0.1847	0.0303	-0.0720
pac.bayes.magnitude	-0.1135	-0.2131	0.2947	-0.1873	-0.0402	-0.1847	0.0303	-0.0720
vcdim	0.0005	0.0002	0.0006	0.0006	-0.0337	-0.1730	-0.0168	-0.0704
pac.bayes.bound	-0.2112	-0.1858	0.1902	-0.2500	-0.0789	-0.1451	-0.1503	-0.1805
aic.bias.term	0.0000	0.0000	0.0000	0.0000	-0.0044	-0.0919	-0.0170	-0.0706
params	0.0000	0.0000	0.0000	0.0000	-0.0044	-0.0919	-0.0170	-0.0706
path.norm	0.1671	-0.2180	0.4915	0.1049	0.1126	-0.0584	0.1379	-0.0581
gradient.noise.scale	0.1085	0.0848	0.1000	-0.0574	0.0838	-0.0368	0.0389	-0.0532
l1.over.margin.p10	0.0776	0.0216	0.3251	-0.1591	-0.0012	-0.0095	0.0043	-0.0700
l2.over.margin.p10	0.0359	0.0354	0.2949	-0.1278	-0.0708	0.0173	0.0007	-0.0238
margin.normalized.param.norm	0.0359	0.0354	0.2949	-0.1278	-0.0708	0.0173	0.0007	-0.0238
pac.bayes.magflat	0.0182	0.1473	-0.2787	0.1939	0.0243	0.0375	-0.0367	-0.0049
waic.bias.term	0.2257	0.2702	-0.1596	0.1143	-0.0987	0.1600	-0.0833	0.1629
cross.entropy	0.1743	0.2494	-0.3214	0.1227	-0.0564	0.1821	-0.0957	0.1309
temperature.scaling	0.2038	0.2836	-0.2368	0.1621	-0.0383	0.2011	-0.0236	0.1958
mce	0.3258	0.3082	-0.0996	0.1870	0.0636	0.2140	0.0709	0.2499
fisher.rao.norm	0.2175	0.2932	-0.1920	0.1597	0.0135	0.2202	-0.0270	0.1671
ece	0.2544	0.2824	-0.2429	0.2084	-0.0107	0.2228	-0.0222	0.1931
ace	0.2562	0.2817	-0.2454	0.2074	-0.0102	0.2231	-0.0254	0.1901
reliability.diagram	0.3413	0.2983	-0.0953	0.1938	0.0684	0.2271	0.0697	0.2538
inverse.margin.p10	0.3616	0.3923	-0.2205	0.2245	0.1745	0.2779	0.0508	0.2325
gradient.norm	0.2823	0.3624	-0.2501	0.2081	0.0407	0.2800	-0.0003	0.2352
gradient.noise.var	0.2904	0.3602	-0.2268	0.1983	0.0412	0.2801	-0.0176	0.2320
input.gradient.norm	0.2565	0.3554	-0.2509	0.1988	0.0437	0.2957	-0.0319	0.2249
flatness.proxy	0.2878	0.3606	-0.2362	0.1967	0.0570	0.2961	-0.0115	0.2410
gradient.noise.final.var	0.2894	0.3603	-0.2279	0.1967	0.0590	0.2983	-0.0142	0.2413
tic.bias.term	0.3198	0.3885	-0.2270	0.2116	0.0805	0.3053	-0.0080	0.2286
hessian.trace	0.3168	0.4360	-0.2448	0.2091	0.1491	0.3678	0.0338	0.2470
hessian.top.eigenvalue	0.3152	0.4245	-0.2313	0.2086	0.1503	0.3693	0.0250	0.2406
sharpness.magnitude.init	0.3376	0.4064	0.1583	0.1581	0.2550	0.4044	0.1530	0.2918
sharpness.magnitude	0.3544	0.4128	0.2065	0.0448	0.2967	0.4169	0.1673	0.2411
sharpness	0.3301	0.4594	-0.1329	0.2552	0.2527	0.4437	0.1250	0.2919
sharpness.magflat	0.3970	0.4433	0.1354	0.0694	0.3571	0.4836	0.1716	0.2659
adaptive.sharpness	0.3381	0.4759	0.0118	0.1603	0.3488	0.5025	0.1940	0.2367

Table 8: Average summary of IID correlations and OODTestGap_C OOD sensitivities across input directories.

Measure	lr^{IID}	lr^{OOD}	wd^{IID}	wd^{OOD}	τ^{IID}	τ^{OOD}	Ψ^{IID}	Ψ^{OOD}
vcdim	0.0005	0.0008	0.0006	0.0000	-0.0337	-0.1444	-0.0168	-0.0550
pac.bayes.bound	-0.2112	-0.0842	0.1902	-0.2810	-0.0789	-0.1429	-0.1503	-0.0628
pac.bayes.magflat	0.0182	-0.0630	-0.2787	0.3093	0.0243	-0.1250	-0.0367	-0.0291
spec.prod	-0.1743	0.0282	0.2927	-0.2947	-0.1413	-0.0922	-0.0598	-0.0153
l1.over.margin.p10	0.0776	-0.1048	0.3251	-0.2857	-0.0012	-0.0839	0.0043	-0.0745
aic.bias.term	0.0000	0.0000	0.0000	0.0000	-0.0044	-0.0779	-0.0170	-0.0552
params	0.0000	0.0000	0.0000	0.0000	-0.0044	-0.0779	-0.0170	-0.0552
spec.sum	-0.2089	0.0617	0.2964	-0.3020	-0.1339	-0.0640	-0.0565	-0.0274
gradient.noise.scale	0.1085	0.0029	0.1000	-0.1083	0.0838	-0.0624	0.0389	-0.0542
l2.over.margin.p10	0.0359	-0.0891	0.2949	-0.2615	-0.0708	-0.0379	0.0007	-0.0402
margin.normalized.param.norm	0.0359	-0.0891	0.2949	-0.2615	-0.0708	-0.0379	0.0007	-0.0402
pac.bayes.magnitude	-0.1135	0.0660	0.2947	-0.2941	-0.0402	-0.0266	0.0303	-0.0593
magnitude	-0.1135	0.0660	0.2947	-0.2941	-0.0402	-0.0266	0.0303	-0.0593
cross.entropy	0.1743	-0.1410	-0.3214	0.2090	-0.0564	-0.0085	-0.0957	0.0844
negative.entropy	-0.1802	0.1374	0.3254	-0.2210	0.0503	0.0040	0.0900	-0.0873
fisher.rao.norm	0.2175	-0.1048	-0.1920	0.1736	0.0135	0.0074	-0.0270	0.0732
temperature.scaling	0.2038	-0.0976	-0.2368	0.2240	-0.0383	0.0077	-0.0236	0.1064
path.norm	0.1671	-0.1464	0.4915	0.1135	0.1126	0.0135	0.1379	-0.0481
frobenius.distance	-0.3710	0.2114	0.1300	-0.0473	-0.3393	0.0214	-0.1300	0.0715
ace	0.2562	-0.1302	-0.2454	0.2604	-0.0102	0.0237	-0.0254	0.1111
ece	0.2544	-0.1277	-0.2429	0.2613	-0.0107	0.0237	-0.0222	0.1110
spectral.norm.per.layer	-0.2090	0.0611	0.2930	-0.2990	-0.1111	0.0244	-0.0301	0.0315
gradient.norm	0.2823	-0.1269	-0.2501	0.2832	0.0407	0.0338	-0.0003	0.1225
gradient.noise.var	0.2904	-0.1301	-0.2268	0.2610	0.0412	0.0358	-0.0176	0.1269
tic.bias.term	0.3198	-0.1050	-0.2270	0.2739	0.0805	0.0459	-0.0080	0.1112
flatness.proxy	0.2878	-0.1243	-0.2362	0.2645	0.0570	0.0465	-0.0115	0.1361
gradient.noise.final.var	0.2894	-0.1300	-0.2279	0.2613	0.0590	0.0472	-0.0142	0.1359
mce	0.3258	-0.0496	-0.0996	0.1980	0.0636	0.0511	0.0709	0.1156
sharpness.magnitude	0.3544	-0.0620	0.2065	-0.0957	0.2967	0.0538	0.1673	0.0499
reliability.diagram	0.3413	-0.0579	-0.0953	0.2057	0.0684	0.0617	0.0697	0.1230
hessian.trace	0.3168	-0.0860	-0.2448	0.2842	0.1491	0.0639	0.0338	0.1121
hessian.top.eigenvalue	0.3152	-0.0873	-0.2313	0.2774	0.1503	0.0658	0.0250	0.1111
sharpness	0.3301	-0.0812	-0.1329	0.2503	0.2527	0.0662	0.1250	0.0924
sharpness.magflat	0.3970	-0.0606	0.1354	-0.0237	0.3571	0.0750	0.1716	0.0600
waic.bias.term	0.2257	-0.1544	-0.1596	0.1687	-0.0987	0.0797	-0.0833	0.1081
input.gradient.norm	0.2565	-0.0821	-0.2509	0.2535	0.0437	0.0842	-0.0319	0.1503
sharpness.magnitude.init	0.3376	-0.0147	0.1583	0.0047	0.2550	0.0896	0.1530	0.0896
inverse.margin.p10	0.3616	0.0322	-0.2205	0.2615	0.1745	0.0963	0.0508	0.1009
adaptive.sharpness	0.3381	-0.0352	0.0118	0.1691	0.3488	0.1009	0.1940	0.0551
pac.bayes.magnitude.init	-0.3319	0.2310	0.2730	-0.2836	-0.2925	0.1536	-0.0415	0.0882

Table 9: Average summary of IID correlations and OODTestGap_P OOD sensitivities across input directories.

Measure	lr^{IID}	lr^{OOD}	wd^{IID}	wd^{OOD}	τ^{IID}	τ^{OOD}	Ψ^{IID}	Ψ^{OOD}
spec.prod	-0.1743	-0.1036	0.2927	-0.3644	-0.1413	-0.1949	-0.0598	-0.0543
pac.bayes.bound	-0.2112	-0.1146	0.1902	-0.3377	-0.0789	-0.1603	-0.1503	-0.0795
vcdim	0.0005	0.0008	0.0006	0.0000	-0.0337	-0.1599	-0.0168	-0.0675
spec.sum	-0.2089	-0.0693	0.2964	-0.3686	-0.1339	-0.1523	-0.0565	-0.0736
magnitude	-0.1135	-0.0703	0.2947	-0.3637	-0.0402	-0.0940	0.0303	-0.1169
pac.bayes.magnitude	-0.1135	-0.0703	0.2947	-0.3637	-0.0402	-0.0940	0.0303	-0.1169
aic.bias.term	0.0000	0.0000	0.0000	0.0000	-0.0044	-0.0924	-0.0170	-0.0677
params	0.0000	0.0000	0.0000	0.0000	-0.0044	-0.0924	-0.0170	-0.0677
frobenius.distance	-0.3710	0.0771	0.1300	-0.1295	-0.3393	-0.0867	-0.1300	0.0244
pac.bayes.magflat	0.0182	0.0299	-0.2787	0.3739	0.0243	-0.0856	-0.0367	-0.0013
path.norm	0.1671	-0.3101	0.4915	0.0274	0.1126	-0.0807	0.1379	-0.0862
l1.over.margin.p10	0.0776	-0.1182	0.3251	-0.3335	-0.0012	-0.0782	0.0043	-0.0698
gradient.noise.scale	0.1085	0.0290	0.1000	-0.1152	0.0838	-0.0639	0.0389	-0.0808
negative.entropy	-0.1802	0.0116	0.3254	-0.3359	0.0503	-0.0635	0.0900	-0.1763
spectral.norm.per.layer	-0.2090	-0.0701	0.2930	-0.3655	-0.1111	-0.0594	-0.0301	-0.0118
l2.over.margin.p10	0.0359	-0.0976	0.2949	-0.2792	-0.0708	-0.0379	0.0007	-0.0253
margin.normalized.param.norm	0.0359	-0.0976	0.2949	-0.2792	-0.0708	-0.0379	0.0007	-0.0253
pac.bayes.magnitude.init	-0.3319	0.0766	0.2730	-0.3439	-0.2925	0.0478	-0.0415	0.0532
cross.entropy	0.1743	-0.0231	-0.3214	0.3250	-0.0564	0.0558	-0.0957	0.1749
temperature.scaling	0.2038	-0.0075	-0.2368	0.3167	-0.0383	0.0660	-0.0236	0.1844
fisher.rao.norm	0.2175	0.0039	-0.1920	0.2771	0.0135	0.0694	-0.0270	0.1531
mce	0.3258	-0.0217	-0.0996	0.2568	0.0636	0.0729	0.0709	0.1599
reliability.diagram	0.3413	-0.0322	-0.0953	0.2539	0.0684	0.0853	0.0697	0.1621
ece	0.2544	-0.0155	-0.2429	0.3764	-0.0107	0.0899	-0.0222	0.1958
ace	0.2562	-0.0177	-0.2454	0.3722	-0.0102	0.0901	-0.0254	0.1943
waic.bias.term	0.2257	-0.0511	-0.1596	0.2178	-0.0987	0.1214	-0.0833	0.1952
gradient.noise.var	0.2904	0.0195	-0.2268	0.3456	0.0412	0.1215	-0.0176	0.2088
gradient.norm	0.2823	0.0269	-0.2501	0.3775	0.0407	0.1217	-0.0003	0.2086
tic.bias.term	0.3198	0.0472	-0.2270	0.3607	0.0805	0.1335	-0.0080	0.1995
flatness.proxy	0.2878	0.0256	-0.2362	0.3496	0.0570	0.1348	-0.0115	0.2208
gradient.noise.final.var	0.2894	0.0200	-0.2279	0.3435	0.0590	0.1352	-0.0142	0.2176
inverse.margin.p10	0.3616	0.1211	-0.2205	0.3502	0.1745	0.1414	0.0508	0.1622
input.gradient.norm	0.2565	0.0518	-0.2509	0.3676	0.0437	0.1587	-0.0319	0.2211
sharpness.magnitude	0.3544	0.0546	0.2065	-0.0945	0.2967	0.1648	0.1673	0.0811
hessian.trace	0.3168	0.0816	-0.2448	0.3633	0.1491	0.1694	0.0338	0.1888
hessian.top.eigenvalue	0.3152	0.0836	-0.2313	0.3516	0.1503	0.1746	0.0250	0.1883
sharpness.magflat	0.3970	0.0563	0.1354	-0.0300	0.3571	0.1917	0.1716	0.1076
sharpness.magnitude.init	0.3376	0.0703	0.1583	0.0188	0.2550	0.1918	0.1530	0.1271
sharpness	0.3301	0.0915	-0.1329	0.3274	0.2527	0.2003	0.1250	0.1566
adaptive.sharpness	0.3381	0.1214	0.0118	0.2032	0.3488	0.2258	0.1940	0.0837

Table 10: nin summary of IID correlations and OODGenGap_C OOD sensitivities for each measure.

Measure	lr^{IID}	lr^{OOD}	wd^{IID}	wd^{OOD}	τ^{IID}	τ^{OOD}	Ψ^{IID}	Ψ^{OOD}
vcdim	0.0014	0.0014	0.0019	0.0019	-0.1010	-0.4718	-0.0503	-0.1780
frobenius.distance	-0.0917	-0.2671	0.0704	0.0111	-0.1200	-0.4046	-0.1719	-0.1150
spec.sum	0.0963	-0.2699	0.2778	-0.3148	-0.0134	-0.3476	-0.0625	-0.2117
spec.prod	0.1185	-0.2532	0.2741	-0.2963	-0.0179	-0.3453	-0.0441	-0.1719
pac.bayes.bound	-0.2269	-0.3542	0.1796	-0.3852	-0.0957	-0.2616	-0.2208	-0.2615
gradient.noise.scale	0.0898	0.0125	0.1259	-0.1389	0.0245	-0.2422	0.0172	-0.1308
aic.bias.term	0.0000	0.0000	0.0000	0.0000	-0.0133	-0.2265	-0.0510	-0.1785
params	0.0000	0.0000	0.0000	0.0000	-0.0133	-0.2265	-0.0510	-0.1785
pac.bayes.magflat	-0.1213	0.2051	-0.2889	0.3241	-0.0509	-0.2066	-0.1421	-0.1162
magnitude	0.1389	-0.2097	0.2981	-0.3148	0.0665	-0.2047	0.0409	-0.1990
pac.bayes.magnitude	0.1389	-0.2097	0.2981	-0.3148	0.0665	-0.2047	0.0409	-0.1990
l1.over.margin.p10	0.0500	-0.1551	0.3463	-0.2796	-0.3049	-0.1943	-0.1466	-0.1817
negative.entropy	0.0824	-0.1218	0.3444	-0.1500	0.3927	-0.1371	0.1724	-0.2641
l2.over.margin.p10	0.1130	-0.0995	0.3352	-0.2870	-0.3264	-0.0809	-0.1077	-0.0795
margin.normalized.param.norm	0.1130	-0.0995	0.3352	-0.2870	-0.3264	-0.0809	-0.1077	-0.0795
spectral.norm.per.layer	0.0954	-0.2708	0.2722	-0.3056	0.0546	-0.0471	0.0133	-0.0507
pac.bayes.magnitude.init	-0.0120	-0.2338	0.2667	-0.3000	-0.0161	0.0066	0.0041	0.0482
fisher.rao.norm	-0.0657	0.1218	-0.1759	0.1500	-0.3872	0.0650	-0.1345	0.2130
waic.bias.term	0.0398	0.1644	-0.0907	0.1704	-0.4471	0.1091	-0.0918	0.2527
cross.entropy	-0.0713	0.1181	-0.3370	0.1556	-0.4115	0.1241	-0.1786	0.2556
temperature.scaling	0.0412	0.2389	-0.2352	0.2204	-0.3946	0.1460	-0.1250	0.3033
path.norm	0.2694	-0.2049	0.2611	-0.4963	0.1767	0.1518	0.1889	-0.1252
gradient.noise.var	0.0380	0.2347	-0.1981	0.2852	-0.3597	0.1651	-0.1189	0.3163
tic.bias.term	0.0389	0.2505	-0.1981	0.3000	-0.3530	0.1679	-0.1111	0.3254
ece	0.1037	0.1884	-0.2083	0.2787	-0.3472	0.1698	-0.0782	0.3380
ace	0.1106	0.1833	-0.2148	0.2759	-0.3430	0.1710	-0.0811	0.3343
gradient.norm	0.0176	0.2477	-0.2222	0.2963	-0.3498	0.1717	-0.1019	0.3301
sharpness.magnitude	0.2352	0.2588	0.3106	-0.0218	0.0055	0.1730	0.1052	0.2972
sharpness.magnitude.init	0.2833	0.3042	0.2056	0.1870	-0.0352	0.1734	0.0885	0.3425
mce	0.2968	0.3074	-0.0370	0.3111	-0.1667	0.1909	0.0917	0.3888
input.gradient.norm	-0.0269	0.1699	-0.2556	0.1870	-0.3227	0.2045	-0.1214	0.3227
flatness.proxy	0.0296	0.2394	-0.2222	0.2944	-0.3110	0.2067	-0.1083	0.3417
gradient.noise.final.var	0.0352	0.2338	-0.1981	0.2852	-0.3060	0.2119	-0.1028	0.3445
reliability.diagram	0.3370	0.2894	-0.0278	0.3167	-0.1612	0.2230	0.1114	0.4098
hessian.top.eigenvalue	0.0287	0.3088	-0.2167	0.2981	-0.2270	0.2348	-0.0927	0.3356
inverse.margin.p10	0.2269	0.3162	-0.1630	0.3204	0.0791	0.2511	0.0943	0.4359
sharpness	0.0009	0.3366	-0.0500	0.3278	-0.1193	0.2523	-0.0401	0.3062
hessian.trace	0.0204	0.3208	-0.2389	0.3056	-0.2230	0.2591	-0.0843	0.3530
sharpness.magflat	0.2046	0.2412	0.1722	0.0333	0.0594	0.3165	0.1473	0.3105
adaptive.sharpness	-0.0389	0.3208	0.0000	0.1889	0.0758	0.4181	0.1138	0.3042

Table 11: nin summary of IID correlations and OODGenGap_P OOD sensitivities for each measure.

Measure	lr^{IID}	lr^{OOD}	wd^{IID}	wd^{OOD}	τ^{IID}	τ^{OOD}	Ψ^{IID}	Ψ^{OOD}
vcdim	0.0014	0.0005	0.0019	0.0019	-0.1010	-0.5189	-0.0503	-0.2112
frobenius.distance	-0.0917	-0.3417	0.0704	0.0352	-0.1200	-0.4658	-0.1719	-0.1796
spec.prod	0.1185	-0.2296	0.2741	-0.2167	-0.0179	-0.3720	-0.0441	-0.2000
spec.sum	0.0963	-0.2481	0.2778	-0.2241	-0.0134	-0.3700	-0.0625	-0.2301
pac.bayes.bound	-0.2269	-0.2954	0.1796	-0.2981	-0.0957	-0.3125	-0.2208	-0.2949
gradient.noise.scale	0.0898	0.0065	0.1259	-0.1148	0.0245	-0.2785	0.0172	-0.1545
aic.bias.term	0.0000	0.0000	0.0000	0.0000	-0.0133	-0.2758	-0.0510	-0.2118
params	0.0000	0.0000	0.0000	0.0000	-0.0133	-0.2758	-0.0510	-0.2118
pac.bayes.magflat	-0.1213	0.2065	-0.2889	0.2222	-0.0509	-0.2488	-0.1421	-0.1558
magnitude	0.1389	-0.2167	0.2981	-0.2130	0.0665	-0.2273	0.0409	-0.2207
pac.bayes.magnitude	0.1389	-0.2167	0.2981	-0.2130	0.0665	-0.2273	0.0409	-0.2207
l1.over.margin.p10	0.0500	-0.1056	0.3463	-0.1667	-0.3049	-0.2182	-0.1466	-0.1751
negative.entropy	0.0824	-0.1991	0.3444	-0.1000	0.3927	-0.1618	0.1724	-0.2980
l2.over.margin.p10	0.1130	-0.0333	0.3352	-0.1741	-0.3264	-0.0772	-0.1077	-0.0623
margin.normalized.param.norm	0.1130	-0.0333	0.3352	-0.1741	-0.3264	-0.0772	-0.1077	-0.0623
spectral.norm.per.layer	0.0954	-0.2491	0.2722	-0.2185	0.0546	-0.0598	0.0133	-0.0463
pac.bayes.magnitude.init	-0.0120	-0.3213	0.2667	-0.2241	-0.0161	-0.0291	0.0041	0.0106
fisher.rao.norm	-0.0657	0.1935	-0.1759	0.1444	-0.3872	0.0840	-0.1345	0.2260
waic.bias.term	0.0398	0.2398	-0.0907	0.1500	-0.4471	0.1077	-0.0918	0.2606
path.norm	0.2694	-0.1847	0.2611	-0.5111	0.1767	0.1095	0.1889	-0.1365
cross.entropy	-0.0713	0.1991	-0.3370	0.1093	-0.4115	0.1467	-0.1786	0.2881
temperature.scaling	0.0412	0.2903	-0.2352	0.1556	-0.3946	0.1593	-0.1250	0.2960
mce	0.2968	0.2903	-0.0370	0.2481	-0.1667	0.1740	0.0917	0.3723
gradient.noise.var	0.0380	0.3269	-0.1981	0.2278	-0.3597	0.1881	-0.1189	0.3460
ece	0.1037	0.2324	-0.2083	0.2398	-0.3472	0.1912	-0.0782	0.3684
tic.bias.term	0.0389	0.3389	-0.1981	0.2389	-0.3530	0.1926	-0.1111	0.3587
ace	0.1106	0.2301	-0.2148	0.2370	-0.3430	0.1937	-0.0811	0.3662
gradient.norm	0.0176	0.3324	-0.2222	0.2352	-0.3498	0.2004	-0.1019	0.3644
reliability.diagram	0.3370	0.2630	-0.0278	0.2648	-0.1612	0.2118	0.1114	0.4082
input.gradient.norm	-0.0269	0.2417	-0.2556	0.1556	-0.3227	0.2258	-0.1214	0.3451
flatness.proxy	0.0296	0.3259	-0.2222	0.2259	-0.3110	0.2368	-0.1083	0.3722
inverse.margin.p10	0.2269	0.3528	-0.1630	0.2593	0.0791	0.2381	0.0943	0.4540
sharpness.magnitude.init	0.2833	0.3833	0.2056	0.2815	-0.0352	0.2408	0.0885	0.4078
gradient.noise.final.var	0.0352	0.3259	-0.1981	0.2315	-0.3060	0.2424	-0.1028	0.3779
sharpness.magnitude	0.2352	0.3481	0.3106	0.0949	0.0055	0.2450	0.1052	0.3669
hessian.top.eigenvalue	0.0287	0.3917	-0.2167	0.2370	-0.2270	0.2728	-0.0927	0.3608
hessian.trace	0.0204	0.4130	-0.2389	0.2333	-0.2230	0.2961	-0.0843	0.3888
sharpness	0.0009	0.4009	-0.0500	0.3037	-0.1193	0.2994	-0.0401	0.3482
sharpness.magflat	0.2046	0.3269	0.1722	0.0611	0.0594	0.3837	0.1473	0.3669
adaptive.sharpness	-0.0389	0.3630	0.0000	0.1537	0.0758	0.4604	0.1138	0.3523

Table 12: nin summary of IID correlations and OODTestGap_C OOD sensitivities for each measure.

Measure	lr^{IID}	lr^{OOD}	wd^{IID}	wd^{OOD}	τ^{IID}	τ^{OOD}	Ψ^{IID}	Ψ^{OOD}
vcdim	0.0014	0.0023	0.0019	0.0000	-0.1010	-0.4333	-0.0503	-0.1650
frobenius.distance	-0.0917	-0.1023	0.0704	-0.0120	-0.1200	-0.3678	-0.1719	-0.0506
spec.sum	0.0963	-0.2199	0.2778	-0.5546	-0.0134	-0.3274	-0.0625	-0.2132
negative.entropy	0.0824	-0.0699	0.3444	-0.3083	0.3927	-0.3204	0.1724	-0.3433
spec.prod	0.1185	-0.2051	0.2741	-0.5398	-0.0179	-0.3027	-0.0441	-0.1572
gradient.noise.scale	0.0898	-0.0653	0.1259	-0.2231	0.0245	-0.2632	0.0172	-0.1628
aic.bias.term	0.0000	0.0000	0.0000	0.0000	-0.0133	-0.2338	-0.0510	-0.1656
params	0.0000	0.0000	0.0000	0.0000	-0.0133	-0.2338	-0.0510	-0.1656
magnitude	0.1389	-0.1588	0.2981	-0.5380	0.0665	-0.2264	0.0409	-0.2736
pac.bayes.magnitude	0.1389	-0.1588	0.2981	-0.5380	0.0665	-0.2264	0.0409	-0.2736
pac.bayes.bound	-0.2269	-0.1264	0.1796	-0.4713	-0.0957	-0.2021	-0.2208	-0.1417
pac.bayes.magflat	-0.1213	0.1338	-0.2889	0.5546	-0.0509	-0.1973	-0.1421	-0.0308
spectral.norm.per.layer	0.0954	-0.2208	0.2722	-0.5435	0.0546	-0.0622	0.0133	-0.0353
l1.over.margin.p10	0.0500	-0.0940	0.3463	-0.5102	-0.3049	-0.0446	-0.1466	-0.0840
pac.bayes.magnitude.init	-0.0120	-0.0597	0.2667	-0.5472	-0.0161	0.0259	0.0041	0.0952
l2.over.margin.p10	0.1130	-0.1069	0.3352	-0.4954	-0.3264	0.0860	-0.1077	-0.0026
margin.normalized.param.norm	0.1130	-0.1069	0.3352	-0.4954	-0.3264	0.0861	-0.1077	-0.0026
path.norm	0.2694	-0.2764	0.2611	-0.5963	0.1767	0.1426	0.1889	-0.1554
inverse.margin.p10	0.2269	0.0921	-0.1630	0.3565	0.0791	0.1497	0.0943	0.2775
sharpness.magnitude	0.2352	0.0125	0.3106	-0.2523	0.0055	0.2085	0.1052	0.1739
sharpness.magnitude.init	0.2833	0.0255	0.2056	-0.0324	-0.0352	0.2204	0.0885	0.2291
fisher.rao.norm	-0.0657	0.0440	-0.1759	0.2009	-0.3872	0.2438	-0.1345	0.2347
mce	0.2968	0.0500	-0.0370	0.3213	-0.1667	0.2697	0.0917	0.2809
sharpness.magflat	0.2046	0.0171	0.1722	-0.0657	0.0594	0.2868	0.1473	0.1805
sharpness	0.0009	0.1505	-0.0500	0.3546	-0.1193	0.2978	-0.0401	0.2992
reliability.diagram	0.3370	0.0282	-0.0278	0.3389	-0.1612	0.3002	0.1114	0.2994
waic.bias.term	0.0398	-0.0106	-0.0907	0.1676	-0.4471	0.3048	-0.0918	0.2474
cross.entropy	-0.0713	0.0588	-0.3370	0.3028	-0.4115	0.3119	-0.1786	0.3324
temperature.scaling	0.0412	0.1551	-0.2352	0.3537	-0.3946	0.3323	-0.1250	0.3527
gradient.noise.var	0.0380	0.0838	-0.1981	0.4343	-0.3597	0.3357	-0.1189	0.3609
tic.bias.term	0.0389	0.0977	-0.1981	0.4454	-0.3530	0.3369	-0.1111	0.3604
gradient.norm	0.0176	0.1079	-0.2222	0.4620	-0.3498	0.3414	-0.1019	0.3783
ace	0.1106	0.0426	-0.2148	0.4009	-0.3430	0.3419	-0.0811	0.3825
ece	0.1037	0.0477	-0.2083	0.3944	-0.3472	0.3421	-0.0782	0.3817
hessian.top.eigenvalue	0.0287	0.1523	-0.2167	0.4602	-0.2270	0.3528	-0.0927	0.3644
adaptive.sharpness	-0.0389	0.1866	0.0000	0.2954	0.0758	0.3609	0.1138	0.2344
flatness.proxy	0.0296	0.0995	-0.2222	0.4472	-0.3110	0.3669	-0.1083	0.3974
gradient.noise.final.var	0.0352	0.0829	-0.1981	0.4343	-0.3060	0.3691	-0.1028	0.3934
input.gradient.norm	-0.0269	0.0773	-0.2556	0.3083	-0.3227	0.3693	-0.1214	0.3818
hessian.trace	0.0204	0.1569	-0.2389	0.4731	-0.2230	0.3744	-0.0843	0.3894

Table 13: nin summary of IID correlations and OODTestGap_P OOD sensitivities for each measure.

Measure	lr^{IID}	lr^{OOD}	wd^{IID}	wd^{OOD}	τ^{IID}	τ^{OOD}	Ψ^{IID}	Ψ^{OOD}
vcdim	0.0014	0.0023	0.0019	0.0000	-0.1010	-0.4798	-0.0503	-0.2026
frobenius.distance	-0.0917	-0.1352	0.0704	-0.0389	-0.1200	-0.4116	-0.1719	-0.1002
negative.entropy	0.0824	-0.2148	0.3444	-0.3963	0.3927	-0.3563	0.1724	-0.4266
spec.sum	0.0963	-0.2472	0.2778	-0.5130	-0.0134	-0.3556	-0.0625	-0.2485
spec.prod	0.1185	-0.2361	0.2741	-0.5056	-0.0179	-0.3329	-0.0441	-0.1958
gradient.noise.scale	0.0898	-0.0926	0.1259	-0.2259	0.0245	-0.3027	0.0172	-0.2030
aic.bias.term	0.0000	0.0000	0.0000	0.0000	-0.0133	-0.2772	-0.0510	-0.2031
params	0.0000	0.0000	0.0000	0.0000	-0.0133	-0.2772	-0.0510	-0.2031
magnitude	0.1389	-0.2454	0.2981	-0.4981	0.0665	-0.2543	0.0409	-0.3255
pac.bayes.magnitude	0.1389	-0.2454	0.2981	-0.4981	0.0665	-0.2543	0.0409	-0.3255
pac.bayes.bound	-0.2269	-0.0722	0.1796	-0.4315	-0.0957	-0.2428	-0.2208	-0.1629
pac.bayes.magflat	-0.1213	0.2296	-0.2889	0.5111	-0.0509	-0.2325	-0.1421	-0.0533
spectral.norm.per.layer	0.0954	-0.2481	0.2722	-0.5037	0.0546	-0.0768	0.0133	-0.0610
l1.over.margin.p10	0.0500	-0.1250	0.3463	-0.4741	-0.3049	-0.0681	-0.1466	-0.1007
pac.bayes.magnitude.init	-0.0120	-0.1481	0.2667	-0.5167	-0.0161	0.0054	0.0041	0.0574
l2.over.margin.p10	0.1130	-0.0750	0.3352	-0.4593	-0.3264	0.0837	-0.1077	0.0025
margin.normalized.param.norm	0.1130	-0.0750	0.3352	-0.4593	-0.3264	0.0837	-0.1077	0.0025
path.norm	0.2694	-0.3972	0.2611	-0.6185	0.1767	0.1095	0.1889	-0.2139
inverse.margin.p10	0.2269	0.1333	-0.1630	0.3667	0.0791	0.1428	0.0943	0.2937
mce	0.2968	0.0477	-0.0370	0.3167	-0.1667	0.2560	0.0917	0.2732
sharpness.magnitude	0.2352	0.1509	0.3106	-0.1718	0.0055	0.2562	0.1052	0.2471
fisher.rao.norm	-0.0657	0.1815	-0.1759	0.2815	-0.3872	0.2671	-0.1345	0.2998
sharpness.magnitude.init	0.2833	0.1213	0.2056	0.0296	-0.0352	0.2684	0.0885	0.2898
reliability.diagram	0.3370	0.0148	-0.0278	0.3185	-0.1612	0.2894	0.1114	0.2904
waic.bias.term	0.0398	0.1241	-0.0907	0.2389	-0.4471	0.3151	-0.0918	0.3091
sharpness	0.0009	0.2759	-0.0500	0.3704	-0.1193	0.3349	-0.0401	0.3665
cross.entropy	-0.0713	0.2000	-0.3370	0.3907	-0.4115	0.3450	-0.1786	0.4123
sharpness.magflat	0.2046	0.1315	0.1722	-0.0463	0.0594	0.3468	0.1473	0.2426
temperature.scaling	0.0412	0.2431	-0.2352	0.3944	-0.3946	0.3540	-0.1250	0.4089
gradient.noise.var	0.0380	0.2204	-0.1981	0.4500	-0.3597	0.3647	-0.1189	0.4196
tic.bias.term	0.0389	0.2324	-0.1981	0.4611	-0.3530	0.3669	-0.1111	0.4237
ece	0.1037	0.1676	-0.2083	0.4676	-0.3472	0.3741	-0.0782	0.4530
ace	0.1106	0.1616	-0.2148	0.4667	-0.3430	0.3745	-0.0811	0.4510
gradient.norm	0.0176	0.2444	-0.2222	0.4870	-0.3498	0.3749	-0.1019	0.4471
adaptive.sharpness	-0.0389	0.2935	0.0000	0.2907	0.0758	0.3892	0.1138	0.2729
hessian.top.eigenvalue	0.0287	0.2870	-0.2167	0.4519	-0.2270	0.3920	-0.0927	0.4230
input.gradient.norm	-0.0269	0.2185	-0.2556	0.3963	-0.3227	0.4010	-0.1214	0.4537
flatness.proxy	0.0296	0.2361	-0.2222	0.4667	-0.3110	0.4033	-0.1083	0.4617
gradient.noise.final.var	0.0352	0.2194	-0.1981	0.4500	-0.3060	0.4051	-0.1028	0.4542
hessian.trace	0.0204	0.2806	-0.2389	0.4667	-0.2230	0.4157	-0.0843	0.4520

Table 14: resnet summary of IID correlations and OODGenGap_C OOD sensitivities for each measure.

Measure	lr^{IID}	lr^{OOD}	wd^{IID}	wd^{OOD}	τ^{IID}	τ^{OOD}	Ψ^{IID}	Ψ^{OOD}
negative.entropy	-0.4478	-0.2058	0.4039	-0.2017	-0.2661	-0.1924	0.0243	0.0279
spec.prod	-0.3106	-0.1119	0.3717	-0.2128	-0.1297	-0.1648	-0.0626	-0.0476
spec.sum	-0.4039	-0.0197	0.3939	-0.2094	-0.1910	-0.1033	-0.0717	-0.0196
spectral.norm.per.layer	-0.4033	-0.0192	0.3894	-0.2161	-0.1910	-0.1033	-0.0693	-0.0175
frobenius.distance	-0.6822	0.0919	0.1317	-0.0417	-0.5833	-0.0814	-0.1413	0.1229
pac.bayes.magnitude.init	-0.6600	0.0997	0.3650	-0.1506	-0.5285	-0.0791	-0.0034	0.0714
magnitude	-0.2872	0.0325	0.3772	-0.2028	-0.1449	-0.0753	0.0445	0.0777
pac.bayes.magnitude	-0.2872	0.0325	0.3772	-0.2028	-0.1449	-0.0753	0.0445	0.0777
pac.bayes.bound	-0.1217	0.0503	0.2894	-0.2706	0.0364	-0.0108	-0.0685	-0.0818
aic.bias.term	0.0000	0.0000	0.0000	0.0000	0.0000	0.0000	0.0000	0.0000
params	0.0000	0.0000	0.0000	0.0000	0.0000	0.0000	0.0000	0.0000
vcdim	0.0000	0.0000	0.0000	0.0000	0.0000	0.0000	0.0000	0.0000
gradient.noise.scale	0.0622	0.0064	0.1439	-0.0483	0.0814	0.0152	0.0547	-0.0050
l1.over.margin.p10	0.1544	0.0797	0.4339	-0.2228	0.2338	0.0399	0.2190	-0.0224
path.norm	0.4524	0.0048	1.0000	1.0000	0.3136	0.0484	0.3016	0.0829
l2.over.margin.p10	0.1017	0.2169	0.4106	-0.1850	0.1890	0.1230	0.2068	0.0224
margin.normalized.param.norm	0.1017	0.2169	0.4106	-0.1850	0.1890	0.1230	0.2068	0.0224
waic.bias.term	0.5178	0.2219	-0.3672	0.2094	0.1949	0.1651	-0.0599	0.1029
cross.entropy	0.4339	0.2108	-0.3883	0.1739	0.2671	0.1972	-0.0309	-0.0252
ace	0.4511	0.2203	-0.3450	0.2350	0.2817	0.2088	0.0330	0.0279
ece	0.4528	0.2219	-0.3394	0.2439	0.2832	0.2110	0.0410	0.0348
pac.bayes.magflat	0.2456	0.0925	-0.3583	0.2450	0.1907	0.2238	0.0595	0.0775
temperature.scaling	0.4153	0.2428	-0.3017	0.1994	0.2873	0.2281	0.0833	0.1138
gradient.norm	0.5250	0.1819	-0.3383	0.2361	0.3442	0.2489	0.0992	0.1216
reliability.diagram	0.4614	0.3078	-0.1872	0.1928	0.2632	0.2505	0.0621	0.1290
hessian.trace	0.5700	0.1836	-0.3106	0.2383	0.4038	0.2508	0.1396	0.0866
tic.bias.term	0.5533	0.1936	-0.2939	0.2339	0.4025	0.2520	0.0814	0.0846
flatness.proxy	0.5178	0.1903	-0.3039	0.2061	0.3456	0.2596	0.0784	0.1325
gradient.noise.var	0.5189	0.1892	-0.3006	0.2128	0.3468	0.2598	0.0738	0.1396
gradient.noise.final.var	0.5183	0.1897	-0.3039	0.2006	0.3465	0.2598	0.0674	0.1336
mce	0.4667	0.3203	-0.1794	0.1861	0.2659	0.2601	0.0928	0.1530
fisher.rao.norm	0.4694	0.2686	-0.2461	0.1739	0.3490	0.2639	0.0797	0.0893
hessian.top.eigenvalue	0.5611	0.1903	-0.2939	0.2606	0.3966	0.2642	0.1322	0.1171
adaptive.sharpness	0.5928	0.2497	0.0672	0.1872	0.4458	0.2676	0.2471	0.0527
input.gradient.norm	0.4689	0.2947	-0.3217	0.2772	0.3094	0.2846	0.0270	0.1500
sharpness	0.5994	0.2108	-0.2161	0.3017	0.4510	0.3019	0.2428	0.1872
inverse.margin.p10	0.4300	0.3869	-0.3106	0.2683	0.1560	0.3023	0.0310	0.0617
sharpness.magflat	0.5394	0.3958	0.1061	0.0161	0.5047	0.3696	0.1958	0.1301
sharpness.magnitude	0.4435	0.3923	0.1550	0.0106	0.4434	0.3971	0.2316	0.1357
sharpness.magnitude.init	0.3728	0.4425	0.1439	0.1083	0.3885	0.4430	0.2158	0.2283

Table 15: resnet summary of IID correlations and OODGenGap_P OOD sensitivities for each measure.

Measure	lr^{IID}	lr^{OOD}	wd^{IID}	wd^{OOD}	τ^{IID}	τ^{OOD}	Ψ^{IID}	Ψ^{OOD}
negative.entropy	-0.4478	-0.3878	0.4039	-0.1667	-0.2661	-0.3257	0.0243	-0.0233
frobenius.distance	-0.6822	-0.1189	0.1317	-0.0733	-0.5833	-0.2646	-0.1413	0.0732
pac.bayes.magnitude.init	-0.6600	-0.1122	0.3650	-0.1444	-0.5285	-0.2599	-0.0034	0.0266
spec.prod	-0.3106	-0.2250	0.3717	-0.1800	-0.1297	-0.2124	-0.0626	-0.0712
spectral.norm.per.layer	-0.4033	-0.1422	0.3894	-0.1833	-0.1910	-0.1768	-0.0693	-0.0381
spec.sum	-0.4039	-0.1428	0.3939	-0.1722	-0.1910	-0.1768	-0.0717	-0.0364
magnitude	-0.2872	-0.0550	0.3772	-0.1700	-0.1449	-0.1361	0.0445	0.0595
pac.bayes.magnitude	-0.2872	-0.0550	0.3772	-0.1700	-0.1449	-0.1361	0.0445	0.0595
aic.bias.term	0.0000	0.0000	0.0000	0.0000	0.0000	0.0000	0.0000	0.0000
params	0.0000	0.0000	0.0000	0.0000	0.0000	0.0000	0.0000	0.0000
vcdim	0.0000	0.0000	0.0000	0.0000	0.0000	0.0000	0.0000	0.0000
gradient.noise.scale	0.0622	0.0144	0.1439	-0.0444	0.0814	0.0149	0.0547	-0.0054
path.norm	0.4524	-0.0619	1.0000	1.0000	0.3136	0.0402	0.3016	0.0597
pac.bayes.bound	-0.1217	0.1117	0.2894	-0.2133	0.0364	0.0653	-0.0685	-0.0619
l1.over.margin.p10	0.1544	0.2067	0.4339	-0.1611	0.2338	0.1560	0.2190	0.0069
l2.over.margin.p10	0.1017	0.3350	0.4106	-0.1167	0.1890	0.2289	0.2068	0.0538
margin.normalized.param.norm	0.1017	0.3350	0.4106	-0.1167	0.1890	0.2289	0.2068	0.0538
waic.bias.term	0.5178	0.4222	-0.3672	0.1856	0.1949	0.2666	-0.0599	0.1609
inverse.margin.p10	0.4300	0.3911	-0.3106	0.2378	0.1560	0.2672	0.0310	0.0831
pac.bayes.magflat	0.2456	0.1867	-0.3583	0.1989	0.1907	0.2837	0.0595	0.1110
cross.entropy	0.4339	0.3961	-0.3883	0.1522	0.2671	0.3318	-0.0309	0.0322
ace	0.4511	0.4133	-0.3450	0.2111	0.2817	0.3435	0.0330	0.0802
reliability.diagram	0.4614	0.4531	-0.1872	0.1633	0.2632	0.3452	0.0621	0.1568
ece	0.4528	0.4139	-0.3394	0.2178	0.2832	0.3461	0.0410	0.0895
mce	0.4667	0.4622	-0.1794	0.1700	0.2659	0.3517	0.0928	0.1858
temperature.scaling	0.4153	0.4342	-0.3017	0.1856	0.2873	0.3673	0.0833	0.1612
gradient.norm	0.5250	0.3894	-0.3383	0.2300	0.3442	0.3906	0.0992	0.1824
adaptive.sharpness	0.5928	0.4306	0.0672	0.2300	0.4458	0.3914	0.2471	0.1434
flatness.proxy	0.5178	0.3978	-0.3039	0.2067	0.3456	0.4022	0.0784	0.1933
hessian.trace	0.5700	0.3900	-0.3106	0.2256	0.4038	0.4025	0.1396	0.1417
gradient.noise.final.var	0.5183	0.3972	-0.3039	0.1989	0.3465	0.4031	0.0674	0.1903
gradient.noise.var	0.5189	0.3967	-0.3006	0.2089	0.3468	0.4032	0.0738	0.1956
hessian.top.eigenvalue	0.5611	0.3911	-0.2939	0.2322	0.3966	0.4102	0.1322	0.1571
tic.bias.term	0.5533	0.4022	-0.2939	0.2322	0.4025	0.4112	0.0814	0.1487
fisher.rao.norm	0.4694	0.4706	-0.2461	0.1678	0.3490	0.4141	0.0797	0.1402
input.gradient.norm	0.4689	0.4922	-0.3217	0.2644	0.3094	0.4154	0.0270	0.1942
sharpness	0.5994	0.4072	-0.2161	0.2733	0.4510	0.4302	0.2428	0.2555
sharpness.magflat	0.5394	0.5706	0.1061	0.0667	0.5047	0.5096	0.1958	0.1937
sharpness.magnitude	0.4435	0.5398	0.1550	0.0811	0.4434	0.5122	0.2316	0.2033
sharpness.magnitude.init	0.3728	0.5417	0.1439	0.1700	0.3885	0.5189	0.2158	0.2812

Table 16: resnet summary of IID correlations and OODTestGap_C OOD sensitivities for each measure.

Measure	lr^{IID}	lr^{OOD}	wd^{IID}	wd^{OOD}	τ^{IID}	τ^{OOD}	Ψ^{IID}	Ψ^{OOD}
hessian.trace	0.5700	-0.5456	-0.3106	0.3044	0.4038	-0.3619	0.1396	-0.1133
tic.bias.term	0.5533	-0.5211	-0.2939	0.3056	0.4025	-0.3453	0.0814	-0.0881
hessian.top.eigenvalue	0.5611	-0.5356	-0.2939	0.3033	0.3966	-0.3402	0.1322	-0.0873
sharpness	0.5994	-0.5200	-0.2161	0.3300	0.4510	-0.3343	0.2428	-0.0600
adaptive.sharpness	0.5928	-0.4644	0.0672	0.1689	0.4458	-0.3267	0.2471	-0.0974
gradient.norm	0.5250	-0.5406	-0.3383	0.3189	0.3442	-0.3226	0.0992	-0.0577
cross.entropy	0.4339	-0.4628	-0.3883	0.2767	0.2671	-0.3194	-0.0309	-0.1006
gradient.noise.var	0.5189	-0.5211	-0.3006	0.2778	0.3468	-0.3110	0.0738	-0.0283
gradient.noise.final.var	0.5183	-0.5206	-0.3039	0.2789	0.3465	-0.3105	0.0674	-0.0334
flatness.proxy	0.5178	-0.5200	-0.3039	0.2778	0.3456	-0.3104	0.0784	-0.0368
ace	0.4511	-0.4589	-0.3450	0.3044	0.2817	-0.3093	0.0330	-0.0931
ece	0.4528	-0.4561	-0.3394	0.3133	0.2832	-0.3087	0.0410	-0.0930
temperature.scaling	0.4153	-0.4297	-0.3017	0.2506	0.2873	-0.3056	0.0833	-0.0697
fisher.rao.norm	0.4694	-0.4139	-0.2461	0.2456	0.3490	-0.2967	0.0797	-0.0718
sharpness.magflat	0.5394	-0.2933	0.1061	-0.0122	0.5047	-0.2801	0.1958	-0.0437
input.gradient.norm	0.4689	-0.4111	-0.3217	0.3711	0.3094	-0.2357	0.0270	0.0196
sharpness.magnitude	0.4435	-0.2344	0.1550	-0.0156	0.4434	-0.2180	0.2316	-0.0365
l1.over.margin.p10	0.1544	-0.1833	0.4339	-0.2900	0.2338	-0.2174	0.2190	-0.1450
pac.bayes.magflat	0.2456	-0.3422	-0.3583	0.3144	0.1907	-0.2099	0.0595	-0.0646
reliability.diagram	0.4614	-0.2258	-0.1872	0.2233	0.2632	-0.1667	0.0621	0.0246
mce	0.4667	-0.2222	-0.1794	0.2200	0.2659	-0.1654	0.0928	0.0194
waic.bias.term	0.5178	-0.4822	-0.3672	0.3167	0.1949	-0.1609	-0.0599	0.0286
l2.over.margin.p10	0.1017	-0.0794	0.4106	-0.2489	0.1890	-0.1509	0.2068	-0.1162
margin.normalized.param.norm	0.1017	-0.0794	0.4106	-0.2489	0.1890	-0.1509	0.2068	-0.1162
pac.bayes.bound	-0.1217	0.0239	0.2894	-0.2889	0.0364	-0.1092	-0.0685	-0.0107
sharpness.magnitude.init	0.3728	-0.0904	0.1439	0.0522	0.3885	-0.1086	0.2158	0.0209
gradient.noise.scale	0.0622	-0.0394	0.1439	-0.1100	0.0814	-0.0251	0.0547	-0.0133
inverse.margin.p10	0.4300	-0.1394	-0.3106	0.3444	0.1560	-0.0249	0.0310	-0.0409
aic.bias.term	0.0000	0.0000	0.0000	0.0000	0.0000	0.0000	0.0000	0.0000
params	0.0000	0.0000	0.0000	0.0000	0.0000	0.0000	0.0000	0.0000
vcdim	0.0000	0.0000	0.0000	0.0000	0.0000	0.0000	0.0000	0.0000
path.norm	0.4524	-0.0857	1.0000	1.0000	0.3136	0.0079	0.3016	0.0101
spec.prod	-0.3106	0.3950	0.3717	-0.2833	-0.1297	0.1799	-0.0626	0.1149
magnitude	-0.2872	0.4361	0.3772	-0.2822	-0.1449	0.2154	0.0445	0.1109
pac.bayes.magnitude	-0.2872	0.4361	0.3772	-0.2822	-0.1449	0.2154	0.0445	0.1109
spectral.norm.per.layer	-0.4033	0.5133	0.3894	-0.2933	-0.1910	0.2616	-0.0693	0.1426
spec.sum	-0.4039	0.5139	0.3939	-0.2911	-0.1910	0.2616	-0.0717	0.1435
negative.entropy	-0.4478	0.4722	0.4039	-0.3044	-0.2661	0.3207	0.0243	0.1042
pac.bayes.magnitude.init	-0.6600	0.8389	0.3650	-0.2522	-0.5285	0.5757	-0.0034	0.1665
frobenius.distance	-0.6822	0.8322	0.1317	-0.0767	-0.5833	0.5924	-0.1413	0.2695

Table 17: resnet summary of IID correlations and OODTestGap_P OOD sensitivities for each measure.

Measure	lr^{IID}	lr^{OOD}	wd^{IID}	wd^{OOD}	τ^{IID}	τ^{OOD}	Ψ^{IID}	Ψ^{OOD}
hessian.trace	0.5700	-0.4861	-0.3106	0.3211	0.4038	-0.3017	0.1396	-0.1007
adaptive.sharpness	0.5928	-0.4122	0.0672	0.1856	0.4458	-0.2829	0.2471	-0.0812
tic.bias.term	0.5533	-0.4583	-0.2939	0.3211	0.4025	-0.2817	0.0814	-0.0511
hessian.top.eigenvalue	0.5611	-0.4728	-0.2939	0.3300	0.3966	-0.2807	0.1322	-0.0663
sharpness	0.5994	-0.4611	-0.2161	0.3444	0.4510	-0.2804	0.2428	-0.0274
gradient.norm	0.5250	-0.4767	-0.3383	0.3456	0.3442	-0.2612	0.0992	-0.0178
cross.entropy	0.4339	-0.3989	-0.3883	0.3144	0.2671	-0.2575	-0.0309	-0.0619
ace	0.4511	-0.3939	-0.3450	0.3444	0.2817	-0.2492	0.0330	-0.0612
gradient.noise.var	0.5189	-0.4572	-0.3006	0.2956	0.3468	-0.2492	0.0738	0.0104
gradient.noise.final.var	0.5183	-0.4567	-0.3039	0.2878	0.3465	-0.2487	0.0674	0.0032
flatness.proxy	0.5178	-0.4561	-0.3039	0.2933	0.3456	-0.2485	0.0784	0.0056
ece	0.4528	-0.3922	-0.3394	0.3578	0.2832	-0.2481	0.0410	-0.0584
temperature.scaling	0.4153	-0.3653	-0.3017	0.2933	0.2873	-0.2420	0.0833	-0.0343
sharpness.magflat	0.5394	-0.2389	0.1061	-0.0089	0.5047	-0.2302	0.1958	-0.0316
fisher.rao.norm	0.4694	-0.3489	-0.2461	0.2611	0.3490	-0.2297	0.0797	-0.0455
input.gradient.norm	0.4689	-0.3461	-0.3217	0.3956	0.3094	-0.1755	0.0270	0.0571
l1.over.margin.p10	0.1544	-0.1328	0.4339	-0.2678	0.2338	-0.1674	0.2190	-0.1317
pac.bayes.magflat	0.2456	-0.2994	-0.3583	0.3344	0.1907	-0.1618	0.0595	-0.0452
sharpness.magnitude	0.4435	-0.1696	0.1550	-0.0033	0.4434	-0.1600	0.2316	-0.0375
reliability.diagram	0.4614	-0.1864	-0.1872	0.2244	0.2632	-0.1334	0.0621	0.0298
mce	0.4667	-0.1839	-0.1794	0.2367	0.2659	-0.1328	0.0928	0.0334
waic.bias.term	0.5178	-0.4161	-0.3672	0.3367	0.1949	-0.1190	-0.0599	0.0662
l2.over.margin.p10	0.1017	-0.0200	0.4106	-0.2211	0.1890	-0.0955	0.2068	-0.0977
margin.normalized.param.norm	0.1017	-0.0200	0.4106	-0.2211	0.1890	-0.0955	0.2068	-0.0977
pac.bayes.bound	-0.1217	0.0589	0.2894	-0.2911	0.0364	-0.0723	-0.0685	0.0015
sharpness.magnitude.init	0.3728	-0.0467	0.1439	0.0767	0.3885	-0.0623	0.2158	0.0267
gradient.noise.scale	0.0622	-0.0439	0.1439	-0.1111	0.0814	-0.0220	0.0547	-0.0298
path.norm	0.4524	-0.1238	1.0000	1.0000	0.3136	-0.0137	0.3016	0.0163
inverse.margin.p10	0.4300	-0.1039	-0.3106	0.3689	0.1560	-0.0000	0.0310	-0.0158
aic.bias.term	0.0000	0.0000	0.0000	0.0000	0.0000	0.0000	0.0000	0.0000
params	0.0000	0.0000	0.0000	0.0000	0.0000	0.0000	0.0000	0.0000
vcdim	0.0000	0.0000	0.0000	0.0000	0.0000	0.0000	0.0000	0.0000
spec.prod	-0.3106	0.3567	0.3717	-0.2956	-0.1297	0.1457	-0.0626	0.0965
magnitude	-0.2872	0.4144	0.3772	-0.2922	-0.1449	0.1912	0.0445	0.1004
pac.bayes.magnitude	-0.2872	0.4144	0.3772	-0.2922	-0.1449	0.1912	0.0445	0.1004
spectral.norm.per.layer	-0.4033	0.4772	0.3894	-0.3056	-0.1910	0.2278	-0.0693	0.1277
spec.sum	-0.4039	0.4778	0.3939	-0.3056	-0.1910	0.2279	-0.0717	0.1281
negative.entropy	-0.4478	0.4094	0.4039	-0.3289	-0.2661	0.2607	0.0243	0.0766
pac.bayes.magnitude.init	-0.6600	0.7961	0.3650	-0.2689	-0.5285	0.5261	-0.0034	0.1444
frobenius.distance	-0.6822	0.7906	0.1317	-0.0844	-0.5833	0.5409	-0.1413	0.2564

Table 18: simplecnn summary of IID correlations and OODGenGap_C OOD sensitivities for each measure.

Measure	lr^{IID}	lr^{OOD}	wd^{IID}	wd^{OOD}	τ^{IID}	τ^{OOD}	Ψ^{IID}	Ψ^{OOD}
frobenius.distance	-0.3391	-0.1753	0.1880	-0.0200	-0.3146	-0.2264	-0.0768	-0.0040
spec.prod	-0.3307	-0.1828	0.2325	-0.0258	-0.2764	-0.2160	-0.0727	-0.0123
pac.bayes.magnitude.init	-0.3238	-0.1652	0.1872	-0.0198	-0.3330	-0.2132	-0.1252	-0.0130
spec.sum	-0.3191	-0.1823	0.2174	-0.0252	-0.1973	-0.1751	-0.0353	-0.0066
spectral.norm.per.layer	-0.3191	-0.1825	0.2174	-0.0254	-0.1971	-0.1750	-0.0345	-0.0068
pac.bayes.bound	-0.2851	-0.2029	0.1015	-0.0755	-0.1772	-0.1507	-0.1616	-0.0703
path.norm	-0.2206	-0.1242	0.2134	-0.0284	-0.1524	-0.1469	-0.0767	-0.0077
pac.bayes.magnitude	-0.1921	-0.1192	0.2087	-0.0274	-0.0421	-0.0837	0.0055	-0.0003
magnitude	-0.1921	-0.1192	0.2087	-0.0274	-0.0421	-0.0837	0.0055	-0.0003
l2.over.margin.p10	-0.1069	-0.0999	0.1388	-0.0179	-0.0749	-0.0671	-0.0972	-0.0238
margin.normalized.param.norm	-0.1069	-0.0999	0.1388	-0.0179	-0.0749	-0.0671	-0.0972	-0.0238
cross.entropy	0.1602	0.0230	-0.2389	0.0099	-0.0248	-0.0087	-0.0776	0.0004
aic.bias.term	0.0000	0.0000	0.0000	0.0000	0.0000	0.0000	0.0000	0.0000
params	0.0000	0.0000	0.0000	0.0000	0.0000	0.0000	0.0000	0.0000
vcdim	0.0000	0.0000	0.0000	0.0000	0.0000	0.0000	0.0000	0.0000
negative.entropy	-0.1751	-0.0345	0.2278	-0.0130	0.0242	0.0019	0.0733	-0.0024
temperature.scaling	0.1549	0.0226	-0.1735	0.0436	-0.0076	0.0058	-0.0292	0.0291
pac.bayes.magflat	-0.0696	0.0062	-0.1888	0.0270	-0.0670	0.0205	-0.0275	-0.0074
l1.over.margin.p10	0.0284	-0.0214	0.1952	-0.0263	0.0674	0.0241	-0.0595	-0.0076
ece	0.2068	0.0681	-0.1810	0.0525	0.0320	0.0499	-0.0292	0.0329
ace	0.2070	0.0684	-0.1763	0.0523	0.0308	0.0505	-0.0283	0.0325
waic.bias.term	0.1196	0.0522	-0.0208	0.0120	-0.0439	0.0697	-0.0981	0.0221
mce	0.2139	0.0859	-0.0822	0.0444	0.0916	0.0739	0.0282	0.0627
reliability.diagram	0.2253	0.0890	-0.0710	0.0499	0.1032	0.0792	0.0356	0.0640
fisher.rao.norm	0.2487	0.1013	-0.1541	0.0533	0.0786	0.0874	-0.0263	0.0464
gradient.norm	0.3044	0.1135	-0.1897	0.0409	0.1276	0.1140	0.0018	0.0466
gradient.noise.var	0.3143	0.1100	-0.1818	0.0448	0.1365	0.1150	-0.0078	0.0470
gradient.noise.final.var	0.3145	0.1101	-0.1818	0.0444	0.1364	0.1150	-0.0071	0.0469
flatness.proxy	0.3159	0.1103	-0.1826	0.0423	0.1364	0.1152	-0.0046	0.0472
gradient.noise.scale	0.1735	0.1461	0.0302	0.0112	0.1454	0.1284	0.0448	0.0222
input.gradient.norm	0.3274	0.1442	-0.1755	0.0561	0.1446	0.1426	-0.0014	0.0535
tic.bias.term	0.3673	0.1705	-0.1889	0.0432	0.1919	0.1766	0.0057	0.0573
inverse.margin.p10	0.4279	0.2384	-0.1880	0.0612	0.2885	0.2266	0.0272	0.0709
hessian.trace	0.3600	0.1956	-0.1850	0.0494	0.2665	0.2281	0.0463	0.0667
sharpness.magnitude.init	0.3567	0.1035	0.1253	0.0154	0.4116	0.2337	0.1546	0.0544
hessian.top.eigenvalue	0.3558	0.1855	-0.1834	0.0437	0.2814	0.2353	0.0356	0.0605
sharpness.magnitude	0.3844	0.1228	0.1538	0.0014	0.4412	0.2530	0.1651	0.0481
sharpness.magflat	0.4470	0.1874	0.1277	0.0353	0.5071	0.3068	0.1716	0.0794
sharpness	0.3899	0.2120	-0.1325	0.0464	0.4265	0.3152	0.1725	0.0765
adaptive.sharpness	0.4603	0.2767	-0.0317	0.0309	0.5249	0.3659	0.2212	0.0717

Table 19: simplecnn summary of IID correlations and OODGenGap_P OOD sensitivities for each measure.

Measure	lr^{IID}	lr^{OOD}	wd^{IID}	wd^{OOD}	τ^{IID}	τ^{OOD}	Ψ^{IID}	Ψ^{OOD}
pac.bayes.magnitude.init	-0.3238	-0.5013	0.1872	-0.1385	-0.3330	-0.4376	-0.1252	-0.1054
frobenius.distance	-0.3391	-0.5045	0.1880	-0.1425	-0.3146	-0.4220	-0.0768	-0.0601
spec.prod	-0.3307	-0.4925	0.2325	-0.1639	-0.2764	-0.4170	-0.0727	-0.0755
spec.sum	-0.3191	-0.4846	0.2174	-0.1615	-0.1973	-0.3352	-0.0353	-0.0431
spectral.norm.per.layer	-0.3191	-0.4846	0.2174	-0.1631	-0.1971	-0.3350	-0.0345	-0.0442
path.norm	-0.2206	-0.4073	0.2134	-0.1742	-0.1524	-0.3249	-0.0767	-0.0974
magnitude	-0.1921	-0.3677	0.2087	-0.1790	-0.0421	-0.1906	0.0055	-0.0550
pac.bayes.magnitude	-0.1921	-0.3677	0.2087	-0.1790	-0.0421	-0.1906	0.0055	-0.0550
pac.bayes.bound	-0.2851	-0.3737	0.1015	-0.2386	-0.1772	-0.1882	-0.1616	-0.1847
l2.over.margin.p10	-0.1069	-0.1955	0.1388	-0.0926	-0.0749	-0.0996	-0.0972	-0.0629
margin.normalized.param.norm	-0.1069	-0.1955	0.1388	-0.0926	-0.0749	-0.0996	-0.0972	-0.0629
negative.entropy	-0.1751	-0.1808	0.2278	-0.1225	0.0242	-0.0795	0.0733	-0.0769
aic.bias.term	0.0000	0.0000	0.0000	0.0000	0.0000	0.0000	0.0000	0.0000
params	0.0000	0.0000	0.0000	0.0000	0.0000	0.0000	0.0000	0.0000
vcdim	0.0000	0.0000	0.0000	0.0000	0.0000	0.0000	0.0000	0.0000
l1.over.margin.p10	0.0284	-0.0362	0.1952	-0.1496	0.0674	0.0336	-0.0595	-0.0418
cross.entropy	0.1602	0.1531	-0.2389	0.1066	-0.0248	0.0677	-0.0776	0.0724
temperature.scaling	0.1549	0.1265	-0.1735	0.1451	-0.0076	0.0766	-0.0292	0.1301
pac.bayes.magflat	-0.0696	0.0487	-0.1888	0.1607	-0.0670	0.0776	-0.0275	0.0303
waic.bias.term	0.1196	0.1484	-0.0208	0.0075	-0.0439	0.1056	-0.0981	0.0673
mce	0.2139	0.1721	-0.0822	0.1430	0.0916	0.1163	0.0282	0.1917
reliability.diagram	0.2253	0.1789	-0.0710	0.1534	0.1032	0.1242	0.0356	0.1962
ece	0.2068	0.2010	-0.1810	0.1677	0.0320	0.1311	-0.0292	0.1212
ace	0.2070	0.2017	-0.1763	0.1741	0.0308	0.1322	-0.0283	0.1239
gradient.noise.scale	0.1735	0.2334	0.0302	-0.0130	0.1454	0.1531	0.0448	0.0004
fisher.rao.norm	0.2487	0.2156	-0.1541	0.1670	0.0786	0.1625	-0.0263	0.1352
input.gradient.norm	0.3274	0.3323	-0.1755	0.1765	0.1446	0.2457	-0.0014	0.1355
gradient.norm	0.3044	0.3652	-0.1897	0.1590	0.1276	0.2491	0.0018	0.1588
gradient.noise.var	0.3143	0.3571	-0.1818	0.1582	0.1365	0.2491	-0.0078	0.1546
gradient.noise.final.var	0.3145	0.3578	-0.1818	0.1598	0.1364	0.2493	-0.0071	0.1557
flatness.proxy	0.3159	0.3582	-0.1826	0.1574	0.1364	0.2494	-0.0046	0.1575
tic.bias.term	0.3673	0.4244	-0.1889	0.1638	0.1919	0.3120	0.0057	0.1783
inverse.margin.p10	0.4279	0.4331	-0.1880	0.1766	0.2885	0.3285	0.0272	0.1603
hessian.trace	0.3600	0.5050	-0.1850	0.1685	0.2665	0.4047	0.0463	0.2103
hessian.top.eigenvalue	0.3558	0.4907	-0.1834	0.1566	0.2814	0.4250	0.0356	0.2039
sharpness.magnitude.init	0.3567	0.2941	0.1253	0.0227	0.4116	0.4534	0.1546	0.1862
sharpness.magnitude	0.3844	0.3504	0.1538	-0.0415	0.4412	0.4934	0.1651	0.1529
sharpness.magflat	0.4470	0.4324	0.1277	0.0806	0.5071	0.5575	0.1716	0.2370
sharpness	0.3899	0.5702	-0.1325	0.1885	0.4265	0.6016	0.1725	0.2718
adaptive.sharpness	0.4603	0.6341	-0.0317	0.0972	0.5249	0.6557	0.2212	0.2145

Table 20: simplecnn summary of IID correlations and OODTestGap_C OOD sensitivities for each measure.

Measure	lr^{IID}	lr^{OOD}	wd^{IID}	wd^{OOD}	τ^{IID}	τ^{OOD}	Ψ^{IID}	Ψ^{OOD}
frobenius.distance	-0.3391	-0.0957	0.1880	-0.0531	-0.3146	-0.1603	-0.0768	-0.0042
spec.prod	-0.3307	-0.1054	0.2325	-0.0610	-0.2764	-0.1539	-0.0727	-0.0037
pac.bayes.magnitude.init	-0.3238	-0.0860	0.1872	-0.0513	-0.3330	-0.1408	-0.1252	0.0030
spec.sum	-0.3191	-0.1089	0.2174	-0.0603	-0.1973	-0.1263	-0.0353	-0.0125
spectral.norm.per.layer	-0.3191	-0.1091	0.2174	-0.0600	-0.1971	-0.1262	-0.0345	-0.0129
pac.bayes.bound	-0.2851	-0.1501	0.1015	-0.0828	-0.1772	-0.1173	-0.1616	-0.0358
path.norm	-0.2206	-0.0770	0.2134	-0.0632	-0.1524	-0.1099	-0.0767	0.0011
pac.bayes.magnitude	-0.1921	-0.0794	0.2087	-0.0620	-0.0421	-0.0689	0.0055	-0.0151
magnitude	-0.1921	-0.0794	0.2087	-0.0620	-0.0421	-0.0689	0.0055	-0.0151
l2.over.margin.p10	-0.1069	-0.0810	0.1388	-0.0401	-0.0749	-0.0488	-0.0972	-0.0019
margin.normalized.param.norm	-0.1069	-0.0810	0.1388	-0.0401	-0.0749	-0.0488	-0.0972	-0.0019
cross.entropy	0.1602	-0.0191	-0.2389	0.0476	-0.0248	-0.0178	-0.0776	0.0214
temperature.scaling	0.1549	-0.0180	-0.1735	0.0679	-0.0076	-0.0036	-0.0292	0.0363
aic.bias.term	0.0000	0.0000	0.0000	0.0000	0.0000	0.0000	0.0000	0.0000
params	0.0000	0.0000	0.0000	0.0000	0.0000	0.0000	0.0000	0.0000
vcdim	0.0000	0.0000	0.0000	0.0000	0.0000	0.0000	0.0000	0.0000
l1.over.margin.p10	0.0284	-0.0371	0.1952	-0.0570	0.0674	0.0104	-0.0595	0.0056
negative.entropy	-0.1751	0.0097	0.2278	-0.0501	0.0242	0.0115	0.0733	-0.0228
pac.bayes.magflat	-0.0696	0.0195	-0.1888	0.0589	-0.0670	0.0322	-0.0275	0.0080
ece	0.2068	0.0254	-0.1810	0.0761	0.0320	0.0377	-0.0292	0.0443
ace	0.2070	0.0256	-0.1763	0.0760	0.0308	0.0384	-0.0283	0.0439
mce	0.2139	0.0235	-0.0822	0.0526	0.0916	0.0489	0.0282	0.0464
reliability.diagram	0.2253	0.0239	-0.0710	0.0548	0.1032	0.0516	0.0356	0.0450
fisher.rao.norm	0.2487	0.0555	-0.1541	0.0744	0.0786	0.0751	-0.0263	0.0568
gradient.norm	0.3044	0.0520	-0.1897	0.0687	0.1276	0.0827	0.0018	0.0469
gradient.noise.var	0.3143	0.0472	-0.1818	0.0710	0.1365	0.0827	-0.0078	0.0482
gradient.noise.final.var	0.3145	0.0476	-0.1818	0.0707	0.1364	0.0829	-0.0071	0.0476
flatness.proxy	0.3159	0.0474	-0.1826	0.0686	0.1364	0.0831	-0.0046	0.0476
waic.bias.term	0.1196	0.0296	-0.0208	0.0217	-0.0439	0.0952	-0.0981	0.0483
gradient.noise.scale	0.1735	0.1134	0.0302	0.0082	0.1454	0.1011	0.0448	0.0135
input.gradient.norm	0.3274	0.0874	-0.1755	0.0811	0.1446	0.1190	-0.0014	0.0493
tic.bias.term	0.3673	0.1083	-0.1889	0.0708	0.1919	0.1461	0.0057	0.0613
sharpness.magnitude.init	0.3567	0.0208	0.1253	-0.0058	0.4116	0.1571	0.1546	0.0186
inverse.margin.p10	0.4279	0.1438	-0.1880	0.0836	0.2885	0.1643	0.0272	0.0662
sharpness.magnitude	0.3844	0.0360	0.1538	-0.0191	0.4412	0.1710	0.1651	0.0122
hessian.trace	0.3600	0.1305	-0.1850	0.0751	0.2665	0.1792	0.0463	0.0600
hessian.top.eigenvalue	0.3558	0.1214	-0.1834	0.0688	0.2814	0.1849	0.0356	0.0561
sharpness.magflat	0.4470	0.0943	0.1277	0.0069	0.5071	0.2182	0.1716	0.0431
sharpness	0.3899	0.1261	-0.1325	0.0663	0.4265	0.2350	0.1725	0.0381
adaptive.sharpness	0.4603	0.1723	-0.0317	0.0429	0.5249	0.2686	0.2212	0.0281

Table 21: simplecnn summary of IID correlations and OODTestGap_P OOD sensitivities for each measure.

Measure	lr^{IID}	lr^{OOD}	wd^{IID}	wd^{OOD}	τ^{IID}	τ^{OOD}	Ψ^{IID}	Ψ^{OOD}
spec.prod	-0.3307	-0.4314	0.2325	-0.2921	-0.2764	-0.3975	-0.0727	-0.0637
frobenius.distance	-0.3391	-0.4240	0.1880	-0.2651	-0.3146	-0.3895	-0.0768	-0.0829
pac.bayes.magnitude.init	-0.3238	-0.4181	0.1872	-0.2460	-0.3330	-0.3881	-0.1252	-0.0423
path.norm	-0.2206	-0.4091	0.2134	-0.2992	-0.1524	-0.3379	-0.0767	-0.0609
spec.sum	-0.3191	-0.4383	0.2174	-0.2873	-0.1973	-0.3293	-0.0353	-0.1005
spectral.norm.per.layer	-0.3191	-0.4393	0.2174	-0.2873	-0.1971	-0.3291	-0.0345	-0.1022
magnitude	-0.1921	-0.3800	0.2087	-0.3008	-0.0421	-0.2190	0.0055	-0.1257
pac.bayes.magnitude	-0.1921	-0.3800	0.2087	-0.3008	-0.0421	-0.2190	0.0055	-0.1257
pac.bayes.bound	-0.2851	-0.3306	0.1015	-0.2906	-0.1772	-0.1657	-0.1616	-0.0771
l2.over.margin.p10	-0.1069	-0.1977	0.1388	-0.1573	-0.0749	-0.1019	-0.0972	0.0192
margin.normalized.param.norm	-0.1069	-0.1977	0.1388	-0.1573	-0.0749	-0.1019	-0.0972	0.0192
negative.entropy	-0.1751	-0.1597	0.2278	-0.2824	0.0242	-0.0950	0.0733	-0.1789
aic.bias.term	0.0000	0.0000	0.0000	0.0000	0.0000	0.0000	0.0000	0.0000
params	0.0000	0.0000	0.0000	0.0000	0.0000	0.0000	0.0000	0.0000
vcdim	0.0000	0.0000	0.0000	0.0000	0.0000	0.0000	0.0000	0.0000
l1.over.margin.p10	0.0284	-0.0968	0.1952	-0.2587	0.0674	0.0008	-0.0595	0.0229
cross.entropy	0.1602	0.1296	-0.2389	0.2697	-0.0248	0.0801	-0.0776	0.1744
temperature.scaling	0.1549	0.0998	-0.1735	0.2622	-0.0076	0.0859	-0.0292	0.1786
mce	0.2139	0.0710	-0.0822	0.2172	0.0916	0.0954	0.0282	0.1731
reliability.diagram	0.2253	0.0748	-0.0710	0.2188	0.1032	0.1000	0.0356	0.1660
gradient.noise.scale	0.1735	0.2236	0.0302	-0.0086	0.1454	0.1332	0.0448	-0.0097
pac.bayes.magflat	-0.0696	0.1594	-0.1888	0.2762	-0.0670	0.1376	-0.0275	0.0948
ece	0.2068	0.1780	-0.1810	0.3038	0.0320	0.1435	-0.0292	0.1927
ace	0.2070	0.1792	-0.1763	0.3054	0.0308	0.1451	-0.0283	0.1931
waic.bias.term	0.1196	0.1389	-0.0208	0.0777	-0.0439	0.1680	-0.0981	0.2103
fisher.rao.norm	0.2487	0.1792	-0.1541	0.2888	0.0786	0.1707	-0.0263	0.2049
gradient.noise.var	0.3143	0.2954	-0.1818	0.2911	0.1365	0.2491	-0.0078	0.1964
gradient.noise.final.var	0.3145	0.2972	-0.1818	0.2927	0.1364	0.2494	-0.0071	0.1954
flatness.proxy	0.3159	0.2968	-0.1826	0.2888	0.1364	0.2496	-0.0046	0.1951
input.gradient.norm	0.3274	0.2829	-0.1755	0.3110	0.1446	0.2508	-0.0014	0.1526
gradient.norm	0.3044	0.3129	-0.1897	0.2999	0.1276	0.2513	0.0018	0.1964
inverse.margin.p10	0.4279	0.3338	-0.1880	0.3151	0.2885	0.2814	0.0272	0.2088
tic.bias.term	0.3673	0.3676	-0.1889	0.2999	0.1919	0.3153	0.0057	0.2260
sharpness.magnitude.init	0.3567	0.1362	0.1253	-0.0499	0.4116	0.3692	0.1546	0.0649
hessian.trace	0.3600	0.4504	-0.1850	0.3023	0.2665	0.3941	0.0463	0.2152
sharpness.magnitude	0.3844	0.1824	0.1538	-0.1085	0.4412	0.3981	0.1651	0.0337
hessian.top.eigenvalue	0.3558	0.4365	-0.1834	0.2729	0.2814	0.4126	0.0356	0.2082
sharpness.magflat	0.4470	0.2764	0.1277	-0.0349	0.5071	0.4586	0.1716	0.1118
sharpness	0.3899	0.4597	-0.1325	0.2675	0.4265	0.5465	0.1725	0.1307
adaptive.sharpness	0.4603	0.4828	-0.0317	0.1333	0.5249	0.5712	0.2212	0.0594

C.4 Sign-Error Results on CIFAR-10-Suite

Here, we present the full sign-error distributions for the CIFAR-10 suite. The figures cover three architectures and five target gaps: `GenGap_CIFAR10`, `OODGenGap_C`, `OODGenGap_P`, `OODTestGap_C`, and `OODTestGap_P`. Figures 4–8 complement the main-text NiN CIFAR-10-C result by showing the corresponding full distributions across architectures and targets. The CIFAR-10-C and CIFAR-10-P train-to-shifted-test targets show similar qualitative patterns, especially for NiN, supporting the reproducibility across CIFAR-10-C/P discussed in Section 4.2. The clean-to-shifted test-gap targets provide a stricter complementary view: they often retain the same hyperparameter-axis dependence, but expose additional local ranking failures when the target is the degradation from clean CIFAR-10 test accuracy to shifted-test accuracy.

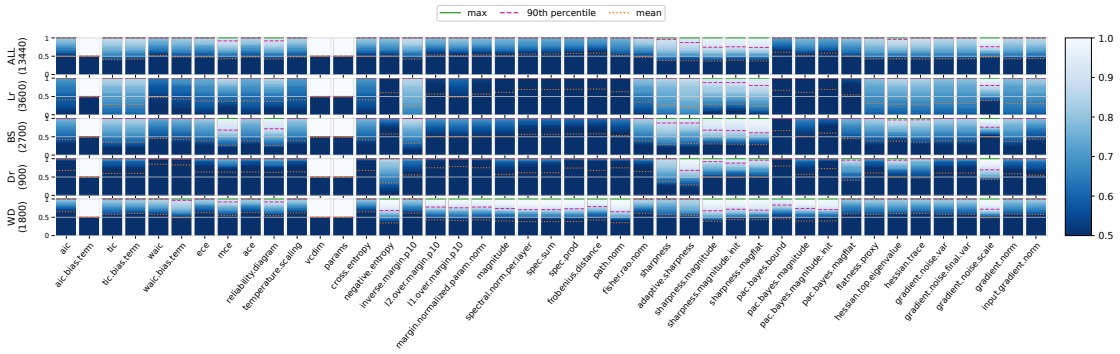

(a) SimpleCNN

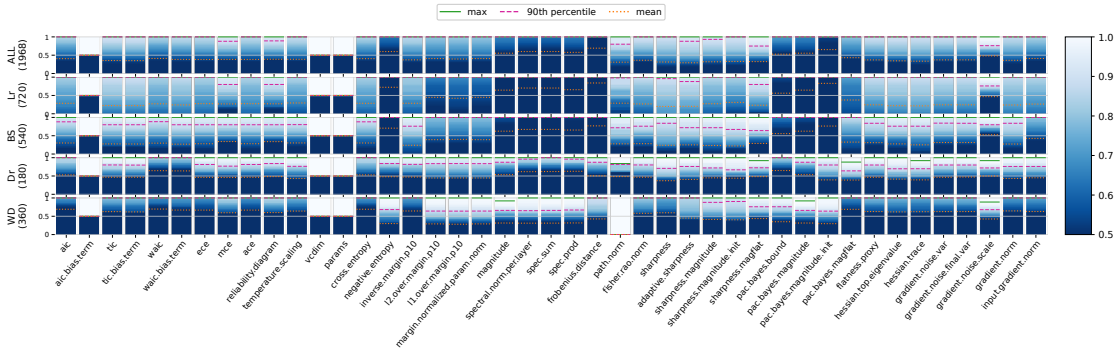

(b) ResNetV2-32

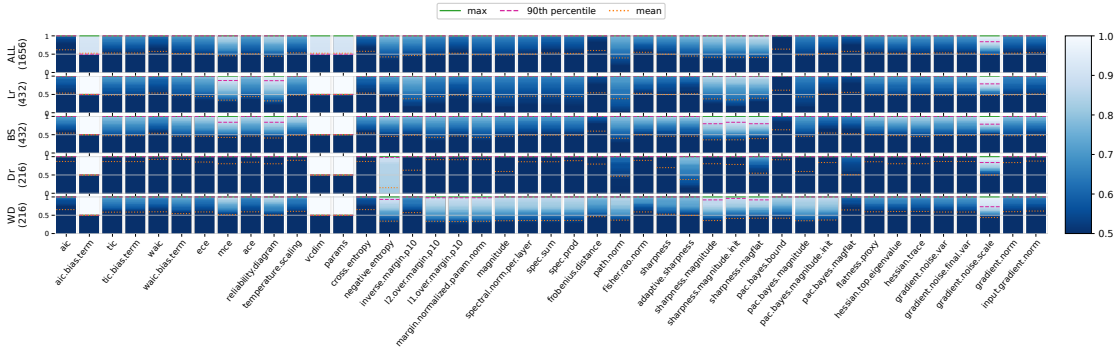

(c) NiN

Figure 4: Sign-error distributions for the IID CIFAR-10 generalization gap. The target is `GenGap_CIFAR10`.

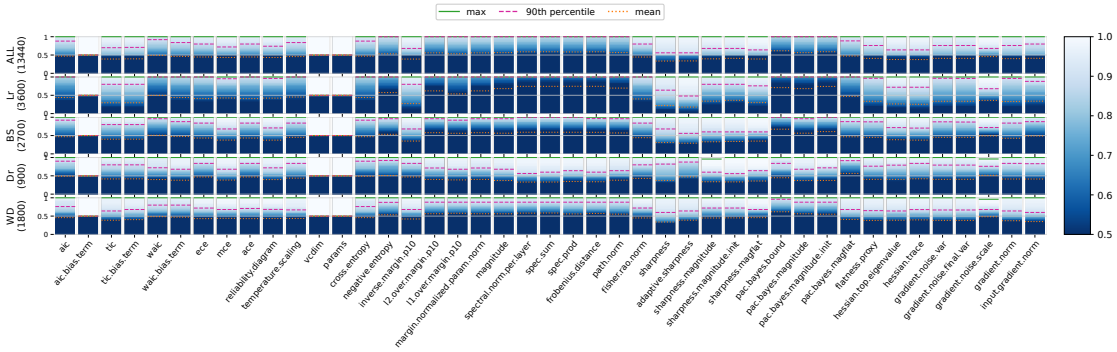

(a) SimpleCNN

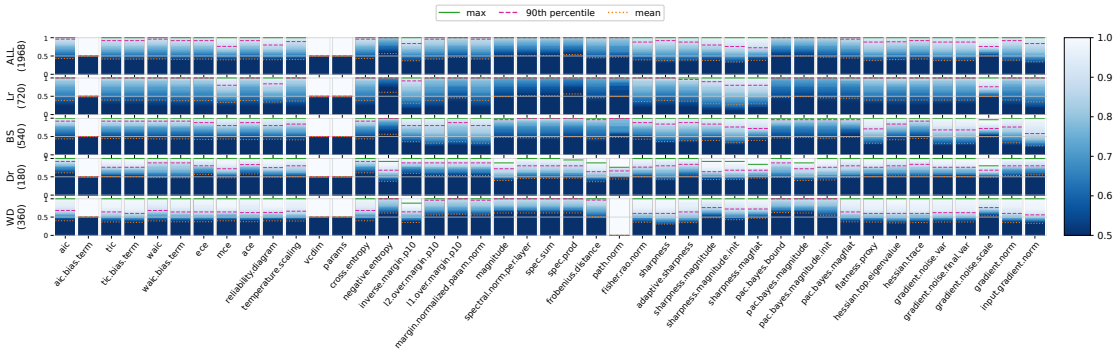

(b) ResNetV2-32

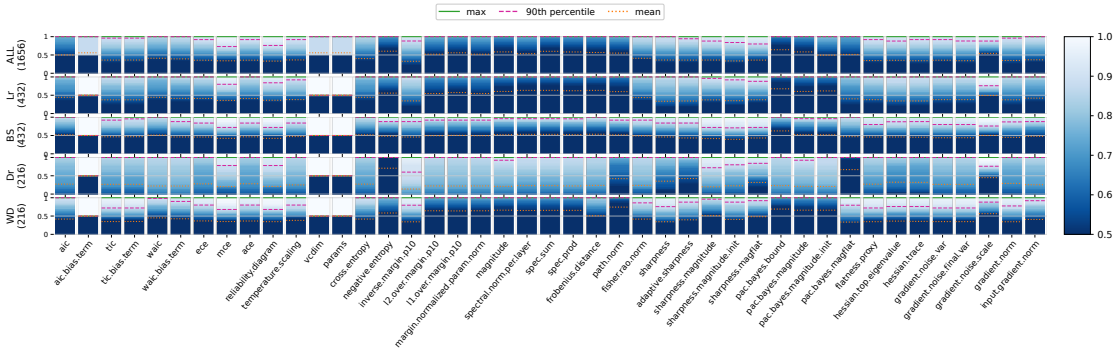

(c) NiN

Figure 5: Sign-error distributions for CIFAR-10-C train-to-shifted-test gap. The target is `OODGenGap_C`, computed from CIFAR-10 training accuracy to CIFAR-10-C test accuracy.

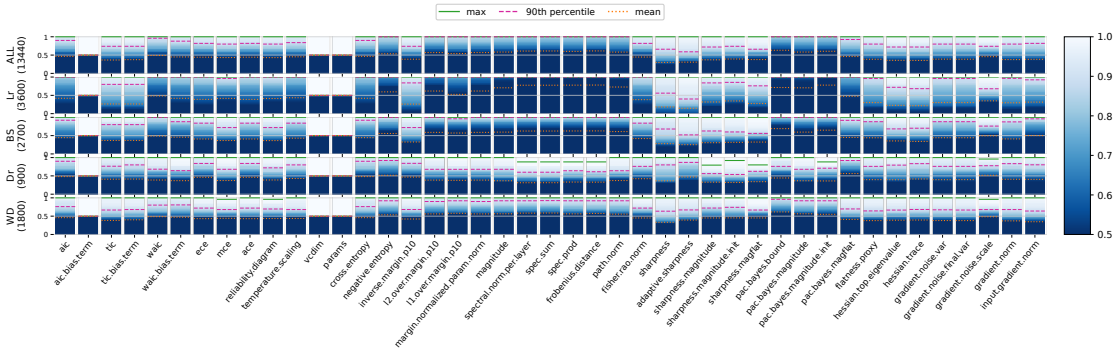

(a) SimpleCNN

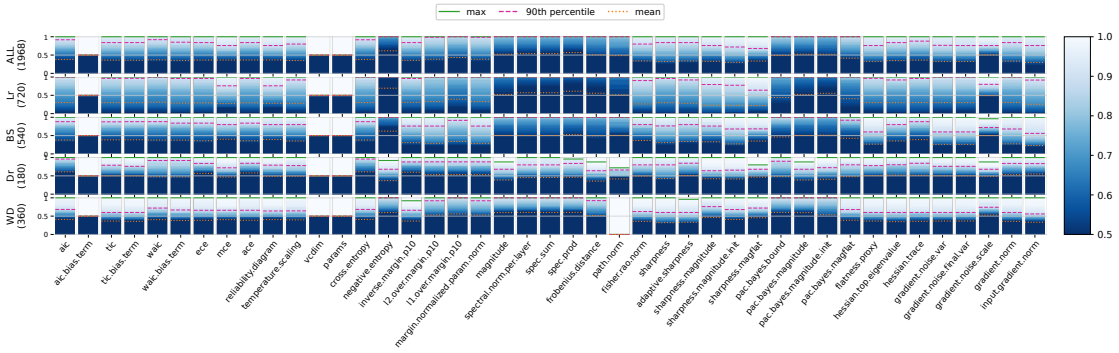

(b) ResNetV2-32

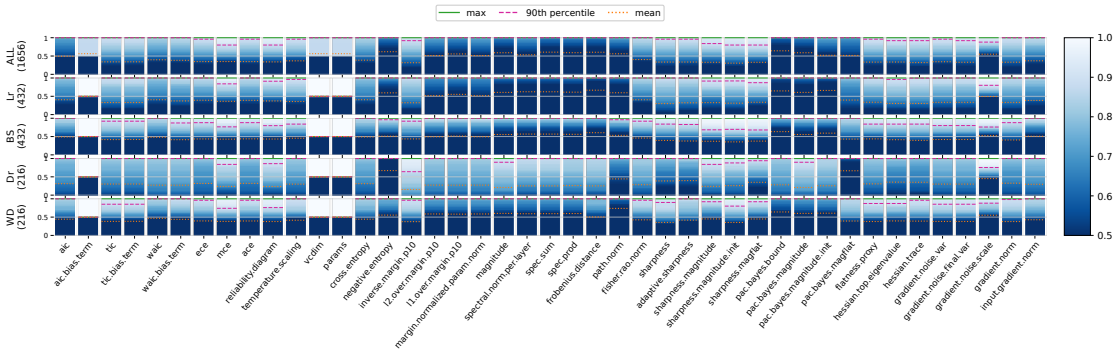

(c) NiN

Figure 6: Sign-error distributions for CIFAR-10-P train-to-shifted-test gap. The target is `OODGenGap_P`, computed from CIFAR-10 training accuracy to CIFAR-10-P test accuracy. The NiN panel is the CIFAR-10-P counterpart to Figure 2.

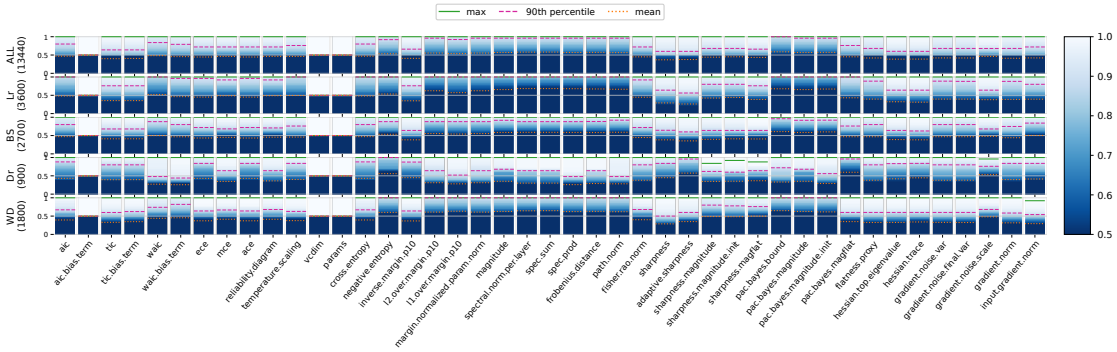

(a) SimpleCNN

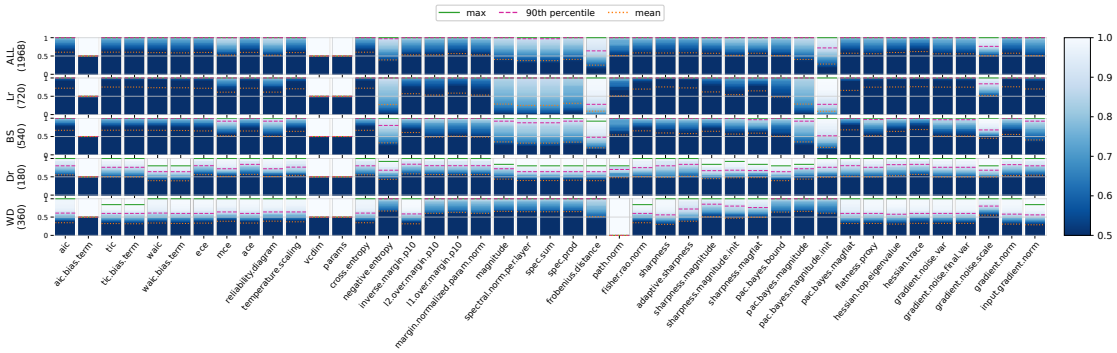

(b) ResNetV2-32

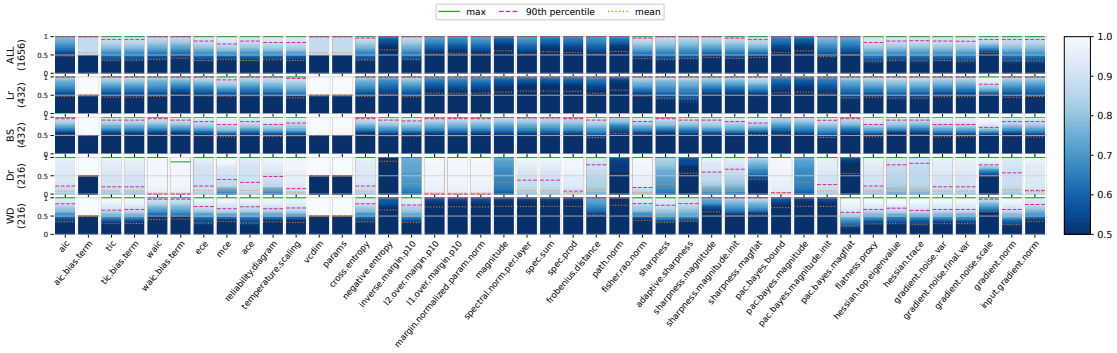

(c) NiN

Figure 7: Sign-error distributions for CIFAR-10-C test degradation. The target is `OODTestGap_C`, computed from clean CIFAR-10 test accuracy to CIFAR-10-C test accuracy.

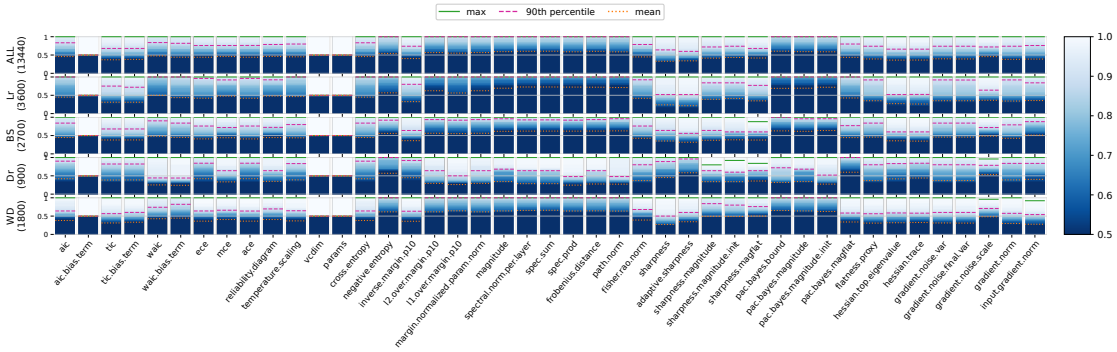

(a) SimpleCNN

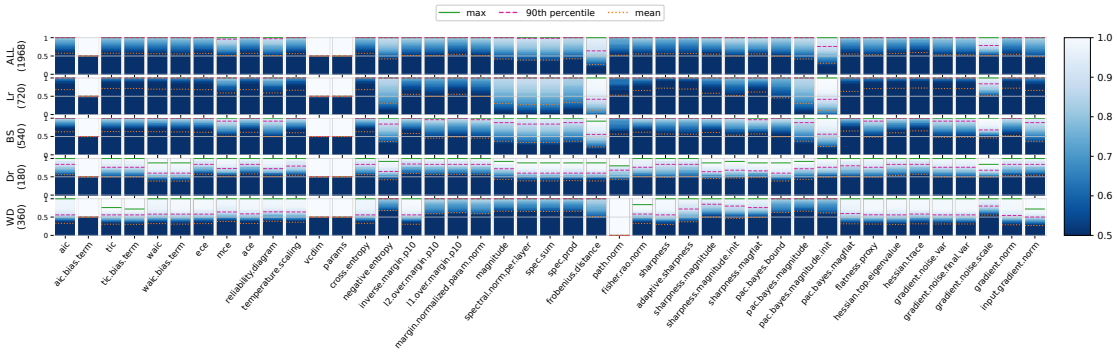

(b) ResNetV2-32

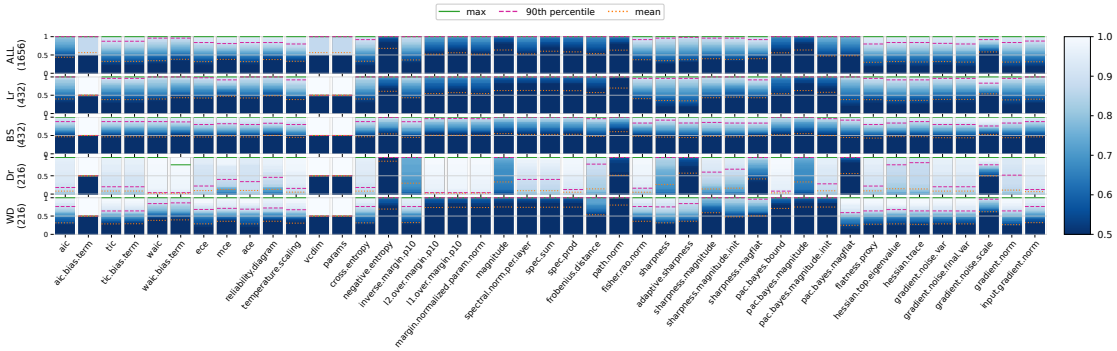

(c) NiN

Figure 8: Sign-error distributions for CIFAR-10-P test degradation. The target is `OODTestGap_P`, computed from clean CIFAR-10 test accuracy to CIFAR-10-P test accuracy.

C.5 Decision-level Model Selection Protocol Details

This appendix gives the exact decision-level model-selection protocol summarized in Section 3.6. The goal is to test whether a pre-target selector can choose a run with strong held-out CIFAR-10-C/P performance, not merely whether its scores correlate with shifted-test metrics.

Candidate sets and filtering. A candidate set $C_{a,s,t}$ is indexed by architecture a, sweep identity s, and shifted target $t \in \{\text{CIFAR-10-C}, \text{CIFAR-10-P}\}$. It contains finished runs that share (a, s, t) and have the selector score and held-out shifted-test metric needed for post-selection evaluation. Selector-level evaluations are restricted to candidate sets with finite selector values and finite held-out shifted-test metrics; if the oracle-to-worst target range is zero, normalized regret is defined as zero because no selector can improve over another on that target metric.

Selectors and leakage check. Generalization-measure selectors use only pre-target measure values, with lower-is-better fixed a priori for all such selectors. Source/clean baselines in the main table use training accuracy, training loss, and clean CIFAR-10 validation loss; clean-test accuracy/loss are excluded from the main Source/clean baseline and reported only as optimistic clean-test references in Table 23. Random samples uniformly from the candidate set, and its metrics are averaged over random draws in the result files. Oracle OOD selects the best run according to the held-out CIFAR-10-C/P metric and is included only as a reference. The leakage check enforces that CIFAR-10-C/P target labels, target accuracies, target losses, target gaps, target ranks, and empirical correlation signs are not used to choose the run or tune the selector direction; they enter only after selection for regret, rank, and hit-rate computation.

Regret and normalized regret. Let $y_t(r)$ be the held-out shifted-test metric for run r on target t, and let $d_t \in \{\text{higher}, \text{lower}\}$ be its direction. Let $r^\star$ be the oracle OOD run, r^- the worst run on the shifted target, and $\hat{r}_q$ the run selected by selector q. The unnormalized regret is

$$R_q(C) = \begin{cases} y_t(r^\star) - y_t(\hat{r}_q), & d_t = \text{higher}, \\ y_t(\hat{r}_q) - y_t(r^\star), & d_t = \text{lower}. \end{cases} \tag{56}$$

The normalized regret divides this by the oracle-to-worst range:

$$\bar{R}_q(C) = \begin{cases} \dfrac{R_q(C)}{y_t(r^\star) - y_t(r^-)}, & d_t = \text{higher}, \\ \dfrac{R_q(C)}{y_t(r^-) - y_t(r^\star)}, & d_t = \text{lower}, \end{cases} \tag{57}$$

with $\bar{R}_q(C) = 0$ when the range is zero.

Hit rates, family-level aggregation, and confidence intervals. The shifted-test rank $\text{rank}_{\text{OOD}}(r)$ orders runs from best to worst under y_t. For $k \in \{10, 20\}$, the top-k hit indicator is

$$\mathbb{I}\left[\text{rank}_{\text{OOD}}(\hat{r}_q) \leq \left\lceil \frac{k}{100}|C| \right\rceil\right]. \tag{58}$$

For each family, we first evaluate each individual measure selector on each candidate set, average the resulting metrics over selectors within the family for that candidate set, and then aggregate these family-level candidate-set values over the 28 candidate sets. Bootstrap confidence intervals are computed by resampling candidate sets, not individual selector rows. Table 1 reports mean normalized regret, top-10% and top-20% hit rates, and the number of candidate sets.

Table 22 reports candidate-set paired bootstrap differences between Calibration & Confidence and key comparator families. The negative regret differences indicate that Calibration & Confidence has lower normalized regret than the comparator on average under this paired candidate-set analysis. Table 23 separately reports clean-test accuracy/loss as optimistic source-domain references; these quantities do not use CIFAR-10-C/P target labels or shifted-test metrics, but they use the clean test split and are therefore excluded from the main Source/clean baseline.

Table 22: Paired decision-level regret differences. Each row reports the candidate-set paired difference in mean normalized regret between Calibration & Confidence and a comparator family. Negative values favor Calibration & Confidence. Intervals are percentile 95% paired bootstrap intervals obtained by resampling candidate sets.

Comparison	Δ normalized regret	95% paired CI	# candidate sets
Calibration - Source/clean baselines	-0.076	[-0.131, -0.023]	28
Calibration - Optimization-based	-0.090	[-0.168, -0.009]	28
Calibration - Random	-0.207	[-0.283, -0.128]	28

Table 23: Source/clean baseline variants. The main decision-selection table excludes clean-test quantities from Source/clean baselines. Clean-test accuracy/loss are shown only as optimistic source-domain references because they use the clean test split, although they still do not use CIFAR-10-C/P target labels or OOD metrics.

Selector group	Included selectors	Mean normalized regret ↓	95% CI	Top-10% hit ↑	Top-20% hit ↑	# candidate sets
Source/clean baselines	train_acc, train_loss, clean_val_loss	0.253	[0.189, 0.325]	0.286	0.405	28
Clean-test optimistic reference	clean_test_acc, clean_test_loss	0.231	[0.162, 0.304]	0.232	0.375	28

Individual selectors, architecture checks, and aggregation diagnostics. Table 24 reports individual selectors under the same decision-level protocol. The lowest non-oracle regrets are obtained by Optimization-based, Sharpness-based, and loss-based selectors, including `gradient.noise.final.var`, `gradient.noise.var`, `sharpness`, `flatness.proxy`, `gradient.norm`, and `cross.entropy`. These results show that strong single selectors exist outside Calibration & Confidence. They also show why the family average should be read as a robustness summary: using those selectors requires choosing a specific measure in advance.

Tables 25–27 report architecture-specific family results. They check whether the pooled result is driven by one architecture. Calibration & Confidence has the lowest point estimate for SimpleCNN and NiN. For ResNetV2-32, its interval overlaps those of Optimization-based selectors and Information Criteria, so the separation is weaker.

Table 24: Decision-level model selection on CIFAR-10-C/P: individual selector results.

Selector	Mean normalized regret ↓	95% CI	# candidate sets	# runs
oracle.ood	0.000	[0.000, 0.000]	28	25948
gradient.noise.final.var	0.098	[0.064, 0.139]	28	25948
gradient.noise.var	0.098	[0.064, 0.139]	28	25948
sharpness	0.106	[0.074, 0.146]	28	25948
flatness.proxy	0.107	[0.066, 0.157]	28	25948
gradient.norm	0.110	[0.068, 0.160]	28	25948
cross.entropy	0.120	[0.072, 0.176]	28	25948
ece	0.149	[0.102, 0.206]	28	25948
ace	0.158	[0.105, 0.222]	28	25948
mce	0.160	[0.107, 0.225]	28	25948
hessian.trace	0.173	[0.093, 0.277]	28	25948
hessian.top.eigenvalue	0.190	[0.111, 0.293]	28	25948
reliability.diagram	0.204	[0.117, 0.313]	28	25948
temperature.scaling	0.218	[0.137, 0.314]	28	25948
pac.bayes.magflat	0.232	[0.148, 0.333]	28	25948
tic.bias.term	0.303	[0.170, 0.442]	28	25948
adaptive.sharpness	0.314	[0.186, 0.456]	28	25948
aic.bias.term	0.326	[0.220, 0.444]	28	25948
params	0.326	[0.220, 0.444]	28	25948
vcdim	0.326	[0.220, 0.444]	28	25948
fisher.rao.norm	0.330	[0.195, 0.471]	28	25948
sharpness.magnitude.init	0.359	[0.213, 0.512]	28	25948
sharpness.magnitude	0.369	[0.222, 0.517]	28	25948
sharpness.magflat	0.390	[0.251, 0.536]	28	25948
pac.bayes.bound	0.397	[0.292, 0.508]	28	25948
input.gradient.norm	0.422	[0.258, 0.581]	28	25948
waic.bias.term	0.465	[0.303, 0.622]	28	25948
frobenius.distance	0.601	[0.490, 0.713]	28	25948
inverse.margin.p10	0.606	[0.477, 0.733]	28	25948
gradient.noise.scale	0.608	[0.465, 0.746]	28	25948
l1.over.margin.p10	0.639	[0.525, 0.750]	28	25948
l2.over.margin.p10	0.640	[0.522, 0.757]	28	25948
margin.normalized.param.norm	0.640	[0.522, 0.757]	28	25948
path.norm	0.666	[0.520, 0.793]	22	24718
spectral.norm.per.layer	0.709	[0.579, 0.826]	28	25948
magnitude	0.712	[0.584, 0.829]	28	25948
pac.bayes.magnitude	0.712	[0.584, 0.829]	28	25948
spec.prod	0.719	[0.599, 0.823]	28	25948
pac.bayes.magnitude.init	0.720	[0.613, 0.824]	28	25948
negative.entropy	0.751	[0.636, 0.856]	28	25948
spec.sum	0.776	[0.670, 0.871]	28	25948
train.loss	0.193	[0.105, 0.297]	28	25948
clean.val.loss	0.270	[0.191, 0.360]	28	25948
train.acc	0.312	[0.212, 0.424]	26	25918
random	0.385	[0.337, 0.429]	28	25948

Note: Clean-test references are excluded from the main table. Selector names use dot notation. Bootstrap confidence intervals resample candidate sets. Lower normalized regret is better. This table is not family-averaged and is used to assess within-family variation.

Table 25: Decision-level model selection on CIFAR-10-C/P for SimpleCNN.

Selector	Mean normalized regret ↓	95% CI	# candidate sets	# runs
Oracle	0.000	[0.000, 0.000]	12	18000
Calibration & Confidence	0.143	[0.052, 0.255]	12	18000
Source/clean baselines	0.168	[0.093, 0.251]	12	18000
Optimization-based	0.227	[0.127, 0.329]	12	18000
Sharpness-based	0.285	[0.190, 0.383]	12	18000
Information Criteria	0.366	[0.170, 0.581]	12	18000
Baseline & Output-based	0.303	[0.187, 0.439]	12	18000
Norm & Margin-based	0.568	[0.424, 0.714]	12	18000
Random	0.368	[0.283, 0.450]	12	18000

Note: The table reports family-level averages over pre-target selectors for a fixed architecture. For each candidate set, selector metrics are averaged within a family, and the resulting candidate-set values are averaged over candidate sets. Bootstrap confidence intervals resample candidate sets. Lower normalized regret is better. This split is one input to Table 29.

Table 26: Decision-level model selection on CIFAR-10-C/P for ResNetV2-32.

Selector	Mean normalized regret ↓	95% CI	# candidate sets	# runs
Oracle	0.000	[0.000, 0.000]	8	3598
Calibration & Confidence	0.287	[0.213, 0.363]	8	3598
Source/clean baselines	0.373	[0.238, 0.527]	8	3598
Optimization-based	0.321	[0.240, 0.410]	8	3598
Sharpness-based	0.395	[0.262, 0.544]	8	3598
Information Criteria	0.340	[0.265, 0.412]	8	3598
Baseline & Output-based	0.351	[0.231, 0.459]	8	3598
Norm & Margin-based	0.676	[0.562, 0.792]	8	3598
Random	0.375	[0.294, 0.451]	8	3598

Note: The table reports family-level averages over pre-target selectors for a fixed architecture. For each candidate set, selector metrics are averaged within a family, and the resulting candidate-set values are averaged over candidate sets. Bootstrap confidence intervals resample candidate sets. Lower normalized regret is better. For ResNetV2-32, the intervals for Calibration & Confidence, Optimization-based selectors, and Information Criteria overlap substantially.

Table 28 reports within-family spread using the individual-selector results in Table 24. Optimization-based and Sharpness-based families contain very strong selectors, but they also have large spread. Calibration & Confidence has a smaller spread, supporting its use as a stable default family when the specific measure is not fixed in advance.

Table 29 gives SimpleCNN, ResNetV2-32, and NiN equal weight using the architecture-level values in Tables 25–27. Calibration & Confidence remains the lowest-regret non-oracle family under this architecture-macro average. Thus, the pooled estimate in Table 1 is not explained solely by SimpleCNN's larger candidate-set count.

Table 27: Decision-level model selection on CIFAR-10-C/P for NiN.

Selector	Mean normalized regret ↓	95% CI	# candidate sets	# runs
Oracle	0.000	[0.000, 0.000]	8	4350
Calibration & Confidence	0.121	[0.078, 0.169]	8	4350
Source/clean baselines	0.262	[0.175, 0.350]	8	4350
Optimization-based	0.274	[0.200, 0.359]	8	4350
Sharpness-based	0.365	[0.267, 0.477]	8	4350
Information Criteria	0.387	[0.233, 0.565]	8	4350
Baseline & Output-based	0.526	[0.468, 0.595]	8	4350
Norm & Margin-based	0.714	[0.618, 0.811]	8	4350
Random	0.420	[0.364, 0.470]	8	4350

Note: The table reports family-level averages over pre-target selectors for a fixed architecture. For each candidate set, selector metrics are averaged within a family, and the resulting candidate-set values are averaged over candidate sets. Bootstrap confidence intervals resample candidate sets. Lower normalized regret is better. This split is one input to Table 29.

Table 28: Within-family spread of individual-selector normalized regret derived from Table 24.

Family	min	max	spread
Calibration & Confidence	0.149 (ece)	0.218 (temperature.scaling)	0.069
Optimization	0.098 (gradient.noise.final.var)	0.608 (gradient.noise.scale)	0.510
Sharpness	0.106 (sharpness)	0.720 (pac.bayes.magnitude.init)	0.614
Information Criteria	0.303 (tic.bias.term)	0.465 (waic.bias.term)	0.162

Note: Min and max entries are computed within each selector family using the individual-selector mean normalized regrets reported in Table 24. Spread is the displayed max-minus-min range of normalized regret; lower normalized regret is better. Large spread indicates sensitivity to the choice of individual selector. Calibration & Confidence has a higher best-selector regret than the strongest Optimization-based, Sharpness-based, and `cross.entropy` selectors, but its smaller spread supports its use as a stable default family when the specific measure is not fixed in advance.

Table 29: Pooled decision-selection estimates compared with equal-architecture macro averages from Tables 25–27.

Family	Pooled	Macro-avg (3 arch equal)
Calibration & Confidence	0.178	0.184
Source/clean	0.253	0.268
Optimization	0.267	0.274
Sharpness	0.339	0.348
Information Criteria	0.365	0.364
Baseline & Output	0.380	0.393
Norm & Margin	0.640	0.653
Random	0.385	0.388

Note: The pooled column reproduces the mean normalized regret values from Table 1. The macro-average column recomputes the displayed architecture-level means from Tables 25–27 with equal weight for SimpleCNN, ResNetV2-32, and NiN; no additional training or selection runs are used. Calibration & Confidence remains lowest under the macro average (0.184), so the pooled value (0.178) is not explained solely by SimpleCNN's larger candidate-set count. Lower normalized regret is better.